



## Review

## Magmatic ore deposits in mafic–ultramafic intrusions of the Giles Event, Western Australia

W.D. Maier<sup>a,\*</sup>, H.M. Howard<sup>b</sup>, R.H. Smithies<sup>b</sup>, S.H. Yang<sup>c</sup>, S.-J. Barnes<sup>d</sup>, H. O'Brien<sup>e</sup>, H. Huhma<sup>e</sup>, S. Gardoll<sup>f</sup><sup>a</sup> School of Earth and Ocean Sciences, Cardiff University, Cardiff, Wales, UK<sup>b</sup> Geological Survey of Western Australia, Perth, Australia<sup>c</sup> Oulu Mining School, University of Oulu, Oulu 90014, Finland<sup>d</sup> Sciences de la Terre, Université du Québec à Chicoutimi, Chicoutimi G7H 2B1, Canada<sup>e</sup> Geological Survey of Finland (GTK), FI-02151 Espoo, Finland<sup>f</sup> Department of Applied Geology, Curtin University, GPO Box U1987, Perth, WA 6845, Australia

## ARTICLE INFO

## Article history:

Received 13 February 2015

Received in revised form 5 June 2015

Accepted 14 June 2015

Available online 17 June 2015

## Keywords:

Musgrave Province

Giles event

Layered intrusions

PGE deposits

Magnetite layers

## ABSTRACT

More than 20 layered intrusions were emplaced at c. 1075 Ma across >100 000 km<sup>2</sup> in the Mesoproterozoic Musgrave Province of central Australia as part of the c. 1090–1040 Ma Giles Event of the Warakurna Large Igneous Province (LIP). Some of the intrusions, including Wingellina Hills, Pirtirri Mulari, The Wart, Ewarara, Kalka, Claude Hills, and Gosse Pile contain thick ultramafic segments comprising wehrlite, harzburgite, and websterite. Other intrusions, notably Hinckley Range, Michael Hills, and Murray Range, are essentially of olivine-gabbroanitic composition. Intrusions with substantial troctolitic portions comprise Morgan Range and Cavenagh Range, as well as the Bell Rock, Blackstone, and Jameson–Finlayson ranges which are tectonically dismembered blocks of an originally single intrusion, here named Mantamaru, with a strike length of >170 km and a width of >20 km, constituting one of the world's largest layered intrusions.

Over a time span of >200 my, the Musgrave Province was affected by near continuous high-temperature reworking under a primarily extensional regime. This began with the 1220–1150 Ma intracratonic Musgrave Orogeny, characterized by ponding of basalt at the base of the lithosphere, melting of lower crust, voluminous granite magmatism, and widespread and near-continuous, mid-crustal ultra-high-temperature (UHT) metamorphism. Direct ascent of basic magmas into the upper crust was inhibited by the ductile nature of the lower crust and the development of substantial crystal-rich magma storage chambers. In the period between c. 1150 and 1090 Ma magmatism ceased, possibly because the lower crust had become too refractory, but mid-crustal reworking was continuously recorded in the crystallization of zircon in anatectic melts. Renewed magmatism in the form of the Giles Event of the Warakurna LIP began at around 1090 Ma and was characterized by voluminous basic and felsic volcanic and intrusive rocks grouped into the Warakurna Supersuite. Of particular interest in the context of the present study are the Giles layered intrusions which were emplaced into localized extensional zones. Rifting, emplacement of the layered intrusions, and significant uplift all occurred between 1078 and 1075 Ma, but mantle-derived magmatism lasted for >50 m.y., with no time progressive geographical trend, suggesting that magmatism was unrelated to a deep mantle plume, but instead controlled by plate architecture.

The Giles layered intrusions and their immediate host rocks are considered to be prospective for (i) platinum-group element (PGE) reefs in the ultramafic–mafic transition zones of the intrusions, and in magnetite layers of their upper portions, (ii) Cu–Ni sulfide deposits hosted within magma feeder conduits of late basaltic pulses, (iii) vanadium in the lowermost magnetite layers of the most fractionated intrusions, (iv) apatite in unexposed magnetite layers towards the evolved top of some layered intrusions, (v) ilmenite as granular disseminated grains within the upper portions of the intrusions, (vi) iron in tectonically thickened magnetite layers or magnetite pipes of the upper portions of intrusions, (vii) gold and copper in the roof rocks and contact aureoles of the large intrusions, and (viii) lateritic nickel in weathered portions of olivine-rich ultramafic intrusions.

© 2015 Elsevier B.V. All rights reserved.

\* Corresponding author.

## Contents

|         |   |     |
|---------|---|-----|
| 1.      | Introduction . . . . .  | 406 |
| 2.      | Past work . . . . .   | 406 |
| 3.      | Regional geology . . . . .  | 408 |
| 4.      | Tectonic subdivision . . . . .  | 408 |
| 5.      | Analytical methods . . . . .  | 408 |
| 6.      | Geology and petrology of the Giles intrusions . . . . .   | 410 |
| 6.1.    | Introduction . . . . .  | 410 |
| 6.2.    | Mafic–ultramafic layered intrusions . . . . .   | 410 |
| 6.2.1.  | Pirntirri Mulari . . . . .  | 410 |
| 6.2.2.  | Wingellina Hills . . . . .  | 412 |
| 6.2.3.  | The Wart . . . . .  | 414 |
| 6.3.    | Predominantly mafic intrusions . . . . .  | 415 |
| 6.3.1.  | Latitude Hill–Michael Hills . . . . .   | 415 |
| 6.3.2.  | Morgan Range . . . . .  | 415 |
| 6.3.3.  | Hinckley Range . . . . .  | 415 |
| 6.3.4.  | Murray Range . . . . .  | 416 |
| 6.3.5.  | Cavenagh Range . . . . .  | 416 |
| 6.3.6.  | Lehmann Hills, Mt Muir, and other small intrusions north of the Blackstone and Wingellina Communities . . . . . | 417 |
| 6.3.7.  | Mantamaru . . . . .   | 417 |
| 6.3.8.  | Alcurra Dolerite suite . . . . .  | 419 |
| 6.3.9.  | Saturn . . . . .  | 419 |
| 6.3.10. | Intrusions in the Halleys–Helena–DB Hill area . . . . .   | 419 |
| 6.3.11. | Nebo–Babel . . . . .  | 419 |
| 6.3.12. | Dyke suites . . . . .   | 420 |
| 7.      | Geochemistry of the intrusions . . . . .  | 421 |
| 7.1.    | Lithophile elements and Nd–Sr–S isotopes . . . . .  | 421 |
| 7.2.    | Sulfur and chalcophile elements . . . . .   | 424 |
| 7.3.    | Mineral chemistry . . . . .   | 424 |
| 8.      | Discussion . . . . .  | 425 |
| 8.1.    | Nature of parent magmas to the Giles intrusions . . . . .   | 425 |
| 8.2.    | Mantle sources of the magmas . . . . .  | 426 |
| 8.3.    | Crustal contamination of the magmas . . . . .   | 426 |
| 8.4.    | Magma emplacement . . . . .   | 427 |
| 8.5.    | Fragmentation of intrusions . . . . .   | 429 |
| 8.6.    | Comparison to other large layered intrusions . . . . .  | 430 |
| 8.7.    | Tectonic setting . . . . .  | 432 |
| 8.8.    | Origin of mineralization . . . . .  | 432 |
| 8.8.1.  | PGE reefs within the Wingellina Hills layered intrusion . . . . .   | 432 |
| 8.8.2.  | Cu–Ni–PGE–Au mineralization at Halleys . . . . .  | 433 |
| 8.8.3.  | Vanadium and PGE mineralization in magnetite seams of the Jameson Range, Mantamaru intrusion . . . . .          | 433 |
| 8.8.4.  | Nebo–Babel Ni–Cu deposit . . . . .  | 433 |
| 9.      | Conclusions . . . . .   | 434 |
|         | Acknowledgements . . . . .  | 434 |
|         | References . . . . .  | 434 |

## 1. Introduction

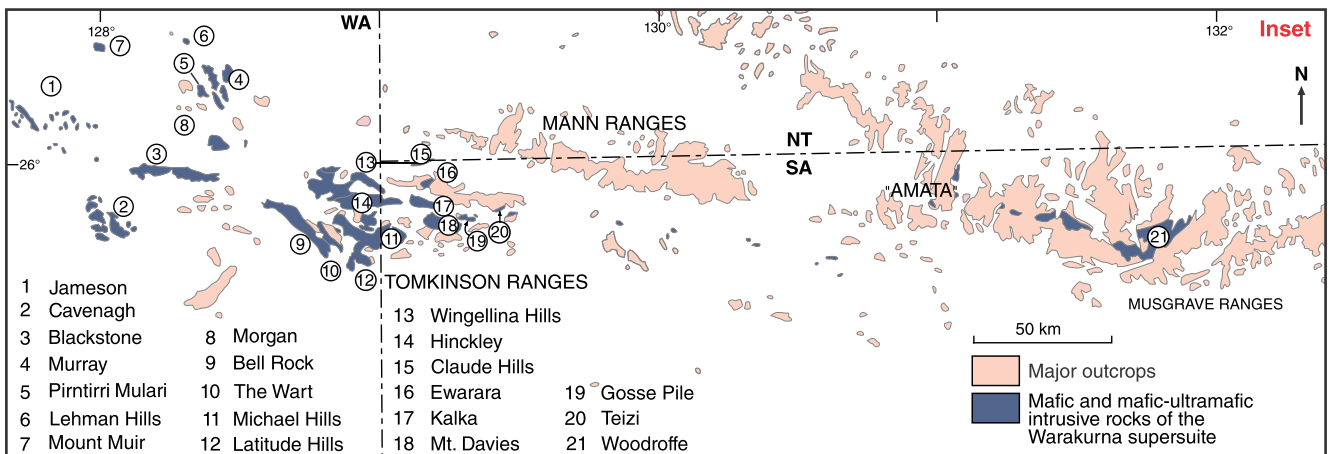
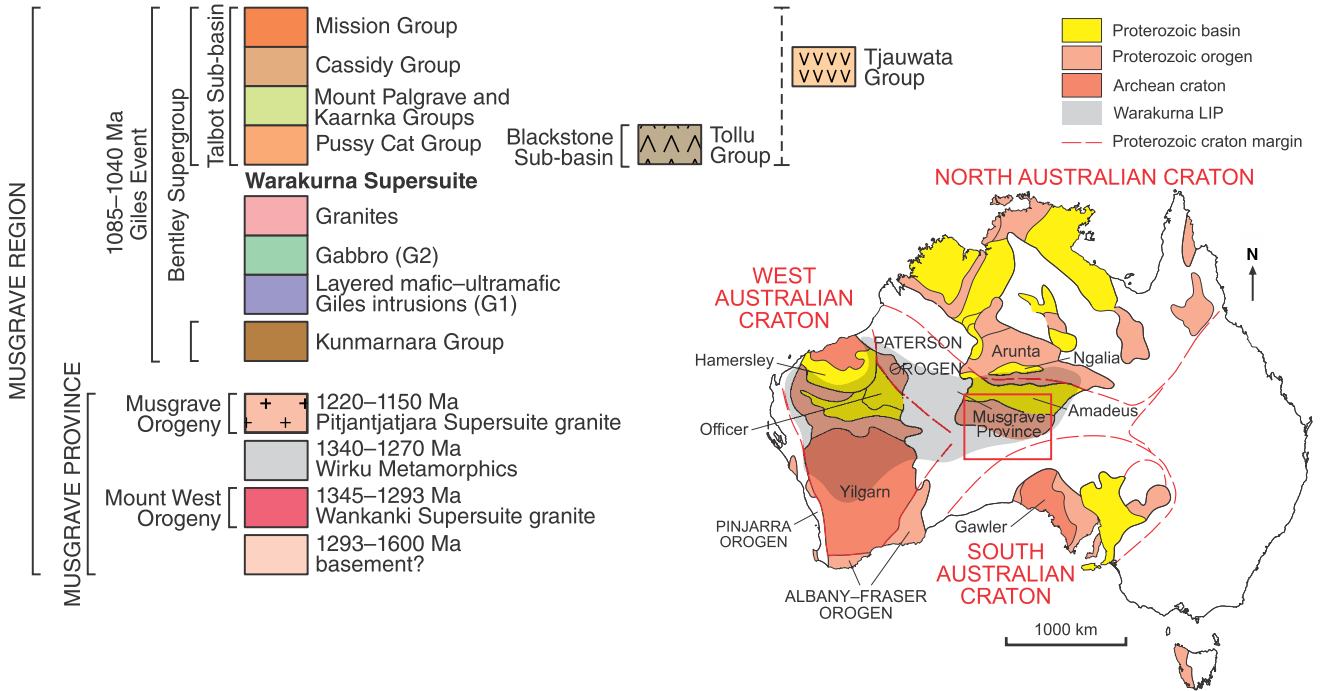
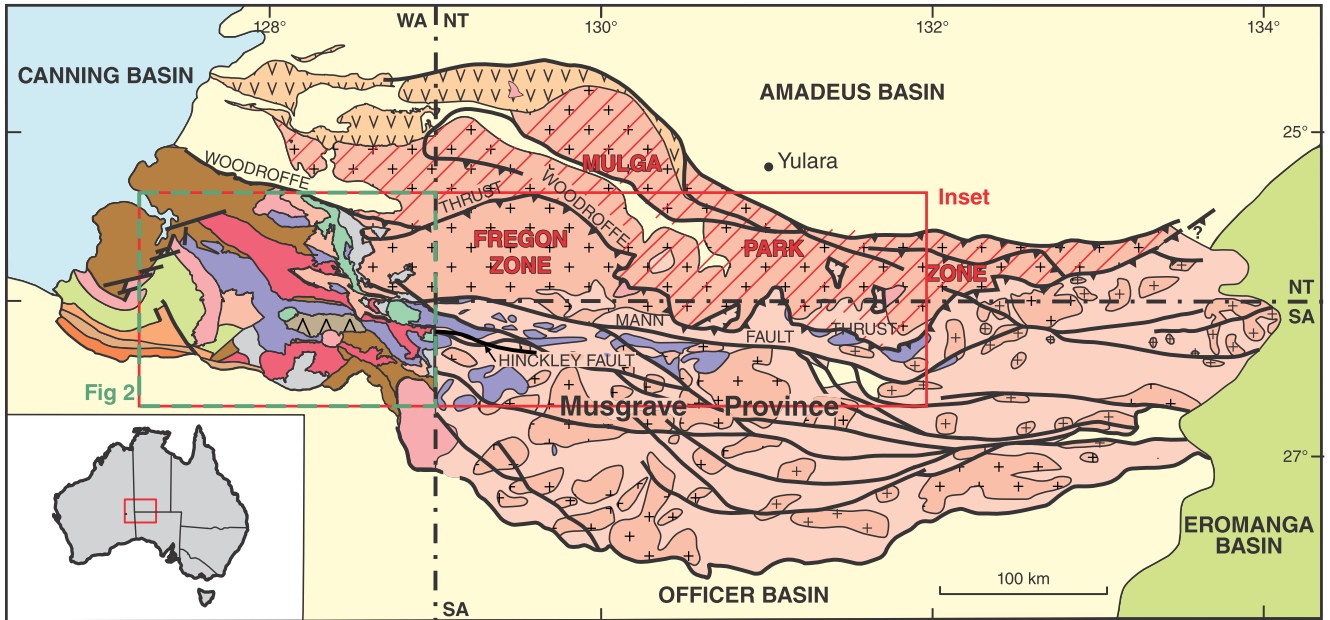
The Musgrave Province of central Australia hosts one of the most important clusters of mafic–ultramafic layered intrusions globally (Fig. 1), referred to as the Giles Complex (Daniels, 1974) or the Giles intrusions (Smithies et al., 2009). Together with broadly contemporaneous bimodal volcanism of the Bentley Supergroup and basic magmatism of the Warakurna Large Igneous Province (LIP) (Wingate et al., 2004), the Giles intrusions constitute the Warakurna Supersuite, formed during the c. 1090 to 1040 Ma Giles Event. The prospectivity of the Giles intrusions for magmatic ore deposits remains poorly understood. This is partly due to sparse exposure and because much of the study area belongs to the Ngaanyatjarra–Anangu Pitjantjatjara–Yankunytjatjara Central Reserve into which access is strictly regulated. However, the enormous volume of mafic igneous rocks and the remarkable size of some of the intrusions (up to several 1000 km<sup>2</sup>) reflect a high flux of mantle derived magma and heat into the crust. This is considered to

be favourable for the formation of magmatic and hydrothermal ore deposits. Two world-class deposits have been discovered so far, namely the Nebo–Babel magmatic Ni–Cu deposit (Seat et al., 2007, 2009) and the Wingellina Ni laterite deposit (Metals X Ltd, 2013). In the present paper we review the ore potential of the Giles intrusions and related mafic intrusive rocks of the Warakurna Supersuite.

## 2. Past work

Systematic geologic research on the Musgrave Province began with a mapping programme (at 1:250 000 scale) in the 1960s (Geological Survey of Western Australia – reported in Daniels, 1974), during which the Blackstone, Murray, and Morgan ranges, and parts of the Cavenagh and Jameson ranges, were mapped (see Fig. 1 for localities). Nesbitt and Talbot (1966) subsequently proposed that some of the layered intrusions are tectonised remnants of an originally much larger body. Other important early contributions on the layered

Fig. 1. Simplified geological map of the Musgrave Province, with mafic–ultramafic intrusions highlighted in bottom panel. From Howard et al. (2011b).



intrusions include the papers by Goode and Krieg (1967), Goode (1970, 1976a,b, 1977a,b,c, 1978), and Goode and Moore (1975). A large multidisciplinary study of the Musgrave Province beginning in the late 1980s (Australian Geological Survey Organisation, now Geoscience Australia: Glikson, 1995; Glikson et al., 1996) also focused mainly on the Giles intrusions (Ballhaus and Glikson, 1989, 1995; Ballhaus and Berry, 1991; Clarke et al., 1995a,b; Glikson, 1995; Sheraton and Sun, 1995; Stewart, 1995). Recent work includes studies by Seat et al. (2007, 2009) and Godel et al. (2011), on the Nebo–Babel Ni–Cu ore deposit, and by Evins et al. (2010a,b) and Aitken et al. (2013), on the structural evolution during the Giles Event.

### 3. Regional geology

In the present paper, the term 'Musgrave Province' is used to refer to high-grade metamorphic rocks affected by the 1220–1150 Ma Musgrave Orogeny, covering an area up to 800 km long and 350 km wide in central Australia (Fig. 1). The Western Australian segment of the Musgrave Province is referred to as the 'west Musgrave Province'. On geophysical images the Province is delineated by a series of east-trending anomalies. It is tectonically bound by the Neoproterozoic to Paleozoic sedimentary rocks of the Amadeus Basin in the north and the Officer Basin in the south (Edgoose et al., 2004).

The Musgrave Province lies at the junction between the North, South and West Australian Cratons. While some models suggest these cratonic elements of the Australian Craton amalgamated as early as c. 1700 Ma (e.g. Li, 2000; Wingate and Evans, 2003), most models agree that final amalgamation pre-dates the Musgrave Orogeny at c. 1220 Ma (Giles et al., 2004; Betts and Giles, 2006; Cawood and Korsch, 2008; Smithies et al., 2010, 2011; Kirkland et al., 2013).

With the exception of c. 1575 Ma rocks in the Wannarn area, the basement to the west Musgrave Province is not exposed. However, isotopic data on the detrital components in paragneisses, and on zircon xenocrysts, indicate that the basement is dominated by two major juvenile crust formation events, at 1600–1550 Ma and 1950–1900 Ma (Kirkland et al., 2013).

The oldest magmatic rocks in the study area comprise felsic calc-alkaline rocks of the Papulankutja Supersuite at c. 1400 Ma (Howard et al., 2011b; Kirkland et al., 2013). However, the oldest event recognizable throughout the west Musgrave Province is the Mount West Orogeny, characterized by emplacement of calc-alkaline granites of the Wankanki Supersuite mainly within the central and southeastern part of the west Musgrave Province (Evins et al., 2009; Smithies et al., 2009). Crystallization ages cluster between c. 1326 and 1312 Ma (Gray, 1971; Sun et al., 1996; White et al., 1999; Bodorkos et al., 2008a, 2008, 2008c, 2008d, 2008e; Kirkland et al., 2008a–f; Smithies et al., 2009). The rocks are typically metaluminous, calcic to calc-alkaline granodiorites and monzogranites, compositionally resembling Phanerozoic granites of the Andean continental arc (Smithies et al., 2010). The Mount West Orogeny may have been triggered by the amalgamation of the North, West, and South Australian Cratons and associated subduction and accretion (Giles et al., 2004; Betts and Giles, 2006; Smithies et al., 2010, 2011; Kirkland et al., 2013).

The 1220–1150 Ma Musgrave Orogeny formed in an intracratonic (Wade et al., 2008; Smithies et al., 2009, 2010) or back-arc setting (Smithies et al., 2013). Deformation and metamorphism was of high grade resulting in abundant mylonites. The main magmatic components are charnockitic and rapakivi granites of the Pitjantjatjara Supersuite. The earliest Pitjantjatjara granites are strongly Yb-depleted interpreted to have formed through deep-crustal melting in the presence of garnet. A transition from these to Yb-undepleted granites derived from shallower depth is diachronous, attributed to removal of the lower crust and mantle lithosphere, previously thickened during the Mount West Orogeny (Smithies et al., 2010, 2011). Intrusion of the high-T Pitjantjatjara granites (Smithies et al., 2010, 2011) coincided with a 70–100 m.y. period of regional ultra-high-temperature (UHT)

metamorphism (King, 2008; Kelsey et al., 2009, 2010; Smithies et al., 2010, 2011), characterized by lower to mid-crustal temperatures of >1000 °C, along a geothermal gradient of  $\geq 35$ –40 °C/km (King, 2008; Kelsey et al., 2009, 2010). Such conditions are consistent with removal of the lithospheric mantle. Thermal modelling and zircon geochronology indicates that mid-crustal temperatures remained elevated (>800 °C) in the period between the Musgrave Orogeny and the Giles Event (Smithies et al., 2015), mainly due to the accumulation of the highly radiogenic Pitjantjatjara granites.

The c. 1090 to 1040 Ma Giles Event was characterized by voluminous mafic to felsic magmatism (Fig. 2), including the layered mafic-ultramafic 'Giles intrusions' (G1), massive gabbro (G2) locally mixed and mingled with granite, various dyke suites including the Alcurra Dolerite suite, granite plutons, as well as mafic and felsic lavas, volcanoclastic and sedimentary rocks forming the Bentley Supergroup. All these components are grouped into the Warakurna Supersuite interpreted to have accumulated in the long-lived intracontinental Ngaanyatjarra Rift (Evins et al., 2010b; Aitken et al., 2013). Based in part on the extensive outcrop of the Warakurna Supersuite across ~1.5 million km<sup>2</sup> the Giles magmatism has been interpreted as the result of a mantle plume (Wingate et al., 2004; Morris and Pirajno, 2005). However, the most conservative estimates for the duration of mantle magmatism are >30 m.y. with a likelihood it continued for significantly longer (Smithies et al., 2015, in press), with no time-progressive geographical trend or track, inconsistent with a simple plume model (Smithies et al., 2013, 2015, in press; Evins et al., 2010a,b).

Younger events include the 580–530 Ma intracratonic Petermann Orogeny, during which many of the Giles intrusions were fragmented. Additional younger events are reflected by several regional dolerite dyke suites (at c. 1000, c. 825, and c. 750 Ma) and low-volume felsic magmatism (at c. 995 Ma and c. 625 Ma) (Howard et al., 2015).

### 4. Tectonic subdivision

Past workers divided the Musgrave Province into a number of sub-zones that show distinct structural and metamorphic characteristics. The sub-zones are separated by major west- and west-northwesterly trending faults, including the south-dipping Woodroffe Thrust (Fig. 1). In the eastern portion of the west Musgrave Province, there is a marked north-to-south change in the pressure of granulite-facies metamorphism. In the northern segment, high-pressure (10–14 kbar) metamorphism during the Petermann Orogeny has masked the effects of older metamorphism (Scrimgeour and Close, 1999). To the south, the metamorphic overprint of the Petermann Orogeny is not as marked and evidence for relatively low-pressure, but high-temperature Mesoproterozoic metamorphism is preserved (Clarke et al., 1995b). The boundary between these two regimes lies close to the west-trending, near vertical Mann Fault (Fig. 1).

The western part of the study area is subdivided into three distinct zones, namely the Walpa Pulka, Tjuni Purlka, and Mamutjarra Zones (from northeast to southwest; Howard et al., 2014; Fig. 2). The Tjuni Purlka Zone represents a northwest-trending belt of multi-generational (c. 1220, 1075, and 550 Ma) shearing and mafic magmatism of the Warakurna Supersuite (Fig. 2) that remained active throughout much of the Giles Event. The Walpa Pulka Zone (Fig. 2) is a deep-crustal domain hosting abundant c. 1220–1150 Ma granites of the Pitjantjatjara Supersuite that were emplaced during the Musgrave Orogeny. Mafic intrusions are rare and restricted to small bodies north of the Hinckley Range. The Mamutjarra Zone in the south (Fig. 2) contains several Giles intrusions and the c. 1345–1293 Ma calc-alkaline granites of the Wankanki Supersuite, emplaced during the Mount West Orogeny.

### 5. Analytical methods

Samples were prepared for analysis at GSWA using a jaw crusher followed by milling in a tungsten carbide mill. The mill was tested for

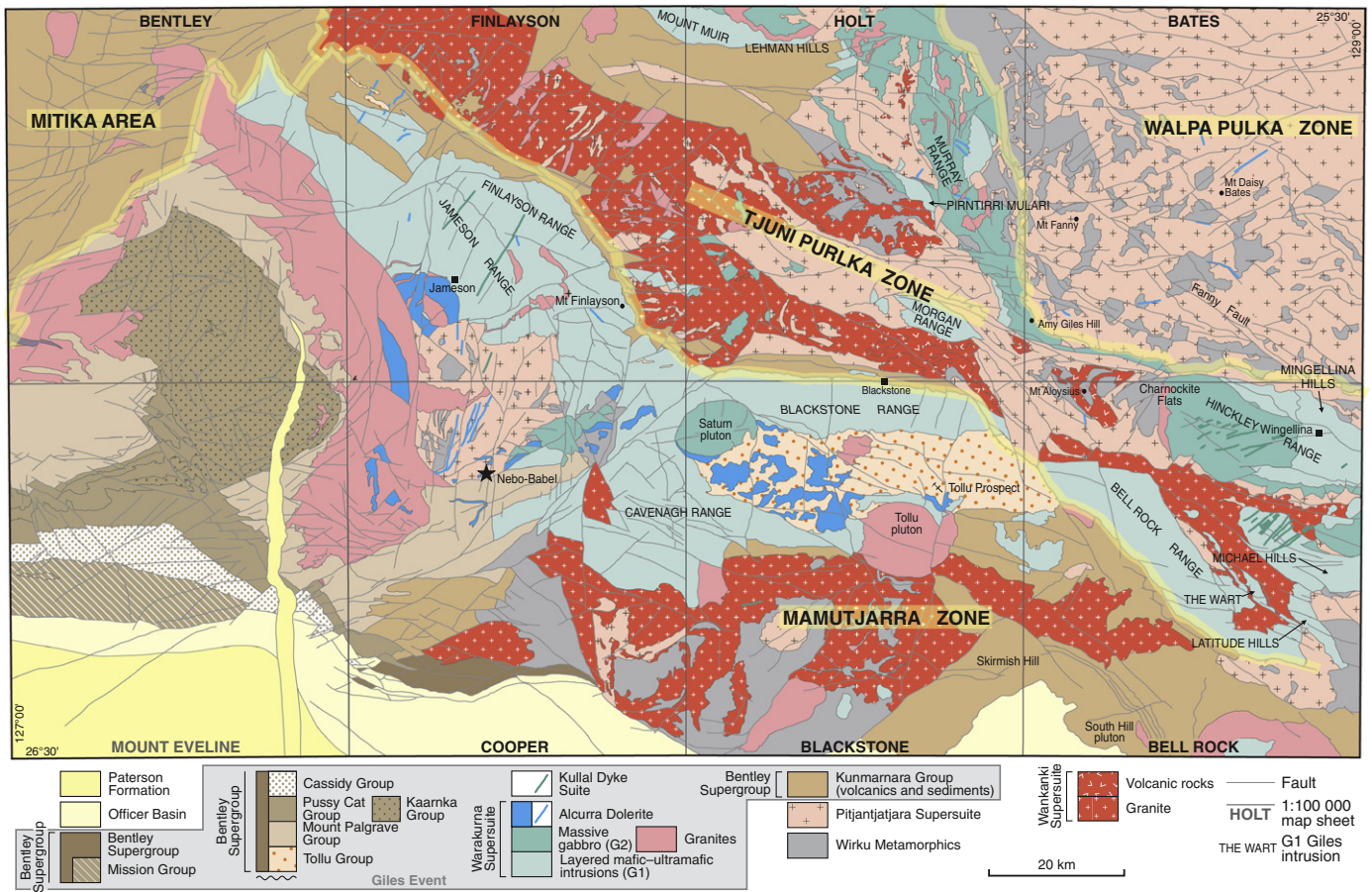


Fig. 2. Interpreted bedrock geology map of the west Musgrave Province. Location of Nebo-Babel deposits is indicated by black star. From Howard et al. (2011b).

possible contaminants, with only cobalt being significant ( $\leq 157$  ppm in grinding tests). Major elements were determined by wavelength-dispersive X-ray fluorescence spectrometry (XRF) on fused disks using methods similar to those of *Norrish and Hutton (1969)*. Precision is better than 1% of the reported values. Concentrations of Ba, Cr, Cu, Ni, Sc, V, Zn, and Zr were determined by wavelength-dispersive XRF on pressed pellets using methods similar to those of *Norrish and Chappell (1977)*, whereas Cs, Ga, Nb, Pb, Rb, Sr, Ta, Th, U, Y, and REE were analysed by inductively coupled plasma-mass spectrometry (ICP-MS) using methods similar to those of *Eggins et al. (1997)*, on solutions obtained by dissolution of fused glass disks. Precision for trace elements is better than 10% of the reported values. All whole-rock major and trace element data for the silicate rocks are listed in Table 1 of the supplementary data. All analyses and analytical details can be obtained from the WACHEM database (at <http://geochem.dmp.wa.gov.au/geochem/>). Selected major and trace elements for the massive magnetite seams were determined by instrumental neutron activation analysis (INAA) at The University of Québec at Chicoutimi, Canada (Table 2, supplementary data).

Platinum, Pd, and Au were analysed by lead collection fire assay of 40 g of sample, followed by ICP quantitation. The detection limit was 1 ppb for each element. For selected samples, complete PGE spectra were obtained by ICP-MS at The University of Québec at Chicoutimi. Analytical details are given in *Barnes et al. (2010)*. Platinum group element data are shown with the bulk of the lithophile element data in Table 1, supplementary data.

Sulfur isotopes were analysed by Rafter GNS Sciences at the New Zealand National Isotope Centre at Lower Hutt, New Zealand.

Samples were measured in duplicate in tin capsules with equal amounts of  $V_2O_5$  on a EuroVector elemental analyser connected to a GVI IsoPrime mass spectrometer. All results are averages and standard deviations of duplicates are reported with respect to Vienna Canyon Diablo Troilite (VCDT) standard, normalized to internal standards R18742, R2268, and R2298 with accepted  $\delta^{34}S$  values of  $-32\%$ ,  $+3.3\%$ , and  $+8.6\%$ , respectively. The external precision for this instrument is better than 0.3 for  $\delta^{34}S$ . All data are listed in Table 3, supplementary data.

In situ Sr isotope data were determined by laser ablation ICP-MS at the Geological Survey of Finland (GTK). Analytical procedures are provided in *Yang et al. (2013b)*, and the data are provided in Table 4, supplementary data.

For most samples, Sm–Nd isotopic analyses were determined by isotope dilution at the VIEPS Radiogenic Isotope Laboratory, Department of Earth Sciences, La Trobe University, Victoria, Australia. Analytical techniques follow those of *Waight et al. (2000)*. All quoted  $\epsilon Nd$  values are initial values calculated at the time of igneous crystallization. For some samples, Nd isotopes were determined at GTK in Espoo, Finland. Analytical details are given in *Maier et al. (2013a)*. All Sm–Nd isotope data are listed in Table 5, supplementary data.

The composition of olivine was determined at The University of Oulu in Oulu, Finland, using a JEOL JXA-8200 electron microprobe at an accelerating voltage of 15 kV and a beam current of 30 nA, which allowed an approximately 150 ppm detection limit for nickel. The accuracy of analyses was monitored using reference material of similar compositions. Compositional data are listed in Table 1.

**Table 1**  
Compositional range of selected minerals.

|                  | Fo (mol.%) | Ni (wt% in ol) | Mg#opx    | Mg#cpx    | An (mol.%) |
|------------------|------------|----------------|-----------|-----------|------------|
| Pirntirri Mulari | 77–85      | 0.37–0.4       | 0.68–0.88 | 0.81–0.92 | 30–88      |
| Wingellina Hills | 77–88      |                | 0.72–0.88 | 0.78–0.87 | 55–92      |
| The Wart         | 78–87      | 0.30–0.39      | 0.79–0.86 | 0.79–0.87 | 53–93      |
| Cavenagh         | 38–74      | 0.04–0.22      | 0.70–0.77 | 0.63–0.79 | 60–73      |
| Morgan           | 71–87      | 0.23–0.29      | 0.74–0.81 | 0.78–0.83 | 69–79      |
| Hinckley         | 57–76      | 0.15–0.16      | 0.55–0.79 | 0.77–0.79 | 45–83      |
| Murray           | 68–81      | 0.23–0.30      | 0.73–0.8  | 0.78–0.84 | 69–79      |
| Lehman Hills     | 71–72      | dl–0.16        | 0.76      | 0.75–0.80 | 70–78      |
| Blackstone       | 40–68      | 0.02–0.18      | 0.59–0.73 | 0.68–0.78 | 50–78      |
| Bell Rock        | 56–68      |                | 0.62–0.71 |           |            |
| Jameson          | 51–66      | dl–0.09        | 0.53–0.70 | 0.74–0.77 | 50–76      |
| Nebo Babel       | 70–74      | 0.11–0.21      | 0.43.0.80 |           | 44–77      |
| Halleys          |            |                | 0.65–0.69 | 0.70–0.71 | 56–82      |
| Saturn           | 56–62      | dl–0.09        | 0.65–0.68 | 0.71–0.73 | 54–55      |

**6. Geology and petrology of the Giles intrusions**

**6.1. Introduction**

The Giles intrusions in western Australia show considerable variation in terms of size (from a few km<sup>2</sup> to >3000 km<sup>2</sup>), depth of emplacement (from <1 kbar to possibly as much as 12 kbar), whole rock and mineral composition, as well as style of associated mineral deposits. In the following section, we group the intrusions by their predominant lithologies. Intrusions with important ultramafic segments of wehrlite, harzburgite,

websterite and (olivine) orthopyroxenite include Wingellina Hills, Pirntirri Mulari and The Wart (Fig. 1). Intrusions that are predominantly leucogabbronoritic are more common, comprising Hinckley Range, Michael Hills, Latitude Hill, Murray Range, Morgan Range, Cavenagh Range and Saturn. The Blackstone, Jameson-Finlayson, and Bell Rock ranges also belong to this group, but they are now believed to be tectonically segmented portions of an originally single body, hereafter called the Mantamaru intrusion. In addition, a number of smaller intrusions or fragments of intrusions occur to the north of the Tjuni Purlka Zone including Mt Muir and Lehmann Hills.

Several of the mafic intrusions contain thick troctolitic successions, namely the Cavenagh and Morgan ranges and Mantamaru. Anorthosites may form relatively thin layers (centimetres to several tens of centimetres) in the mafic intrusions, but attaining thicknesses of several tens of metres at Kalka in South Australia.

**6.2. Mafic–ultramafic layered intrusions**

**6.2.1. Pirntirri Mulari**

The intrusion is located ~30 km north of Blackstone Community (Fig. 2). It was grouped with the gabbonoritic Murray Range by Ballhaus and Glikson (1995), but in view of the distinct lithologies and composition of the intrusions (ultramafic–mafic for Pirntirri Mulari, mafic for Murray) this interpretation is rejected here. The exposed portion of the intrusion has the shape of a wedge, with the upper, predominantly mafic portion being markedly wider than the lower, predominantly ultramafic portion (Fig. 3). The layers strike about 150°

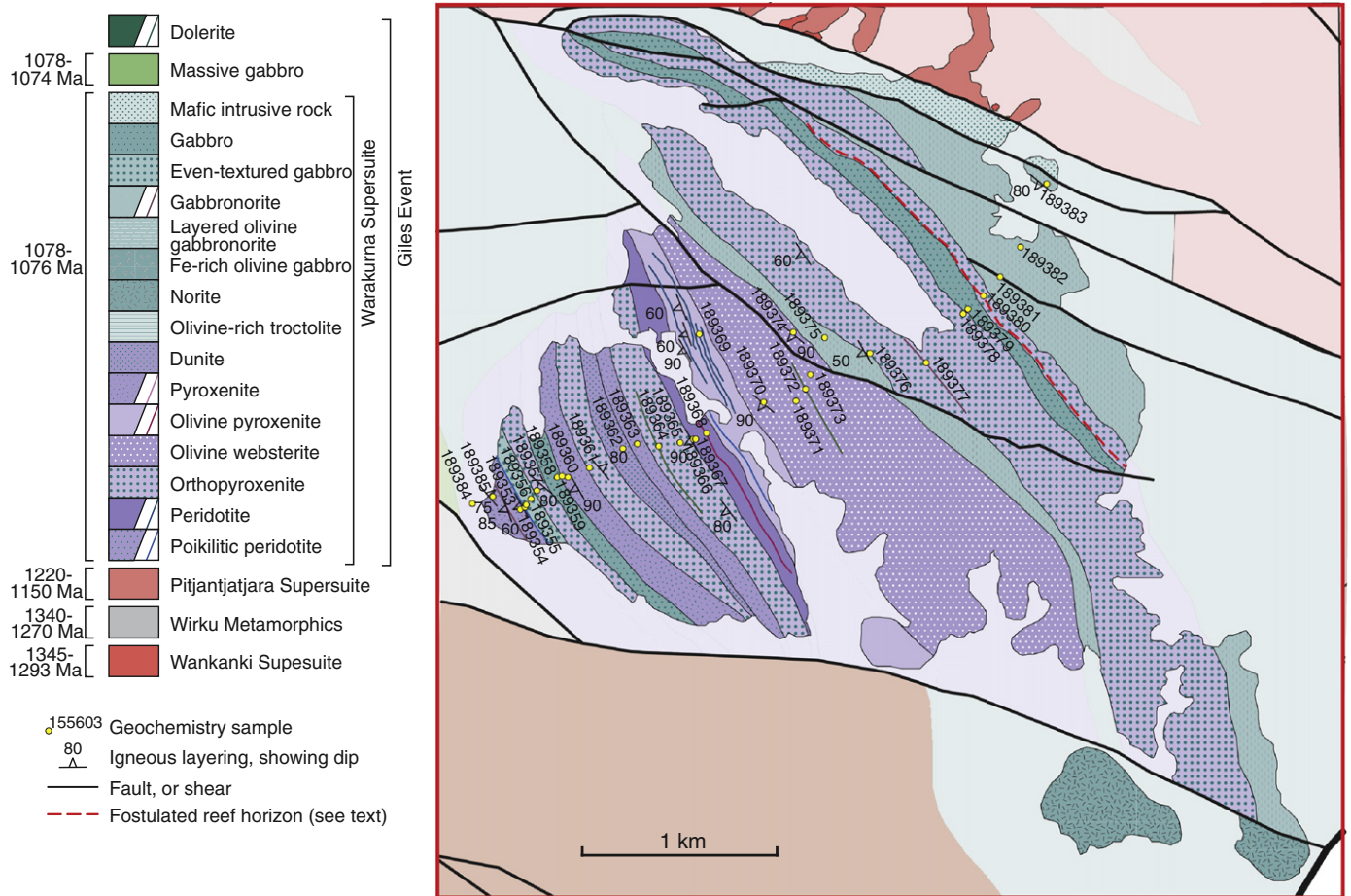


**Fig. 3.** Interpreted bedrock geological map of the Pirntirri Mulari intrusion, showing sample localities (yellow circles). Stippled line indicates position of postulated reef horizon. Light shaded areas indicate regions of regolith cover. Modified from Maier et al. (2014).

and mostly dip steeply to the southwest (60–90°). The body is about 5 km wide and has a stratigraphic thickness of about 3 km.

Most of the rocks are medium-grained (olivine) websterites, peridotites, (olivine) orthopyroxenites, and (olivine) gabbronorites. At the southwestern and northeastern margins of the intrusion occur interlayered websteritic and gabbronoritic orthocumulates, whereas adcumulate peridotites and orthopyroxenites are concentrated in the centre. Based on compositional and field evidence, we propose that the succession youngs to the northeast, implying that the intrusion is slightly overturned. Many of the rocks show textural equilibration, expressed by 120° grain boundaries, abundant bronzite and spinel exsolutions in clinopyroxene, small granoblastic plagioclase grains containing spinel inclusions, orthoclase exsolution blebs and two-pyroxene spinel symplectite at contacts between plagioclase and olivine. These features are common to many other Giles intrusions and were previously interpreted to reflect relatively high crystallization pressures and temperatures (Ballhaus and Glikson, 1989).

The basal contact of the intrusion is not exposed, but in view of the increased proportion of orthocumulates towards the southwestern exposed edge, we argue that the basal contact is proximal to this. The top contact is likely of a tectonic nature, as suggested by the presence of a mylonite zone and by the relatively unevolved chemical composition of the uppermost gabbros (Mg# 0.7, Cr/V > 1) (Table 1 supplementary data).

Exposed contacts between layers can be gradational or sharp (Fig. 4a). In the centre of the intrusion (GSWA189374), coarse-grained websterite underlies gabbronorite with an undulose contact, and has locally injected the gabbronorite (Fig. 4b). The gabbronorite is more deformed than the pyroxenite, and is altered near the contact, consistent with intrusion of pyroxenite below older gabbronorite. Elsewhere (e.g., GSWA189368), fine-grained lherzolite overlies coarse-grained peridotite with an undulose, sharp contact (Fig. 6c in Maier et al., 2014). The lherzolite contains inclusions of the peridotite and is interpreted to have crystallized from a new magma influx that was

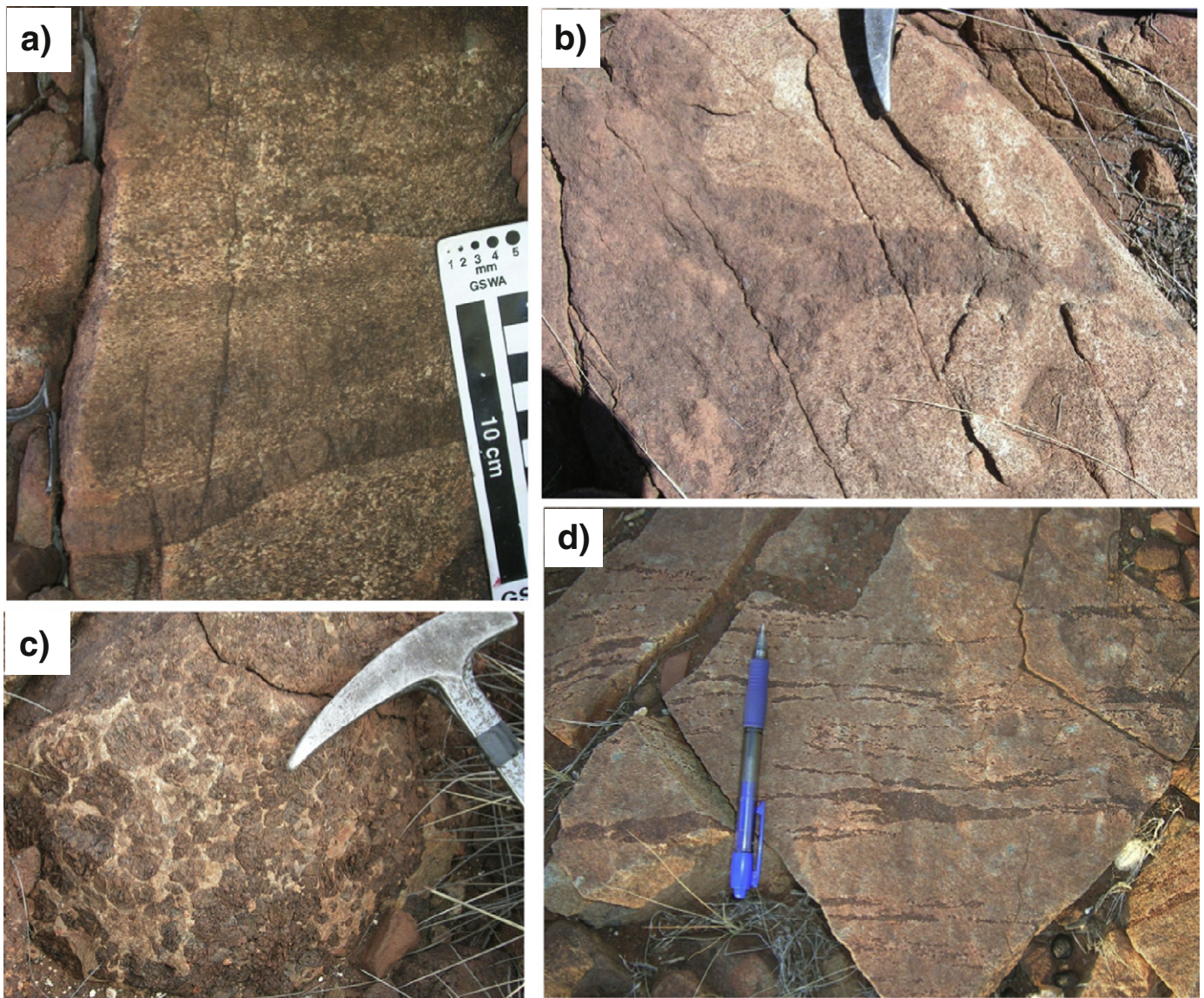


**Fig. 4.** Textures of rocks in the Pirntirri Mulari intrusion. a) Centimetre-scale interlayering of pyroxenite and gabbronorite showing sharp bottom contact and upward grading; note small lenses and schlieren of pyroxenite within gabbronorite (near GSWA 189359); b) contact between pyroxenite and overlying gabbronorite; finger-like structure of pyroxenite is interpreted as injection of pyroxenite mush into gabbronorite (near GSWA 189374); c) pegmatoidal layer within medium-grained pyroxenite (GSWA 189360); d) schlieren of pyroxenite within leucogabbronorite (near GSWA 189358).

Adapted from Maier et al. (2014).

quenched and partially eroded its floor. Other ultramafic layers are underlain by pegmatoidal gabbronoritic orthocumulate layers (Fig. 4c), consisting of 40% plagioclase, 30% orthopyroxene, 20% clinopyroxene, and accessory phlogopite and chromite. Relatively high concentrations of incompatible trace elements (e.g. P, LREE, Nb, Rb) in the pegmatoid suggest that it may have formed in response to upward percolation of evolved melt or fluid.

The lower portion of the intrusion, particularly below and above pyroxenite layers, contains several horizons showing textural evidence for considerable syn-magmatic cumulate mobility, such as abundant ultramafic and anorthositic schlieren within gabbronorite (Fig. 4d).

The concentrations of the platinum-group elements (PGE) in the intrusion are mostly <10 ppb (Fig. 5), and Cu/Pd is at the level of the primitive mantle (4000–7000), suggesting that the magma was fertile and sulfur undersaturated during crystallization. However, at a stratigraphic height of ~2600 m above the base of the intrusion, Cu/Pd increases sharply, suggesting that a sulfide melt had fractionated from the magma at this stage. This sample has low PGE concentrations, although it contains nearly 500 ppm Cu. It is located in the mafic–ultramafic transition interval, analogous to the stratigraphic position of PGE reefs in the Bushveld Complex and many other PGE-mineralized intrusions (Maier, 2005). A sulfide-bearing pyroxenite from an equivalent stratigraphic level collected along the southeastern edge of the intrusion (Fig. 3) has similar chromium, copper, and nickel concentrations to the equivalent internal horizon, but higher Pt + Pd (172 ppb) and gold (17 ppb) concentrations. Assay results using a NITON portable XRF showed elevated Ni and Cu over a stratigraphic interval of 5–10 m, and peak concentrations of 0.43% Cu and 0.7% Ni in weathered rock (Redstone Resources Ltd, 2008a). No detailed sampling of this interval has yet

been conducted to establish the width and grade of a putative reef horizon.

### 6.2.2. Wingellina Hills

The intrusion is approximately 12 km long and up to 3 km wide (Fig. 6). Drilling by Acclaim Minerals and Metals X Ltd, and mapping by GSWA, established dips of about 65–75° to the southwest, and younging in the same direction indicating that the intrusion is not overturned. The strike of the layering is 110–120°. The exposed stratigraphic thickness amounts to 2.5 km, assuming that the stratigraphy is not duplicated by tectonism. The gabbros and pyroxenites tend to be unaltered at the surface, whereas the peridotites are commonly deeply weathered to a depth of about 60 m to >200 m, particularly in shear zones.

The central portion of the intrusion contains numerous cyclic units consisting of basal pegmatoidal (ortho) pyroxenite, overlain by clinopyroxenite and then peridotite (olivine–spinel cumulate), wehrlite, and gabbronorite (Ballhaus and Glikson, 1989). The gabbronorite may contain fragments and schlieren of ultramafic material, and it may display convoluted and folded layering on a scale of 1–2 cm, analogous to Pirntirri Mulari (Fig. 4).

The composition of the basal to central portion of the intrusion has been studied in several stratigraphic boreholes. The basal contact has been intersected by a reverse circulation (RC) borehole (WPRCO-023, see Maier et al., 2014 for details). It is interpreted as intrusive because there is a well-defined, > 100 m wide basal compositional reversal that is characteristic of layered intrusions (Latypov et al., 2011). Overlying the contact is a 1–2 m thick zone consisting of hybrid, possibly contaminated gabbroic rocks (~10% MgO). A rock chip collected ~2 m

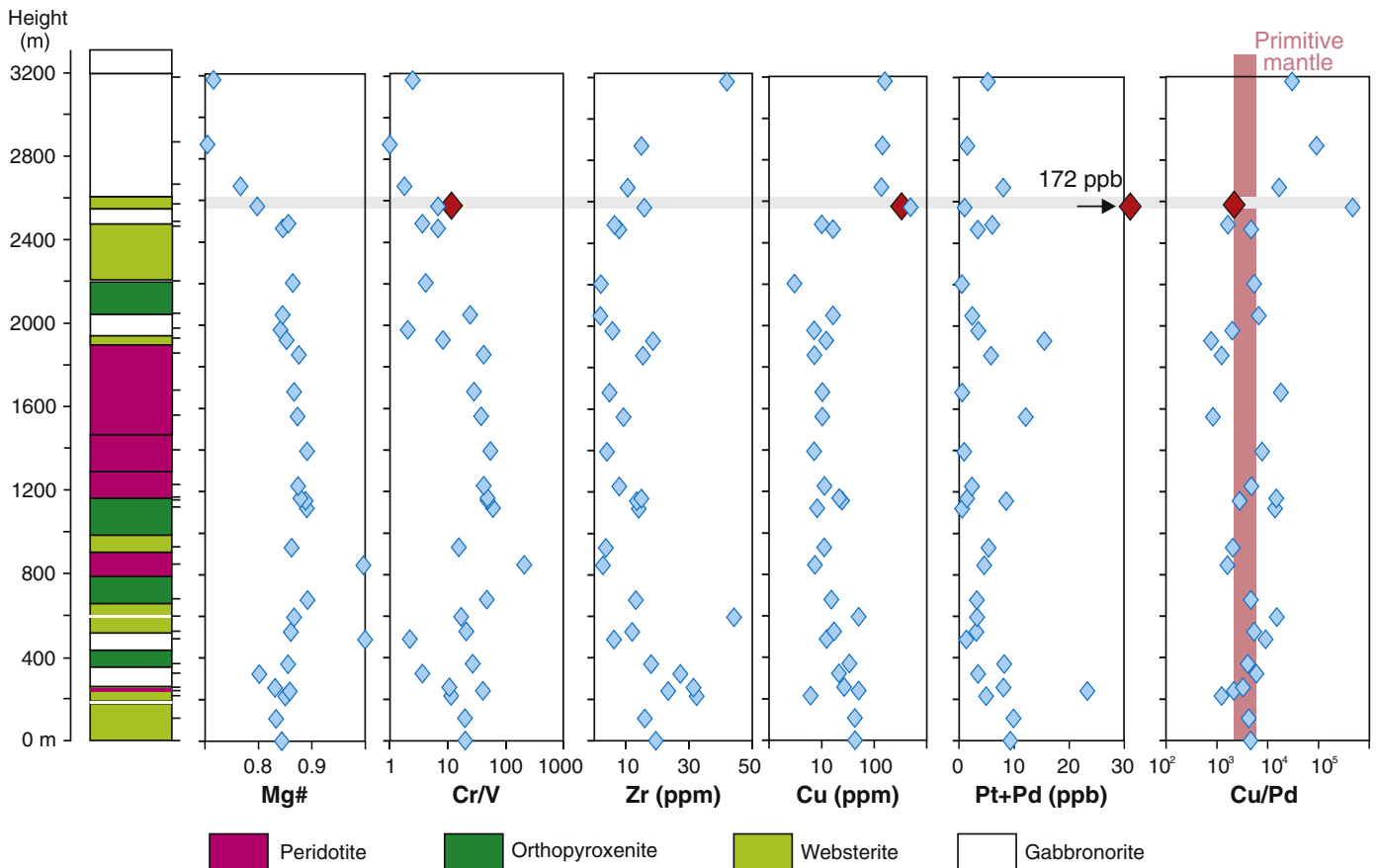


**Fig. 5.** Compositional variation with stratigraphic height in the Pirntirri Mulari intrusion. Red diamonds indicate the platinum-group element – rich sample analysed by Redstone Resources Ltd, and horizontal shaded bar indicates postulated position of platinum-group element reef. Range of primitive mantle composition (for Cu/Pd) is based on Barnes and Maier (1999) and Becker et al. (2006). Figure from Maier et al. (2014).



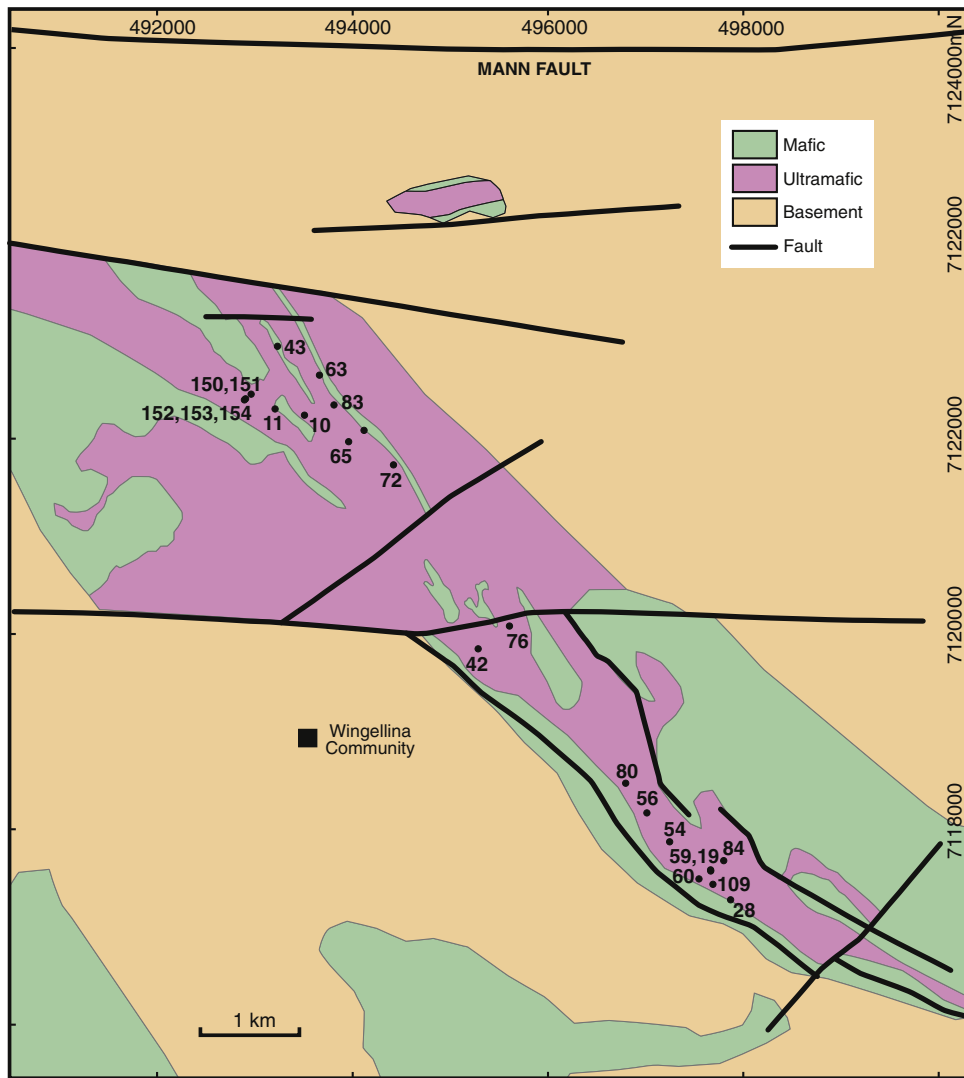


**Fig. 6.** Simplified geological map of Wingellina Hills intrusion, showing location of boreholes where platinum-group element mineralization has been intersected. Figure provided by Metals X Ltd, with permission. Figure from Maier et al. (2014).

above the contact consists of medium-grained, moderately deformed olivine gabbronorite, implying relatively insignificant tectonism of the contact zone (R Coles, 2013, written comm., 27 May).

In the next 300 m of the drill core, basal olivine gabbronorite is first overlain by pyroxenite and then by progressively more magnesian harzburgite. This, in turn, is followed by peridotite and wehrlite and then by about 20 m of websterite and >40 m of olivine gabbronorite. The contacts between rock types can be either sharp or gradational. Within the websterite occurs a PGE reef (described below) that has been identified along a strike length of 2–3 km (Fig. 6). The remainder of the intrusion consists of layers of peridotite, wehrlite, pyroxenite, and olivine gabbronorite, described in more detail in Ballhaus and Glikson (1989).

The compositional variation in the interval hosting the PGE reef is shown for borehole WPRCO-064 (Fig. 7). The contact between websterite and wehrlite is sharp, reflected by a marked decrease in MgO and an increase in Cr concentration. Platinum-group element concentrations increase through the websterite layer to a maximum of 2 ppm Pt + Pd + Au, at a level about 5–7 m beneath the top of the layer. The peak grades occur over a 1-m interval, and grades in excess of 1 ppm PGE occur over 3–5 m. Above the reef, the concentrations of the PGE decrease relatively rapidly over a height of a few metres. Gold and Cu concentrations remain relatively low (<5 ppb Au, <10 ppm

Cu) throughout the PGE-enriched zone, but peak just above the PGE reef, with up to 330 ppb Au in a 1-m interval, and up to 400 ppm Cu in rocks located a further 2 m above the Au peak. Gold and Cu concentrations then decrease with further stratigraphic height, although at a slower rate than the PGE levels. Similar metal distribution patterns have been observed in several other layered intrusions (e.g., the c. 2.58 Ga Great Dyke, Wilson et al., 1989; the c. 2.925 Ga Munni Munni intrusion, Barnes, 1993; and the c. 3.03 Ga Stella intrusion, Maier et al., 2013b), where they were referred to as 'offset patterns' (Barnes, 1993). In comparison to the Bushveld PGE reefs (~1–2% S), the PGE reefs at Wingellina Hills are relatively sulfur-poor (mostly <500 ppm S), possibly due to metamorphic devolatilization. This renders the reefs nearly invisible in hand specimen.

The thickness and grade of the PGE reef shows considerable variation along-strike. In two of the three analysed boreholes (WPRCO-064 and WPRCO-083) concentrations of >500 ppb PGE occur over a thickness of 8 m. The bulk concentrations of PGE + Au normalized to a width of 1 m are similar in the two holes (10.6 ppm in WPRCO-064, 9.6 ppm in WPRCO-083). Borehole WPRCO-043 contains >100 ppb PGE + Au over 12 m, and total PGE + Au contents of 5.5 ppm normalized to 1 m, lower by about 40% than in the two other holes. This is unlikely to be the result of alteration, but implies significant variation in PGE grade of the reef along strike. Notably, the bulk PGE contents normalized to a width of

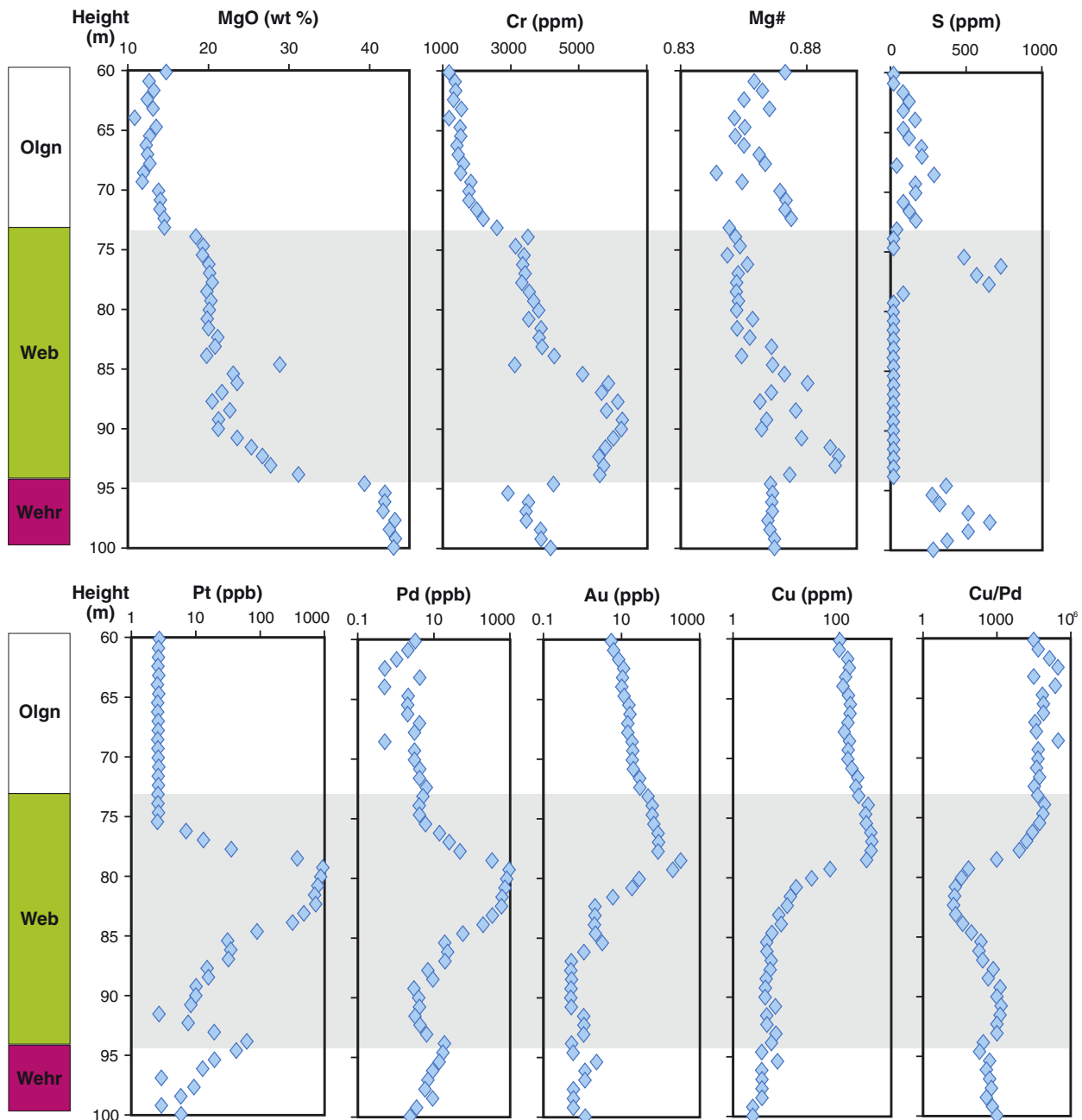


Fig. 7. Log of percussion drillhole WPRCD0-064, Wingellina Hills intrusion (Web = websterite, Wehr = wehrilite). From Maier et al. (2014).

1 m of the reef interval (at least in holes WPRCD0-064 and WPRCD0-083) are broadly similar to the PGE contents of the combined Merensky Reef and UG2 chromitite of the Bushveld Complex. However, the Bushveld reefs are much narrower and thus more economic to mine.

The Wingellina Hills laterite consists of yellow-brown to dark brown ochre material composed of goethite, manganese oxides, gibbsite, and kaolinite produced by weathering of peridotite. This constitutes the Wingellina nickel laterite deposit, discovered by INCO in 1956 (187 Mt at about 1% Ni and 0.08% Co; > 167 Mt is classified as probable mining reserve; Metals X Ltd, 2013). Limonitic ochre is also present at Claude Hills (4.5 Mt at 1.5% Ni; Goode, 2002), in the Pirntirri Mulari intrusion, and in the southeastern part of the Bell Rock intrusion where excavations revealed laterite, ochre, and chalcadonic veins above a zone of saprolite (Howard et al., 2011b). The laterites formed by selective leaching of SiO<sub>2</sub> and MgO, resulting in residual concentration of alumina, iron oxides,

and nickel, developed particularly prominently along shear zones. The ore is exposed at surface and has an average thickness of 80 m (maximum 200 m). The deposit has a high aspect- and very low strip ratio. It is locally cut by semiprecious, pale green chrysoprase mined artisanally since the 1960s, particularly in the Kalka area (Goode, 2002). The lateritic profiles may have some potential for scandium deposits, particularly where the parent rock consisted of clinopyroxenite, but to our knowledge, no relevant investigations have so far been conducted.

### 6.2.3. The Wart

The Wart is a relatively small mafic–ultramafic body, located about 20 km south of the community of Wingellina. The main block of the intrusion measures about 5 km × 2 km striking about 130° and dipping steeply at 80–90° to the southwest. Several smaller mafic slivers occur to the northwest of the main body. The stratigraphic thickness of the

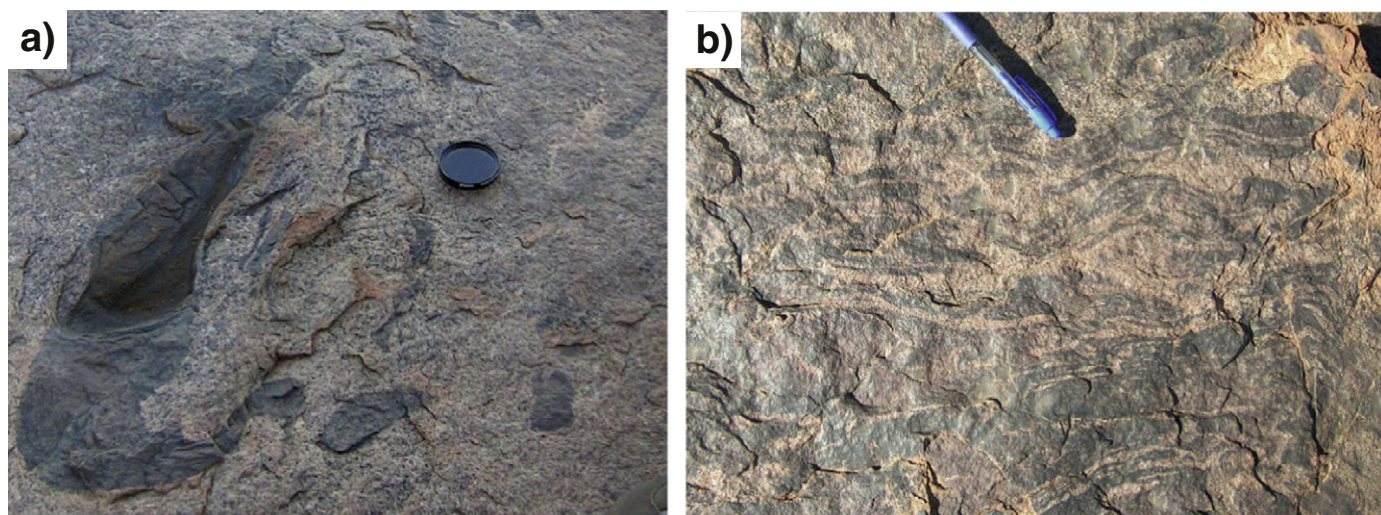


Fig. 8. a, b) Examples of mingling textures between G2 gabbro and granite in the West Hinckley Range. Figure from Maier et al. (2014).

body is ~1–2 km. Ballhaus and Glikson (1995), who studied the Wart in some detail suggested that it represents the lower portion of the Bell Rock intrusion.

The Wart shares certain lithological and compositional characteristics with Pirntirri Mulari. Both contain layers of medium-grained mesocumulate wehrlite–peridotite within a package of adcumulates and mesocumulates of clinopyroxenite and melagabbronorite. Many of the ultramafic layers have sharp contacts and have been interpreted as sills (Ballhaus and Glikson, 1995). We collected only a small number of gabbroic and ultramafic samples because the body is culturally sensitive. However, abundant mineral compositional data are given in Ballhaus and Glikson (1995).

### 6.3. Predominantly mafic intrusions

#### 6.3.1. Latitude Hill–Michael Hills

Latitude Hill is located 5–10 km to the east of The Wart and the Bell Rock intrusions (Fig. 2). Ballhaus and Glikson (1995) proposed that it may be a folded segment of the 8000 m thick Michael Hills gabbro, whereas Pascoe (2012) suggested that Latitude Hill is in faulted contact with Bell Rock. Latitude Hill has an intrusive contact with granulite analogous to Wingellina Hills and The Wart (Ballhaus and Glikson, 1995; present work). It contains numerous layers and lenses of olivine gabbronorite and olivine pyroxenite, as well as rare peridotite, but the dip direction of the layers remains uncertain.

#### 6.3.2. Morgan Range

The Morgan Range is located ~10 km north of Blackstone Community (Fig. 2). It measures approximately 10 km × 5 km (~50 km<sup>2</sup>) in size, striking broadly 120° and with a stratigraphic thickness of >1 km. The intrusion consists mostly of relatively unaltered olivine gabbronorites and troctolites that display modal layering on a scale of centimetres to metres. It forms a boat-shaped structure with steep dips (up to 80°) to the interior, except for the centre where the dip is sub-horizontal. The syncline plunges at a relatively shallow angle towards the southeast and compositional data suggest that the intrusion is not overturned.

At the northeastern tip of the intrusion is a relatively small (~300 m × 300 m) interlayered mafic–ultramafic block consisting of dunite, troctolite and melagabbronorite. The rocks strike ~100° and dip steeply (80°) to the north. They show certain compositional similarities to Wingellina Hills and Pirntirri Mulari, but because the contact with the main Morgan Range is concealed by regolith it is presently unclear whether this segment forms an integral part of the Morgan Range

intrusion, or whether it is a fragment of another intrusion that was tectonically adjoined to the Morgan Range.

#### 6.3.3. Hinckley Range

This is a large (~30 km × 10 km), highly deformed, relatively poorly layered body that has a stratigraphic thickness of about 5800 m, strikes about 100°, and dips steeply to the north at 70–80°. The rocks consist of (olivine) gabbros, troctolites, and microgabbros, with a few layers or lenses of anorthosite, and minor pyroxenite. Abundant pseudotachylites are related to the Petermann Orogeny. Many of our samples have relatively high concentrations of K<sub>2</sub>O and incompatible trace elements, suggesting that the mafic magma assimilated, or mixed with, a granitic component. Our most primitive samples were collected at the southern edge of the intrusion, suggesting that the intrusion youngs towards the northeast (cf Ballhaus and Glikson, 1995).

Where the Hinckley Range intrusion is in contact with the West Hinckley Range intrusion (MGA 472843E 7118953 N), mingling textures between gabbro and granite are prominent. These have been described in Howard et al. (2011b) and Maier et al. (2014), from whom the following description is taken. The gabbro belongs to the unlayered G2 variety which tends to crosscut, engulf, and post-date the layered G1 intrusions. The G2 gabbros locally form agmatites or injection migmatites (Fig. 8), and angular blocks engulfed by granite. Brittle fractures in gabbro may be infilled by granite veins. This indicates that the granite has intruded partially solidified gabbro. Contacts between the felsic and mafic portions may also be cusped, indicating that the mafic component behaved in a ductile manner in the presence of the felsic material. Similar relationships occur some 20 km to the northwest, at Amy Giles Hill (Fig. 2). A leucogranite showing well-developed comingling textures with gabbro (Howard et al., 2006a) has been dated at 1074 ± 3 Ma (GSWA 174589; Bodorkos and Wingate, 2008).

In the West Hinckley Range, mingled gabbro forms a kilometre-scale fold with a steep northwest-trending axial plane that has been intruded by syndeformational leucogranite. A strong ‘gneissic’ fabric has locally formed in mixed or agmatitic rocks as the axial planar fabric continued to develop, and this has been again engulfed within subsequent injections of leucogranite. A sample of undeformed leucogranite from within one of these axial planar zones, approximately 2 km south of the mingled gabbro–granite described above, yielded a crystallization date of 1075 ± 7 Ma (GSWA 174761; Kirkland et al., 2008e). Syn-mylonitic leucogranite has also pooled into boudin necks in a northwest-trending mylonite directly south of Charnockite Flats (~2.5 km northwest of the West Hinckley Range intrusion), and has been dated at 1075 ± 2 Ma (GSWA 185509; Kirkland et al., 2008f). The combined

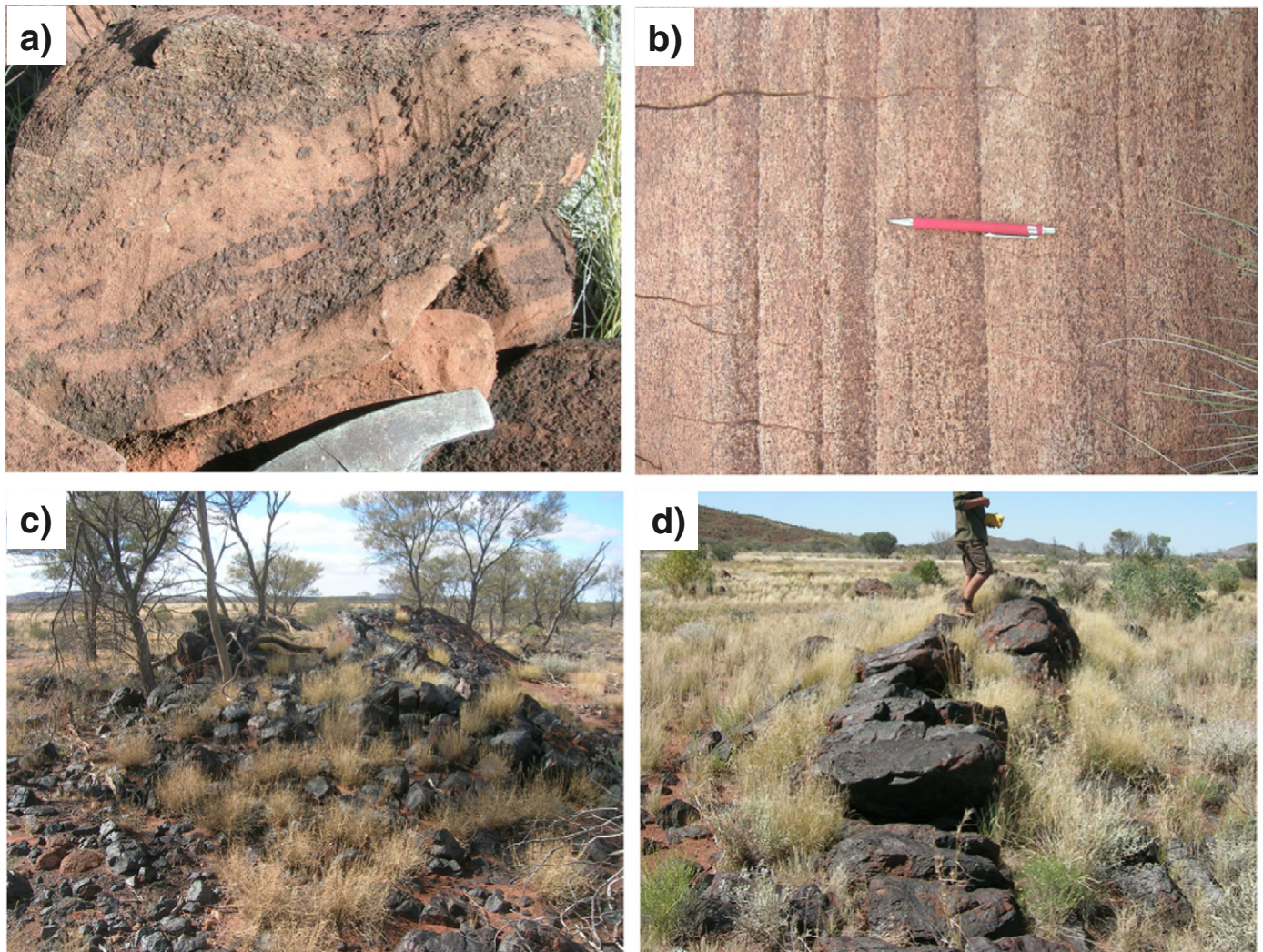


**Fig. 9.** Field photographs of samples from the Lehman Hills, Jameson and Blackstone intrusions: a) banded horizon containing schlieren, lenses and fragments of fine-grained gabbronorite, and medium- to coarse-grained pyroxenite (Lehman Hills, near GSWA 189310); b) modally graded layering in olivine gabbronorite at Jameson Range (MGA 363526E 7149428N); c) basal magnetite layer, Jameson Range; note shallow dip of layer to the right (locality GSWA 194642); d) steeply south-dipping magnetite layer, southern edge of Blackstone Range (GSWA 194679).

Adapted from Maier et al. (2014).

data define a very narrow period of intrusion of massive G2 gabbro and multi-phase intrusion of leucogranites (1078–1074 Ma), northwest-directed folding, and northwest-trending shearing. The relationships between gabbro and granite in the Hinckley Range intrusion confirm earlier suggestions by Clarke et al. (1995b) that substantial deformation occurred during the Giles Event.

#### 6.3.4. Murray Range

The gabbroic Murray Range comprises two distinct segments, (i) a layered portion of >25 km<sup>2</sup> consisting of gabbronorite or olivine gabbronorite, with the most primitive rocks occurring in the centre of the intrusion, and (ii) extensive areas covered by massive gabbro, particularly to the east and northeast of Pirntirri Mulari. The strike of the layering is mostly 50–70°, and the dip is sub-vertical. The intrusion contains abundant stratiform layers and lenses of microgabbro and cross-bedded medium-grained gabbronorites. Due to its location at the contact between the Tjuni Purlka and Walpa Pulka Zones the intrusion was tectonically dismembered, obscuring the true stratigraphic thickness and structure of the intrusion. Like the Hinckley Range, the Murray Range is one of the G1 intrusions that was substantially intruded by G2 gabbro, consistent with the model that during the emplacement of the G2 gabbros, the contact between the Tjuni Purlka and Walpa Pulka

Zones was a syn-magmatic shear zone (Evins et al., 2010a,b). It is thus not surprising that deformation and alteration are commonly more pronounced than in the other Giles intrusions.

#### 6.3.5. Cavenagh Range

The Cavenagh Range remains one of the least known amongst the Giles intrusions because access to it is restricted on cultural grounds. The intrusion is located 10 km south of the Blackstone Range (Fig. 2) and is defined by several circular remanent magnetic highs occurring over an area of approximately 22 km × 18 km. The southern portion forms a syncline with a stratigraphic thickness of about 1 km. It consists predominantly of olivine gabbronorites, olivine gabbros, troctolites, and norites. Websterites, anorthosites and microgabbros form bands and discontinuous pods, schlieren, and autoliths. Xenoliths of basement gneiss have been encountered near the southeastern edge. An east-trending fault separates the southern segment from the northern portion of the intrusion which dips at about 15–30° to the northeast and has a stratigraphic thickness of about 2–4 km (barring structural duplication). It consists dominantly of poorly layered olivine gabbronorite, troctolite, and magnetite-bearing olivine gabbronorite.

Layering in the Cavenagh intrusion is defined predominantly by modal variation between olivine, pyroxene, and plagioclase. Boundaries

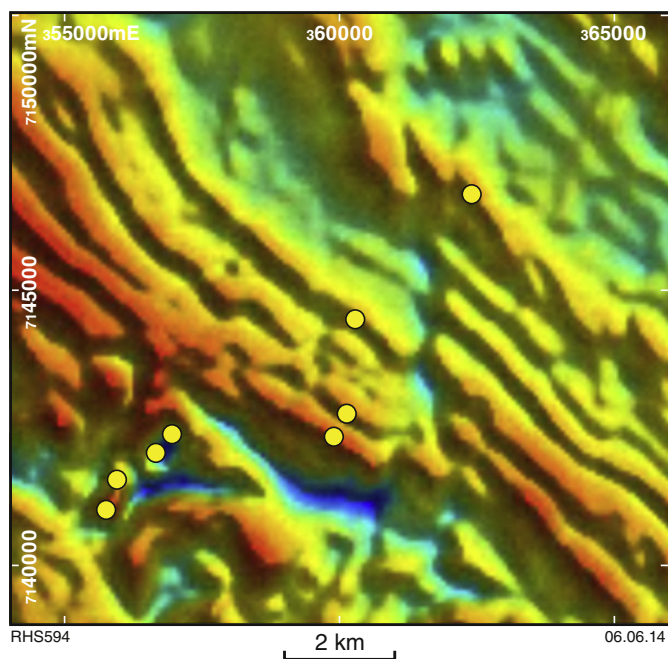


**Fig. 10.** Aeromagnetic total magnetic intensity (TMI) image of the area to the northwest of Jameson, showing interpreted trend of magnetite layers (aeromagnetic highs) within the Jameson intrusion. Yellow circles are GSWA sample sites. Figure from Maier et al. (2014).

between layers are mostly gradational, but pyroxenites, anorthosites, and many microgabbros tend to have sharp contacts. The latter rocks also tend to form lenses, schlieren, and fragments within gabbro and troctolite.

The southern to central portion of the Cavenagh intrusion is the least chemically evolved. The northern portion shows a subtle trend towards more differentiated compositions with height. Simultaneously, the concentrations of PGE increase, reaching 80–100 ppb PGE in two samples.

The microgabbros are interlayered with medium-grained gabbro and may contain autoliths of anorthosite and thin bands, irregular clasts, and circular concretions of granular websterite and clinopyroxene adcumulate. These field relationships suggest that the microgabbros and the associated medium-grained rocks intruded contemporaneously. The microgabbros tend to have equigranular textures with 120° grain boundaries. In places, olivine and pyroxene grains may form strings oriented in a radial configuration that are here interpreted to have resulted from crystal growth in a flowing, supercooled magma. Large olivine oikocrysts can form wispy crystals that are surrounded by rims of anorthosite. The latter may have formed when rapid crystallization due to supercooling or degassing led to depletion in the olivine component within a boundary layer surrounding the growing crystals. The microgabbros may also contain clinopyroxene oikocrysts with abundant inclusions of irregular and rounded exsolved oxide grains.

The microgabbros have variable compositions, broadly overlapping with the medium grained host rocks. Many of the samples contain a cumulus component, as indicated by whole-rock chromium concentrations of up to 1900 ppm, positive strontium anomalies on multi-element variation diagrams, and depleted incompatible trace element levels (e.g., <5 ppm Zr). Microgabbros in the Giles intrusions and elsewhere were previously explained by intraplutonic quenching (Ballhaus and Glikson, 1989; Tegner et al., 1993).

### 6.3.6. Lehmann Hills, Mt Muir, and other small intrusions north of the Blackstone and Wingellina Communities

The intrusions outcrop over relatively small areas and consist of gabbro, olivine gabbro and troctolite (Fig. 9a). The rocks may have a distinct flow structure, containing elongated lenses

and schlieren of anorthosite in pyroxenite, and autoliths of pyroxenite within anorthosite. At Lehmann Hills, sulfides (up to 1% combined pyrrhotite and chalcopyrite) are relatively abundant.

A number of small mafic bodies occur up to 20 km to the north of the Hinckley Range, in the Mt Gosse–Mt Daisy Bates area (termed ‘Northeast’ in Table 1, supplementary data). These bodies consist of metagabbros and metagabbro-norites. They tend to show partial granoblastic textures, with garnet forming fine-grained rims around pyroxene and magnetite, or more rarely porphyroblasts. Pyroxene is commonly replaced by hornblende, and biotite is also common.

### 6.3.7. Mantamaru

Mantamaru is the Ngaanyatjarra name for the Community of Jameson. The intrusion forms one of the world’s largest layered igneous bodies, with an original size of at least 3400 km<sup>2</sup>. This body was dismembered during the Petermann orogeny resulting in the Jameson–Finlayson, Blackstone and Bell Rock ranges.

**6.3.7.1. Jameson–Finlayson Range.** The Jameson–Finlayson Range extends for 66 km along a strike of ~120° and is ~30 km wide (Fig. 2). Layering is in normal orientation and dips at about 20° to 30° to the southwest, implying a stratigraphic thickness of up to about 10 km. Several layer-parallel mylonitic zones occurring near the base of the intrusion could account for limited structural repetition, but we argue that this does not significantly affect the overall thickness estimates.

The bottom and top contacts of the intrusion are not exposed. At the base is magnetite–ilmenite-bearing lherzolite; the rocks contain 20–50 vol.% opaques that have estimated V<sub>2</sub>O<sub>5</sub> contents of about 1.4 wt.% (Daniels, 1974). This is overlain by rhythmically layered troctolite and olivine gabbro (Fig. 9b). At the top of the intrusion, in the southwest, there is a layered succession of troctolite, olivine gabbro, and olivine gabbro, containing at least 11 major titaniferous magnetite seams (Fig. 9c). However, due to poor outcrop, the thickness and contact relationships of most of the seams remain poorly known.

The magnetite seams mostly form bands of rubble. They appear to be separated by silicate intervals several hundreds of metres thick (Fig. 10). All layers that have been sampled consist of massive iron oxide, with <5% silicates. Grain sizes are relatively coarse (≤3 mm), possibly reflecting sintering (Reynolds, 1985). The main minerals are magnetite, granular ilmenite, fine ilmenite lamellae, abundant hematite replacement patches and lamellae (≤20 vol.%), as well as goethite. Layers enriched in apatite were not encountered.

The most reliable observations have been made on the basal magnetite layer. It has been traced along a strike of about 19 km forming an aeromagnetic anomaly with sporadic broken outcrop (Fig. 10). The seam may reach a thickness of 50 m, with up to three sub-seams locally developed. Whether the sub-seams formed due to primary magmatic processes or structural duplication is uncertain. The contacts of the seam with the magnetite-bearing leucotroctolite and anorthosite hanging and footwall are sharp. The host rocks show evidence for deformation. The mineralogy of the seam consists of magnetite and granular ilmenite, as well as fine ilmenite lamellae within magnetite. Hematite and goethite replacement is locally abundant.

Concentrations of Pt, Pd, and Au have been analysed in 39 samples of the layer along strike and in 3 traverses across the layer (Traka Resources, unpublished report). In addition, we analysed three samples of the layer for the complete PGE spectrum (Table 1, supplementary data). The PGE concentrations reach approximately 2 ppm Pt + Pd + Au (Fig. 11). The seam is thus markedly PGE enriched relative to the Bushveld Main Magnetite Layer (Fig. 12), but has significantly lower PGE contents than the main PGE mineralized magnetite layer of the Stella intrusion of South Africa (Maier et al., 2003). The metal concentration patterns of the Jameson seam show depletion in Os–Ir–Ru relative to Rh–Pt–Pd, characteristic of evolved magmatic rocks (Fig. 12). The layer has relatively constant vanadium concentrations throughout (up to 7400 ppm V,

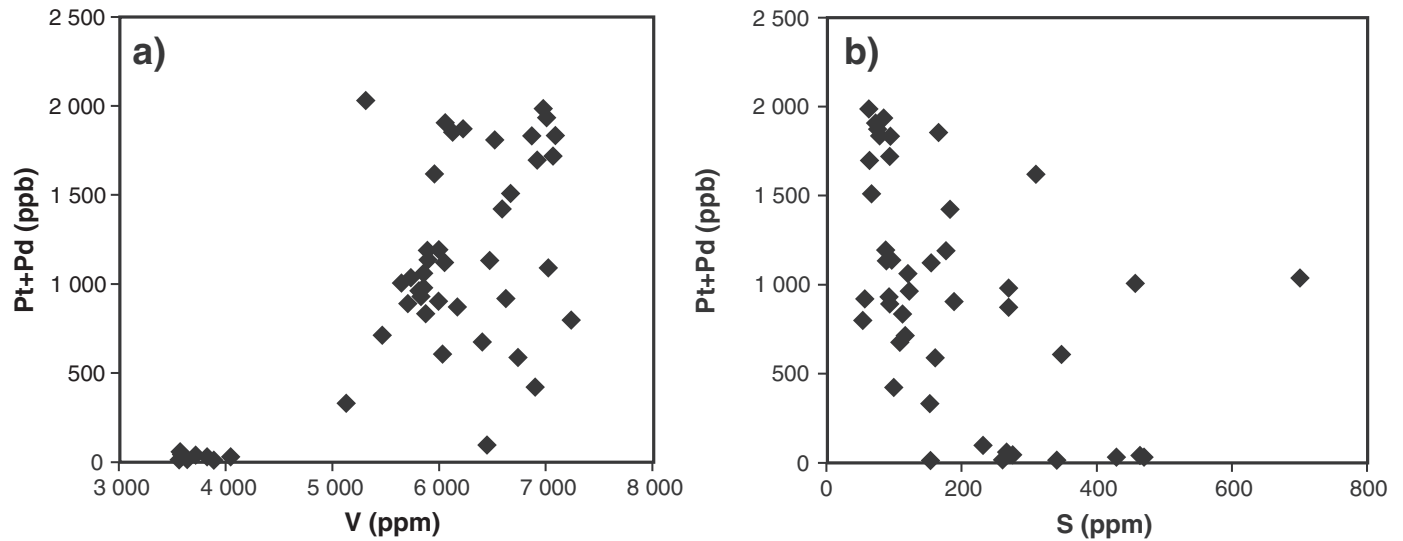


**Fig. 11.** Composition of basal magnetite layer within the Jameson intrusion, based on 32 samples collected along strike by Traka Resources (Traka Resources Ltd, 2011, written comm., 21 October): a) Pt + Pd vs V; b) Pt + Pd vs S. Adapted from Maier et al. (2014).

1.35 wt.%  $V_2O_5$ ; Fig. 11), whereas the PGE tend to be markedly elevated at the base. Sulfur concentrations are mostly 100–150 ppm, locally reaching 700 ppm. Sulfur concentrations do not correlate with Cu and PGE (Fig. 11), suggesting some of the sulfur could have been lost in response to equilibration of sulfide with magnetite (Naldrett and Lehmann, 1988), or in response to low-grade metamorphic devolatilisation. The average Pd/Ir ratio is relatively low (34), consistent with a magmatic origin of the PGE mineralization. Platinum/Pd ratios are above unity, analogous to other PGE mineralized magnetites and magnetite gabbros (see Maier, 2005 and references therein).

Magnetite layers 2, 3, 6 and 7 are not exposed, but their presence is suggested by prominent magnetic anomalies (Fig. 10). Layers 4 and 5 are pervasively altered to goethite and hematite, although they also contain abundant granular ilmenite. Layer 8 may be a plug-like body. Layer 11 is partly exposed and forms a massive, well-layered, possibly rotated layer dipping about  $30^\circ$  to the southwest. The compositional variation in the upper seams is poorly understood, although it is evident that the vanadium and noble metal contents are much lower than in layer 1, whereas iron, chromium, and phosphorus concentrations increase with height (Table 2, supplementary data).

**6.3.7.2. Blackstone Range.** The body is ~50 km long and up to 5 km wide. It strikes about  $90^\circ$  and layering dips at between  $70$  and  $80^\circ$  to the south and is not overturned. The exposed stratigraphic thickness is about 4 km. The body is interpreted to be the exposed northern limb of an upright west-trending structural syncline (the Blackstone Syncline). Relics of its north-dipping southern limb are sporadically exposed 20 km to the south, directly north of the Cavenagh intrusion. The size of the combined body is about 1400 km<sup>2</sup>. It is conformably overlain by felsic volcanic rocks of the Tollu Group (Bentley Supergroup).

The rocks are relatively unaltered and undeformed. Layering can be pronounced where defined by thin (centimetre-scale) magnetite layers. Most of the rocks are (olivine) gabbro-norites and troctolites, each constituting approximately 50% of the total mass of the intrusion. Troctolitic rocks occupy the central and southern portions of the intrusion. The troctolites contain less than 20% olivine, with the exception of two relatively olivine-rich layers (40% olivine, 100–150 m thickness) that can be traced along much of the intrusion, one in the centre (sample GSWA 155669) and another near the southern edge. These two layers are also present in the Bell Rock intrusion where they contain up to 80% olivine. The occurrence of these layers in both intrusions is consistent with an interpretation whereby the two intrusions are fragments of a

large, tectonically dismembered proto intrusion (Nesbitt and Talbot, 1966; Glikson, 1995). At the southern margin of the intrusion occurs a ~1 m-thick magnetite layer that contains 1.5%  $V_2O_5$ . Relatively elevated Cu concentrations of up to 250 ppm suggest the presence of minor sulfides, common to all magnetite-rich rocks in the upper portions of the Blackstone intrusion. Whether this layer can be correlated to magnetite layer 1 in the Jameson–Finlayson intrusion is uncertain, as it is highly PGE depleted whereas the Jameson basal layer is relatively PGE rich.

**6.3.7.3. Bell Rock Range.** This body extends for ~50 km along a strike of ~ $120^\circ$ . The exposed width is ~5–6 km, and the rocks dip at  $70^\circ$  to the southwest. Field exposures of graded and cross-bedded layers, as well as whole rock and mineral compositional data indicate younging of the intrusion to the southwest. A detailed compositional study of the Bell Rock intrusion was conducted by Ballhaus and Glikson (1995), from which some of the following information is taken. Our own sample base is relatively small, comprising 14 samples taken across the body.

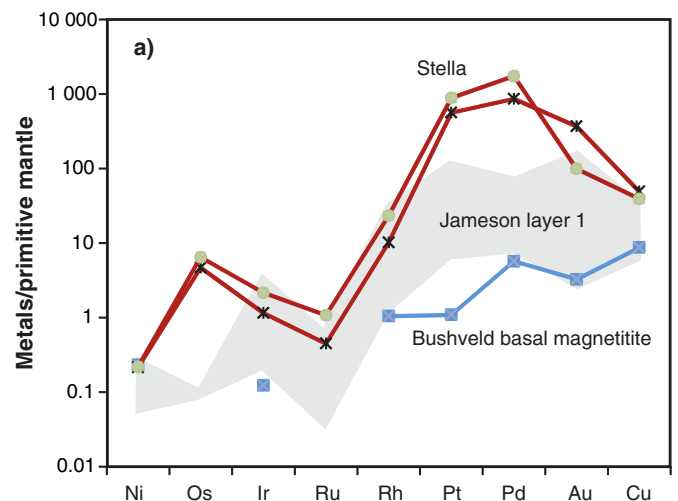


**Fig. 12.** Metal patterns of the basal magnetite layer of the Jameson intrusion (shaded field), compared to basal magnetite layer in Upper Zone of Bushveld Complex (blue line) and PGE-rich magnetite layers of Stella intrusion, South Africa (red lines). Adapted from Maier et al. (2014).

The exposed stratigraphic thickness is about 3800 m, but since the contacts of the body are not exposed, this is a minimum estimate. The top of the intrusion is likely in contact with volcanic rocks of the Bentley Supergroup; this implies that either the intrusion has been deeply eroded after its emplacement or the top contact is faulted. The basal rocks consist of medium- to coarse-grained troctolites and gabbros, whereas the central portion consists of magnetite-bearing troctolite and the upper portion contains centimetre- to tens of centimetre-thick magnetite seams, dunitic layers, numerous microgabbro sills, and a few anorthositic layers. Modal cyclicity occurs on a centimetre to metre scale. A recent drillhole collared at the western edge of the Latitude Hill intrusion with a dip of 70° towards the southwest (MDDH0001, drilled by Anglo American Exploration (Australia) Pty Ltd as part of the Department of Mines and Petroleum's Exploration Incentive Scheme), has intersected deformed magnetite-enriched troctolites that are interpreted to belong to the Bell Rock intrusion (Pascoe, 2012). This suggests that magnetite seams could be present below cover.

### 6.3.8. Alcurra Dolerite suite

The components of the Alcurra Dolerite suite comprise dolerite dykes and sills that constitute the bulk of the 1078–1073 Ma Warakurna Large Igneous Province (Wingate et al., 2004), small basic and intermediate bodies and dykes emplaced near the margins of older G1 layered mafic intrusions, G2 massive gabbro, and comingled gabbro–granite.

Contact relationships constrain the emplacement dates of the Alcurra suite to <1078 Ma, and dating of some of the intrusions indicates that magmatism continued to at least c. 1067 Ma (Howard et al., 2009). However, geochemical data suggest that Alcurra-type rocks were likely formed over a much longer period, including lavas of the Bentley Supergroup until at least 1047 Ma (Howard et al., 2009, 2011a; Smithies et al., 2013). The Alcurra Dolerite suite thus reflects relatively long-lived mantle melting (Smithies et al., 2013).

The c. 1076 Ma mafic to intermediate rocks forming part of the Alcurra Dolerite suite typically consist of fine- to medium-grained olivine gabbro, olivine norite, ferromylonite, and ferrodiorite. The latter rocks have evolved and Fe-rich tholeiitic compositions, resulting in a pronounced aeromagnetic signature and high specific gravity.

Rocks of the Alcurra Dolerite Suite occur throughout the West Musgrave Province, including the Blackstone Syncline, within the marginal zones of the G1 Jameson Range and Murray Range where they intruded along the layer contacts and between the intrusions and their country rocks. The northeast-trending, coarse-grained ferrogabbro dykes that crosscut the G1 Jameson intrusion, and which also occur throughout the northern parts of the COOPER map sheet, used fractures and faults related to the earlier Musgrave Orogeny.

### 6.3.9. Saturn

The Saturn intrusion defines an elliptical aeromagnetic anomaly with a diameter of approximately 10 km, located between the Cavenagh and Blackstone ranges (Figs. 2 and 13). Cross cutting field relationships indicate that Saturn is younger than the Blackstone Range. However, a date of  $1072 \pm 8$  Ma determined by using the U–Pb method on baddeleyite in olivine gabbro (Redstone Resources Ltd, 2008a, 2008b, written comm.) is within error of the c. 1078 to 1075 Ma range for both the G1 and G2 mafic phases of the Giles Event. The concentric magnetite pattern implies zones of magnetite enrichment, but massive magnetite layers have not been found on the surface. Possibly, this is due to the very poor outcrop. The only exposed rocks consist of, medium-grained, leucocratic olivine gabbros, typically containing elevated concentrations of biotite and up to 5% magnetite. The rocks are massive or show flow-banded textures, defined by schlieren of fine-grained gabbro (for example, at the 'Camp' site, Fig. 13).

The rocks have relatively evolved compositions, overlapping with Blackstone and Bell Rock. Samples collected along the Phoebe traverse (Figs. 13, 14) contain up to 6.7% TiO<sub>2</sub> and 800 ppm V, comparable to magnetite gabbros from the Jameson and Blackstone ranges. The rocks

in the centre of the Saturn intrusion are somewhat more primitive than those at the margin, having higher Mg# and lower Ti concentrations (Fig. 14), consistent with a dome-like structure. Sulfide contents are around 1%, higher than in most other Giles intrusions. Copper and PGE concentrations are mostly relatively low, but they increase approximately halfway up the magmatic stratigraphy (Fig. 14). Based on its age, the crosscutting relationships with rocks in the Blackstone syncline, and compositional characteristics such as the enrichment in mica and sulfide, the Saturn intrusion may be of transitional composition between the Alcurra Dolerite Suite and the G1/G2 intrusive phase.

### 6.3.10. Intrusions in the Halleys–Helena–DB Hill area

The mafic rocks to the northeast and south of the Saturn intrusion were explored by Redstone Resources at the Halleys, Halleys NW, Helena, and DB Hill prospects (Report at General Meeting, 2008b; Fig. 13). The intrusion(s) lack the strong remanent magnetic signature of the Cavenagh intrusion and are thus interpreted to be distinct bodies. The crosscutting magnetic patterns suggest that they intruded into the G1 intrusions as well as the volcanic, volcanoclastic, and clastic rocks of the Kunmarnara and lower Tollu Groups.

Most of the rocks are medium-grained, leucocratic ferrogabbros or ferromylonites. They have up to 20% intercumulus or oikocystic magnetite, up to 5% biotite, and several percent sulfide minerals. The rocks tend to be massive, or show a weak, west-trending magmatic foliation. Although whole-rock and mineral compositions are slightly more differentiated than in the upper portions of the Blackstone or Cavenagh intrusions, Cr/V ratios are locally elevated due to chromium enrichment ( $\leq 1.6$  wt.%) within magnetite. The rocks have markedly higher concentrations of mica, sulfide, and incompatible trace elements, and Au/PGE ratios than the Cavenagh and Blackstone intrusions. Instead, the Halleys rocks have distinct chemical and petrographic affinities with the Alcurra Dolerite suite.

Drilling delineated a pipe-like PGE enriched body, with up to 0.33 wt.% Cu and 0.24 ppm PGEs over 74 m, and 0.5 wt.% Cu and 0.53 ppm PGE over 16 m (Redstone Resources Ltd, 2008a, 2008b, comm. at Annual General Meeting, 27 November). The noble metal patterns are less fractionated than in the magnetite seams of the Bushveld Complex or the Stella, Jameson, and Saturn intrusions, having lower PPGE/IPGE ratios. This is consistent with a magmatic origin of the Halleys mineralization.

### 6.3.11. Nebo–Babel

The 1068 ± 4 Ma Nebo–Babel intrusion is located about 25 km south of Jameson Community (Fig. 2). The Nebo–Babel Ni–Cu–PGE deposit was studied in detail by Seat et al. (2007, 2009) and Seat (2008), and the following section has been compiled mostly from their work.

The intrusion has a tubular ('chonolithic') shape traceable for about 5 km and trending north-northeast to east. It is 1 km wide and has a stratigraphic thickness of approximately 0.5 km. The chonolith plunges gently to the west–southwest and dips to the south at about 15°. It is offset by the Jameson Fault, dividing it into 2 portions, the Nebo section in the east and the Babel section in the west. Geochemical data indicate that the body is overturned. It was emplaced along a shearzone in felsic orthogneiss of the Pitjantjatjara Supersuite. The magma flow direction was proposed to have been towards the northeast because some of the units thin in this direction and become progressively more fractionated.

At the stratigraphic base of the intrusion is a breccia zone (MBZ), overlain by a chilled margin (7–9% MgO), variably textured leucogabbro (VLGN), melagabbro (mela-GN) and barren gabbro (BGN), which in the Nebo sector is associated with oxide–apatite gabbro (OAGN). The latter constitutes about 20–30% of the intrusion and is characterized by oxide-rich layers that are 5–30 cm thick, with gradational bases and sharp upper contacts. The Babel segment additionally contains the key Ni–Cu mineralized gabbro unit (MGN) and a 15 m thick massive and coarse-

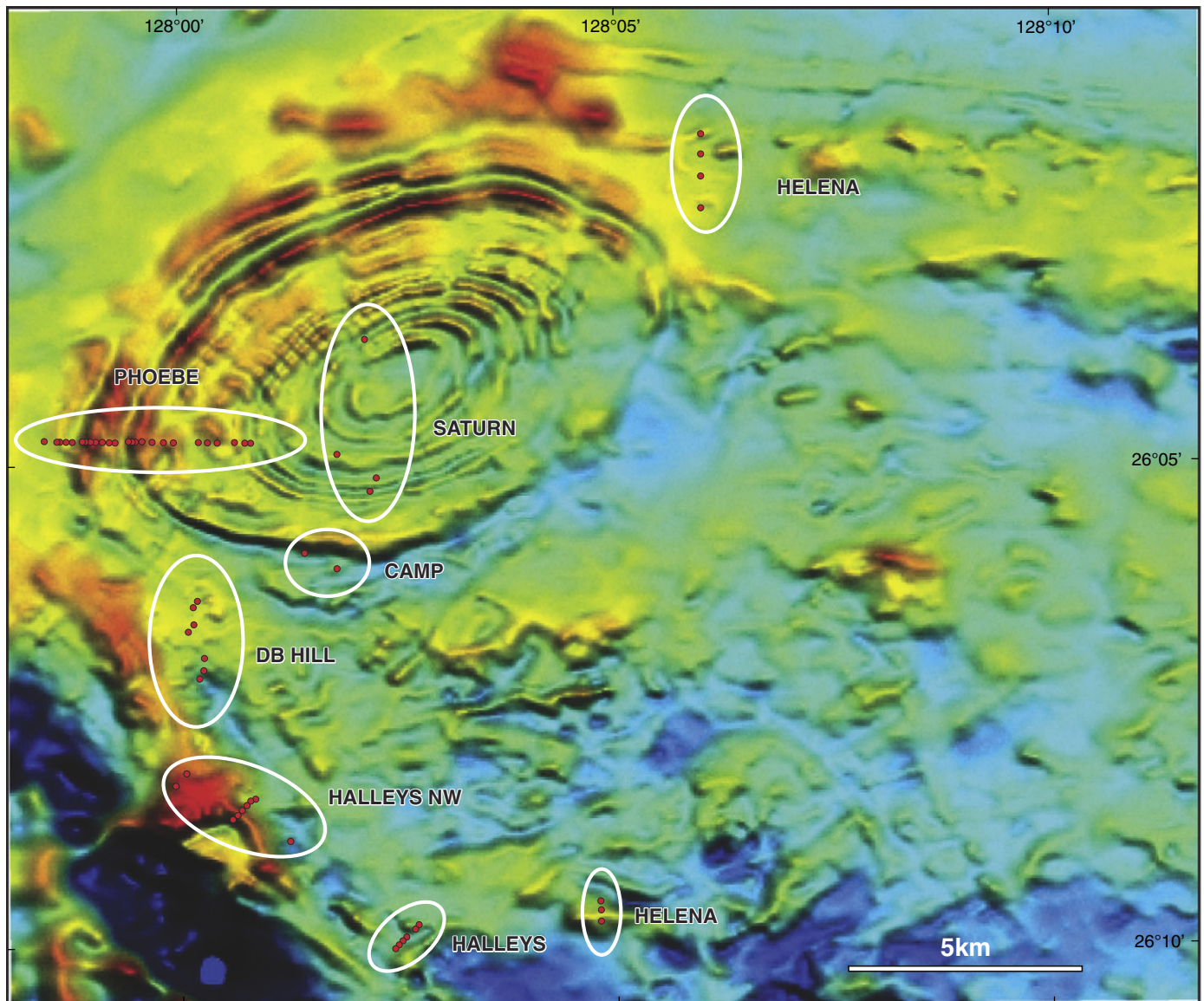


**Fig. 13.** Aeromagnetic image of the Saturn intrusion, between the Cavenagh intrusion (lower left) and the Blackstone intrusion (to the north of the image). Red circles are sampling points for various traverses (named and enclosed in ellipses). Note the concentric pattern defining the Saturn intrusion. Figure from Maier et al. (2014).

grained troctolite unit located between VLGN and BGN in the upper part of the intrusion.

In April 2002, Western Mining Corporation announced a drill intersection of 26 m containing 2.45% Ni, 1.78% Cu, and 0.09% Co at the Nebo–Babel prospect. The resource estimates are 392 Mt at 0.30% Ni and 0.33% Cu, based on 90 drillholes (Seat et al., 2007). The sulfides consist of monoclinic pyrrhotite, pentlandite, chalcopyrite, and pyrite and occur as massive ores with associated sulfide breccias and stringers, and as disseminated ores, typically forming interstitial blebs in the gabbronorite unit (MGN). Sulfur isotopic data show a remarkably narrow range of  $\delta^{34}\text{S}$  values from 0 to +0.8‰. The massive sulfides formed through fractional crystallization of a sulfide liquid, resulting in a cumulate of monosulfide solid solution relatively enriched in Os, Ir, Ru, and Rh and depleted in Pt, Pd, and Au.

#### 6.3.12. Dyke suites

The dyke suites in the west Musgrave Province have been studied by a number of authors, including Nesbitt et al. (1970), Zhao et al. (1994), Clarke et al. (1995b), Glikson et al. (1996), and Scrimgeour and Close

(1999). Howard et al. (2006b) identified seven distinct suites of dykes. The oldest dyke suite (c. 1170 Ma, ~8% MgO) forms part of the Pitjantjatjara Supersuite. Dykes associated with the Giles Event include those belonging to the Alcurra Dolerite suite (6–9% MgO; Zhao et al., 1994; Edgoose et al., 2004) and further include unnamed plagioclase-rich dolerites (~8% MgO) that clearly post-date the G1 intrusions, but may be synchronous with the G2 intrusions. Post-Giles dolerites comprise a suite of unnamed olivine- and plagioclase-porphyratic dykes at c. 1000 Ma (~8% MgO), 825 Ma quartz dolerite dykes of the Gairdner–Willouran LIP (~8% MgO), and c. 800 Ma dykes of the Amata Dolerite (Zhao et al., 1994; Glikson et al., 1996; Wingate et al., 2004). A further suite of dykes (~9.5% MgO) may be broadly coeval with, or younger than, the Gairdner Dyke Swarm.

Godel et al. (2011) distinguished five distinct dyke suites (NB1–5) in the Nebo–Babel area. Types NB1–3 are low-Ti basalts with 5–20% MgO, postulated to be derived from the sub-continental lithospheric mantle (SCLM). Types NB4 and NB5 are high-Ti basalts with 5–14% MgO interpreted to be sourced from a mantle plume. The NB1 type is of approximately similar composition to the plagioclase-phyric dykes of



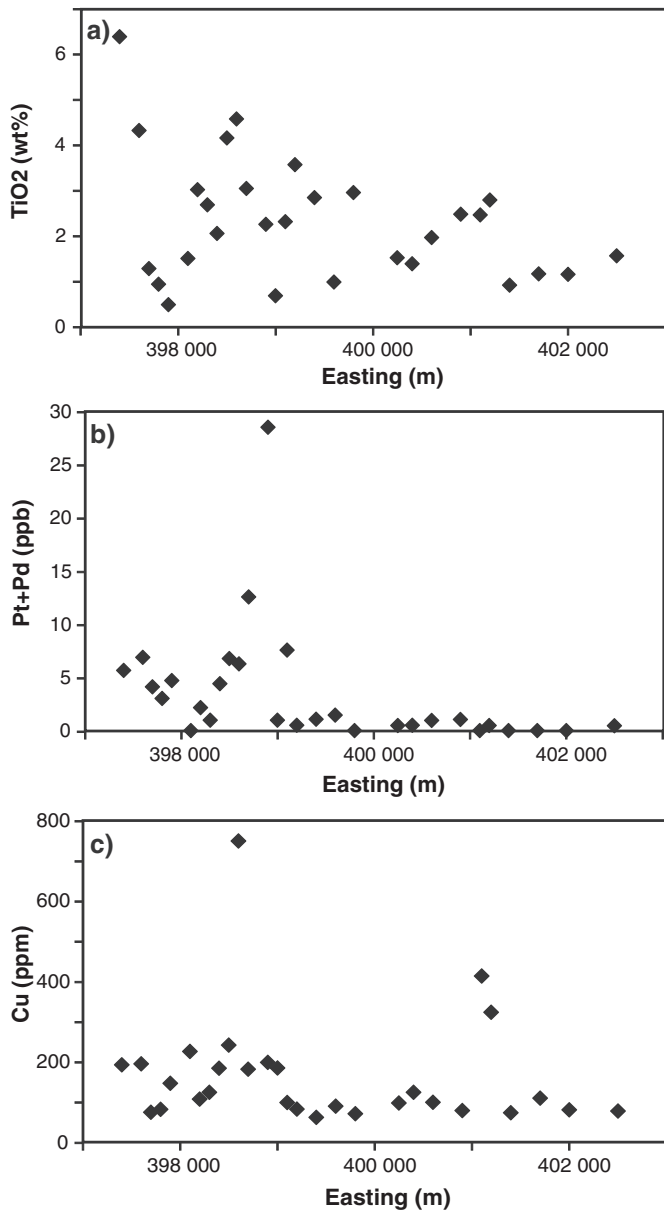


**Fig. 14.** Compositional traverse (west to east) across the Saturn intrusion at Phoebe (see Fig. 13 for sample localities). Note increase in PGE and Cu concentrations approximately halfway along the traverse. Plots of: a) TiO<sub>2</sub>; b) Pt + Pd; c) Cu vs Eastings. Adapted from Maier et al. (2014).

Howard et al. (2006b), containing about 10–13% MgO. NB4 was proposed to represent the Alcurra Dolerite suite.

## 7. Geochemistry of the intrusions

### 7.1. Lithophile elements and Nd–Sr–S isotopes

The concentration of the major elements in the G1 layered intrusions is largely controlled by variation in the proportions of olivine, orthopyroxene, clinopyroxene, plagioclase, and magnetite. The modal proportion of plagioclase in the ultramafic rocks is mostly <10%, resulting in relatively high MgO and FeO contents and low Al<sub>2</sub>O<sub>3</sub> contents (Fig. 15a). Most of the remaining samples collected are gabbro-norites or troctolites with <15% MgO and >10% Al<sub>2</sub>O<sub>3</sub>. Application of the lever rule indicates that the modal proportion of plagioclase in the latter rocks is typically >50%, with the Cavenagh intrusion being least feldspathic (Fig. 15a, b). Titanomagnetite is an important phase

in the Mantamaru, Halleys, and Saturn intrusions, as indicated by high TiO<sub>2</sub> at low MgO and Al<sub>2</sub>O<sub>3</sub> concentrations (Fig. 15b). Elevated K<sub>2</sub>O concentrations in the Hinckley and Murray Range intrusions are likely the result of relatively enhanced crustal contamination (Fig. 15c), whereas the elevated K<sub>2</sub>O levels at the Halleys prospect possibly result from advanced fractionation since the country rocks are K-poor mafic intrusive rocks. Relatively high P<sub>2</sub>O<sub>5</sub> levels at the Halleys prospect and the Saturn, Jameson, and Blackstone intrusions suggest the presence of apatite (Fig. 15d). Relatively P enriched rocks have also been intersected by drilling along the eastern edge of the Bell Rock intrusion (Pascoe, 2012).

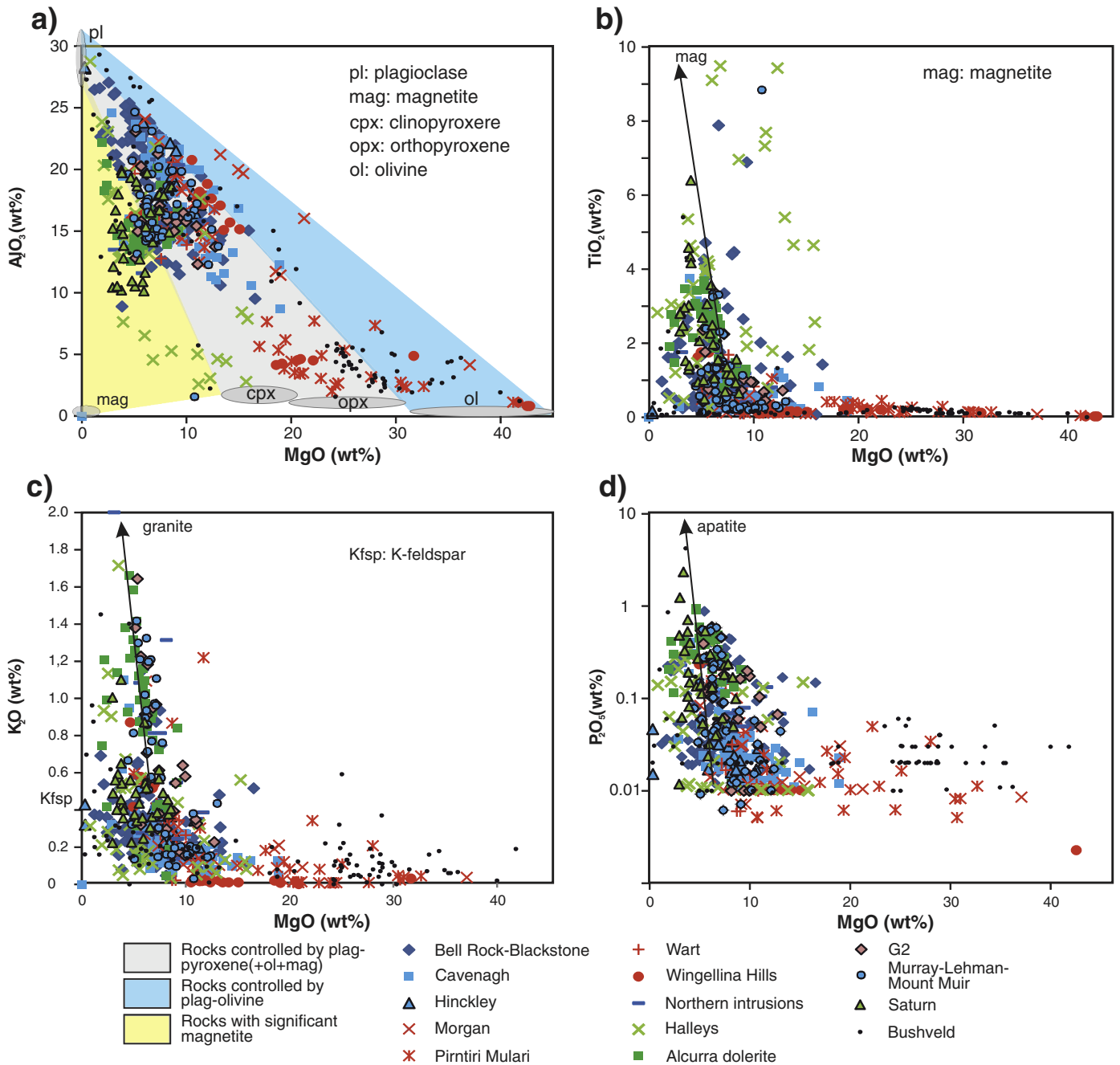
The ultramafic intrusions are characterized by relatively high Cr and Ni contents, controlled mainly by olivine, clinopyroxene, and orthopyroxene (Fig. 16). The basal rocks at Wingellina Hills plot along a trend from olivine to orthopyroxene, reflecting their harzburgitic and olivine-orthopyroxenitic composition. The remainder of the ultramafic rocks at Wingellina Hills and Pirntirri Mulari are wehrlites and websterites. Cumulus chromite is largely confined to Wingellina Hills where Cr contents exceed the levels that can be hosted in pyroxene (Fig. 16a). Most of the gabbroic intrusions contain <1000 ppm Cr, with the exception of samples from the Wingellina Hills and Halleys intrusions. The elevated Cr concentrations at Halleys are the result of abundant Cr-bearing magnetite.

In most intrusions, Ni shows a good positive correlation with MgO (Fig. 16b). Samples with significant amounts of olivine are mostly confined to the Wingellina Hills intrusion which has MgO > 30 wt.% and Ni > 1000 ppm. The trend of the Wingellina Hills samples in Ni–MgO space can be extrapolated to a Ni concentration in olivine of about 2500–3000 ppm, broadly overlapping with measured olivine compositions from Pirntirri Mulari (~3000 ppm Ni). Two ultramafic samples from Pirntirri Mulari and one from the Morgan Range have distinctly higher Ni contents than the other ultramafic rocks. This is possibly a result of alteration, in view of their relatively high loss-on-ignition (LOI) values. The presence of sulfide and magnetite could explain the elevated Ni levels in the Halleys and Blackstone intrusions (up to ~1500 ppm Ni), compared to the other gabbroic–troctolitic intrusions, which tend to contain <500 ppm Ni. Even higher Ni contents occur at the Nebo Babel Ni–Cu sulfide deposit which has a tenor of 5–6% Ni in the sulfides.

The state of differentiation of the intrusions can be compared in a plot of Cr/V ratio vs Mg# (Fig. 17). Wingellina Hills, Pirntirri Mulari, The Wart, and Morgan Range are least evolved, showing some overlap with the Lower Zone of the Bushveld Complex, except that the Bushveld has higher Cr/V ratios due to higher chromite contents. Intrusions with intermediate compositions include Cavenagh, Murray Range, Hinckley Range, the massive G2 gabbros, and the slightly more differentiated Mt. Muir together with the intrusive fragments to the north of Mt. Muir and Hinckley Range ('North' and 'Northeast' in Table 1, supplementary data). The most evolved intrusions are Mantamaru (although Bell Rock contains some relatively unevolved samples), Saturn, Halleys, and dykes belonging to the Alcurra Dolerite suite. However, in the Alcurra Dolerite suite there are also relatively unevolved samples that have up to 9 wt.% MgO.

The mafic intrusions show fractionated lithophile multi-element (spider) patterns, with relative enrichments in the most incompatible elements, but negative Nb anomalies (Maier et al., 2014). Positive Ti anomalies are found at Mantamaru, Halleys, and Lehman Hills and in many samples from Saturn, reflecting the presence of magnetite. The Saturn and Halleys intrusions have distinctly elevated incompatible trace element contents relative to most other intrusions, including Cavenagh and Blackstone, consistent with a distinct magmatic lineage. Notably, the trace element patterns of gabbros from Wingellina Hills are identical to those of Wingellina Hills pyroxenites, indicating crystallization from magmas of broadly similar composition.

Data from sample suites that contain a higher liquid component are plotted in Fig. 18. The Alcurra Dolerite suite (Fig. 18a), G2 gabbros (Fig. 18b), NB1 dykes, and the fine grained marginal rocks from Nebo–Babel show considerable similarity including pronounced negative Nb



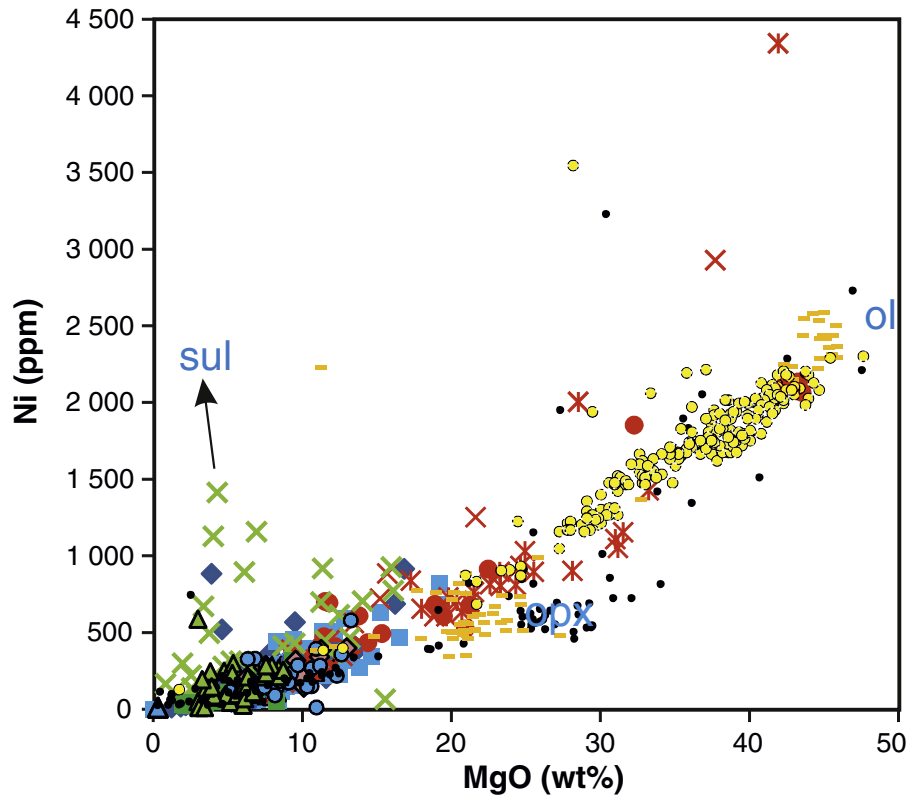
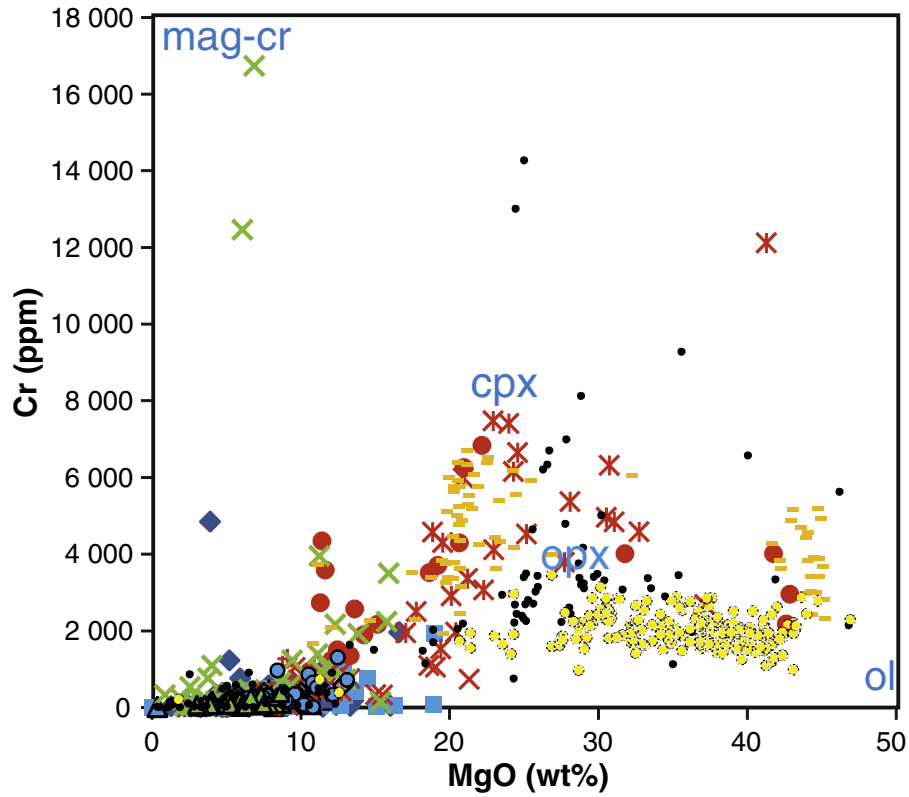
**Fig. 15.** Binary variation diagrams vs MgO of selected major elements in the Giles intrusions: a)  $\text{Al}_2\text{O}_3$ ; b)  $\text{TiO}_2$ ; c)  $\text{K}_2\text{O}$ ; d)  $\text{P}_2\text{O}_5$ . Coloured fields in (a) denote cumulates whose compositions are principally controlled by variation in modal proportions of plagioclase and olivine (blue) and plagioclase + pyroxene (grey). Yellow field indicates rocks that contain significant magnetite. Vectors in b)–d) indicate that some cumulates contain substantial magnetite, apatite, and granite components. 'Northern' intrusions include intrusive fragments to the north of Mt Muir and Hinckley Range.

Figure from Maier et al. (2014).

and Ta anomalies and, in the case of the G2 gabbros and Nebo–Babel chilled margins, negative Ti anomalies. In all suites, the incompatible trace element contents are typically higher than in the G1 intrusions, but the shapes of the multi-element patterns for all mafic intrusives are remarkably similar. Microgabbros from Cavenagh have less fractionated, but more 'spiky' patterns than the other liquid-rich mafic rocks (Fig. 18d). This reflects the elevated cumulate component in most microgabbros.

Mantamaru has systematically higher  $\epsilon\text{Nd}$  (0 to +2) and lower Ce/Nb ratios (mostly 2–7) than the other intrusions (Fig. 19). Some of the least radiogenic Nd isotope compositions occur in the G2 gabbros and the G1 Cavenagh and Morgan Range intrusions ( $\epsilon\text{Nd} = -1$  to  $-4$ , Ce/Nb = 3–13), and in the Kalka intrusion in South Australia (Wade, 2006). Rocks of the Alcurra Dolerite suite have intermediate compositions ( $\epsilon\text{Nd} = -1$  to +2, Ce/Nb ~ 3–5). Most Nebo–Babel samples have compositions overlapping with the Alcurra Dolerite suite ( $\epsilon\text{Nd} = -1.7$  to 0.3,

**Fig. 16.** Rocks of the Giles intrusions plotted into binary variation diagrams vs MgO of: a) Cr; and b) Ni. Approximate compositions of selected silicate and oxide minerals are shown in blue lettering. Mineral abbreviations as for Fig. 15. Figure from Maier et al. (2014).



- |                        |  |   |
|------------------------|--|---|
| ◆ Bell Rock-Blackstone | ◆ G2   | - Wingellina Hills PGE reef horizons (MetalsX data) |
| ■ Cavenagh             | ● Murray-Lehman-Mount Muir                       | ● Bushveld  |
| ▲ Hinckley             | ▲ Saturn   | × Morgan  |
| - Northern intrusions  | ● Wingellina Hills PGE reef horizons (GSWA data) | × Pirntirri Mulari                                  |
| × Halleys              | ● Wingellina Hills basal rocks                   | + Wart  |

Ce/Nb = 5–7, except for the marginal rocks, which show lithological evidence for crustal assimilation and have  $\epsilon_{\text{Nd}}$  as low as  $-3$ ). The data of [Seat et al. \(2009\)](#) indicate that basement rocks at Nebo–Babel have  $\epsilon_{\text{Nd}}$  values of  $-4.5$  to  $-5$  and Ce/Nb ratios of 9, whereas the regionally extensive Pitjantjatjara granite suite has  $\epsilon_{\text{Nd}}$  of  $-2$  to  $-4$  and highly variable Ce/Nb (5 to  $>20$ ).

In situ Sr isotope analyses on plagioclase ([Maier et al., 2014](#)) are consistent with these results in that the least-radiogenic Sr isotopic values are found in the Mantamaru and Halleys intrusions, whereas Morgan Range, Lehman Hills, and Cavenagh have higher initial Sr isotope ratios. Microgabbros from Cavenagh have less radiogenic Sr isotope ratios ( $\text{Sr}_i = (87\text{Sr}/86\text{Sr})_i = 0.7042 - 0.7057$ ) than associated medium-grained gabbros ( $\text{Sr}_i = 0.7052 - 0.7068$ ), and the medium-grained samples show greater isotopic heterogeneity. This is interpreted to reflect lining of the magma conduits by early, relatively contaminated magma pulses, allowing the relatively late-stage microgabbro magma to be emplaced while undergoing relatively less crustal interaction. Of note is that almost the entire range in Sr isotopic ratios seen within the west Musgrave mafic–ultramafic intrusions is present within the Kalka intrusion in South Australia, and in both cases, the ultramafic rocks have the highest initial Sr isotope ratios, whereas anorthosites, leucogabbros, and troctolites have relatively more mantle-like compositions.

Whole-rock sulfur isotope data have been generated for rocks of the Jameson intrusion, the G2 gabbros, and the Alcurra Dolerite suite (Table 3, supplementary data). In addition, we collected sulfur isotope data for sulfide-bearing rhyolites from the Bentley Supergroup in the Palgrave area (Fig. 2), as well as in situ (laser ablation ICP-MS) sulfur isotope data from Halleys. These data can be compared to those from Nebo–Babel ([Seat et al., 2009](#)). All mafic intrusive rocks plot near the composition of the mantle. By contrast, rhyolites of the Mount Palgrave Group have a much wider sulfur isotopic range of  $\delta^{34}\text{S}$ , from  $+3.2$  to  $+7$ . The data could either suggest that the sulfides in the mafic rocks are of mantle derivation, or that any crustal sulfides were juvenile or underwent no sulfur isotopic fractionation, or that assimilated crustal sulfides equilibrated with the magma at high R-factors (mass ratio of silicate melt to sulfide melt; [Campbell and Naldrett, 1979](#); [Leshner and Burnham, 2001](#)). Notably, recent data from the Manhego prospect ([Karykowski, 2014](#)) show strong negative  $\delta^{34}\text{S}$ , representing the only igneous suite amongst the Giles intrusions with markedly non-magmatic S isotope signatures.

## 7.2. Sulfur and chalcophile elements

Most of the Giles intrusions have relatively low sulfur concentrations, at  $<200$  ppm (Fig. 20a). Slightly higher sulfur concentrations are present at Wingellina Hills, The Wart, Murray Range, Hinckley Range, the ‘North’ and ‘Northeast’ intrusive fragments, some of the G2 massive gabbros, and the Alcurra Dolerite suite (up to 2000 ppm). Even higher sulfide contents (in places  $>1$  vol.%) occur at Saturn, and in olivine gabbro and olivine gabbro-norite of the upper Jameson intrusion, with Cu concentrations up to 860 ppm (at 0.12 wt.%  $\text{SO}_3$ ). The relatively high sulfide and Cu contents could be due to protracted fractionation and resulting saturation in sulfide liquid in the magma, analogous to the troctolitic Kiglapait intrusion in Labrador, where sulfur saturation is reached after 93% fractionation ([Morse, 1981](#)). Alternatively, the upper stratigraphic portions of the Jameson Range could have undergone incipient hydrothermal alteration and addition of Cu and S, possibly related to the voluminous volcanic activity that formed the Mount Palgrave Group, directly to the southwest. However, sulfur isotopic data for two troctolitic samples (G2WA 189475 and 189478) indicate  $\delta^{34}\text{S}$  of between  $+2.1$  and  $+2.8$ , broadly consistent with a magmatic origin.

No sulfur data are available for Halleys, but petrographic examination indicates locally several percent sulfides, consistent with Cu concentrations of  $>4000$  ppm in some samples. Sulfide-rich mafic

intrusive rocks, locally containing net textured and massive sulfides were recently intersected at the Manhego Prospect ([Phosphate Australia Ltd, 2014](#); [Karykowski, 2014](#)). The highest sulfide contents amongst the Giles intrusions occur at Nebo–Babel, including thick intervals of massive and disseminated sulfides ([Seat et al., 2007](#)).

The mafic–ultramafic intrusions are typically relatively Cu poor ( $<200$  ppm Cu, Fig. 20b). The relatively unevolved (ultramafic) rocks have particularly low Cu contents, whereas Cu contents progressively increase in the evolved (mafic) rocks, consistent with incompatible behaviour of Cu in fractionating sulfur-undersaturated magma. The highest Cu contents are found in the Nebo Babel (sulfide tenor of 2–8% Cu), Halleys and Manhego intrusions ([Seat et al., 2007](#), [Karykowski, 2014](#)). Slightly lower Cu contents occur in some samples from Saturn, and the uppermost portions of the Jameson intrusion, where some of the massive magnetite layers contain up to 700 ppm Cu. Elevated Cu concentrations are also found in the Wingellina Hills PGE reefs (up to 500 ppm Cu), and in a pyroxenite from the upper portion of Pirntirri Mulari that has 350 ppm Cu.

The majority of the Giles intrusions have low PGE contents ( $<30$  ppb Pt + Pd, Fig. 20c). Higher values occur in the PGE reefs of the Wingellina Hills intrusion, containing up to several ppm PGE, the pyroxenite in the upper portion of Pirntirri Mulari (200 ppb PGE, not shown in Fig. 20c due to lack of major element data), and in samples from Halleys (up to 200 ppb PGE). Other PGE-rich rocks not plotted include those from Nebo–Babel (up to 0.5 ppm PGE in whole rocks, up to  $\sim 7$  ppm PGE in sulfide) and Manhego (up to approximately 1 ppm PGE in sulfide, [Karykowski, 2014](#)). The lowermost magnetite layer in the Jameson intrusion has up to about 2 ppm PGE, at very low sulfide contents. Scattered PGE enrichment, not accompanied by sulfide enrichment, occurs in the Morgan Range ( $\leq 80$  ppb), The Wart (one sample with 120 ppb), and Cavenagh (three samples with 75–100 ppb).

In almost all intrusions, including the sulfide-bearing Nebo Babel, Halleys and Manhego intrusions, Cu/Pd ratios are above the range of the primitive mantle ( $\sim 7000$ ); thus, they are PGE-depleted relative to mantle (Fig. 20d). This could suggest that the magma had equilibrated with sulfide prior to final emplacement, in the mantle or the crust, or that it assimilated Cu-rich crust, or that the mantle source was relatively enriched in Cu. Cu/Pd ratios progressively increase with decreasing Mg# and samples with Cu/Pd  $<$  primitive mantle are mostly confined to Wingellina Hills, Pirntirri Mulari, and the Morgan Range, as well as some Cavenagh samples, that is, rocks with Mg# mostly  $>60$ . We interpret this to reflect sulfide liquid saturation in response to primarily magmatic fractionation rather than contamination. We do not consider it likely that the PGE depletion is due to a relatively small degree of mantle melting, as NB1 is strongly S undersaturated and has lower TiO<sub>2</sub> contents (0.8%) than typical MORB ( $>1\%$ , [Gale et al., 2013](#)).

Most of the sample suites that represent liquids rather than cumulates (NB1 dykes, the Alcurra Dolerite suite, and Nebo–Babel chilled margins) are PGE depleted, with Cu/Pd ratios above primitive mantle values. The main exceptions are the unevolved G2 gabbros, which contain up to 10–15 ppb Pt and Pd each and have Cu/Pd ratios overlapping with primitive mantle. Notably, Nebo Babel chilled margins too have PGE concentrations typical of basaltic magmas ( $\sim 10$ – $20$  ppb Pt and Pd each), but Cu/Pd  $> 10000$ .

## 7.3. Mineral chemistry

We determined the compositions of olivine, orthopyroxene, clinopyroxene, and plagioclase in more than 50 rock samples from the Giles intrusions, excluding the Alcurra Dolerite suite and the G2 massive gabbros. A summary of some key compositions are given in Table 1, and a detailed discussion of the data can be found in [Maier et al. \(2014\)](#). In the present paper, we focus on discussing olivine compositions. The mineral has between 40 and 87 mol% Fo (Fig. 21). Olivine from the

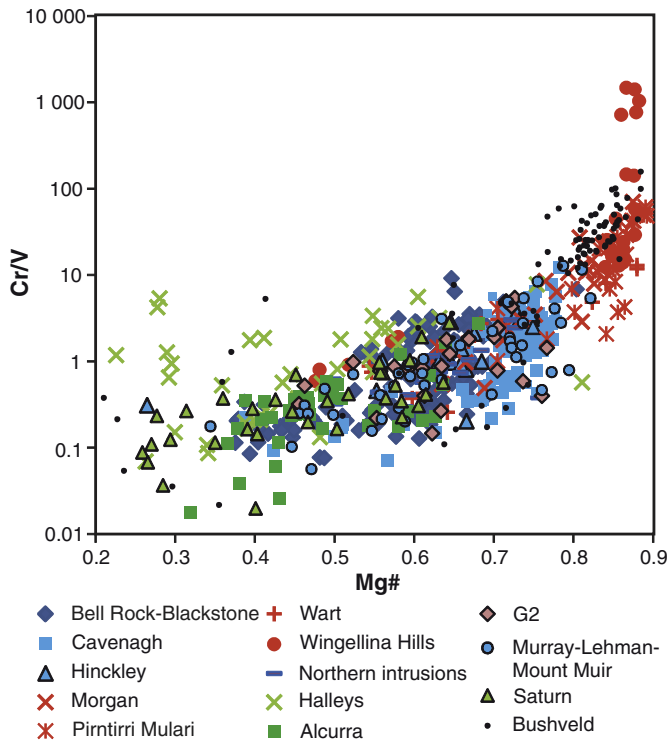


Fig. 17. Binary variation diagram of Cr/V vs Mg# for the Giles intrusions. Bushveld data are from Maier et al. (2013b). 'Northern' intrusions include intrusive fragments North of Mt Muir and the Hinckley Range. Cavenagh data include samples from Staubmann (2010). Figure from Maier et al. (2014).

Blackstone intrusion and parts of Cavenagh show the lowest Fo values, whereas the highest Fo contents occur at Wingellina Hills, Pirntirri Mulari, The Wart, and Morgan Range. Samples from Jameson, Saturn, Hinckley Range, Murray Range, Nebo–Babel, Lehman Hills, and Latitude Hill contain olivine with intermediate Fo contents.

Olivine from the mafic and mafic–ultramafic Giles intrusions has mostly up to 3500 ppm Ni (Fig. 21a). Ni contents show a positive correlation with Fo content and are higher than in olivines of comparable Fo content from many basic magmas globally, although relatively high Ni concentrations appear to be characteristic of many layered intrusions (Fig. 21b). The highest Ni contents in magmatic olivine identified so far occurs in the Kevitsa intrusion of Finland (with up to 1.5 wt.% Ni; Yang et al., 2013a, 2013b).

For the origin of the Ni enrichment in olivine of the layered intrusions several models may be considered. (i) Equilibration of olivine with trapped melt could lower the Fo content without significantly affecting Ni concentrations. This model would be consistent with the observed decoupling of Fo from Ni contents in olivine, and from An contents of plagioclase. However, Godel et al. (2011) found Ni enrichment in olivines from the NB1 dykes. Thus, the observed Ni enrichment must, at least in part, reflect an early magmatic process. (ii) Equilibration of olivine with percolating sulfide liquid. However, there is little evidence for sulfide in most intrusive rocks related to the Giles Event. (iii) Assimilation of Ni-rich sulfide before final magma emplacement. This model is presently also considered unlikely as the West Musgrave crust is relatively poor in magmatic Ni sulfides. (iv) Magma derivation from a pyroxenitic–eclogitic mantle source (Sobolev et al., 2011). This model is equally rejected as it implies that most layered intrusions globally are derived from pyroxenitic mantle sources, for which there is presently no evidence. (v) Contamination leading to magma reduction and relatively low Fo contents. However, the oxygen fugacity of the Giles layered intrusions is thought to be similar to most other

mafic–ultramafic crustal rocks, at around the quartz–fayalite–magnetite buffer (Staubmann, 2010). (vi) Polybaric fractionation, with initial high-P crystallization of pyroxene at depth leading to depletion of the magma in MgO relative to Ni, followed by ascent and final emplacement of the magma at low pressure conditions where olivine may become stable. Such a magma, and any olivine crystallizing from it, could have relatively high Ni to MgO ratios (Maier et al., 2013a, 2013b). In addition, the  $D_{Ni}$  into olivine increases with falling pressure (Li and Ripley, 2010). The model would be consistent with the distinctly lower Cr/Al ratios of pyroxenes in the Giles intrusions relative to the Bushveld Complex (Maier et al., 2014), potentially reflecting high-P pyroxene crystallization. Ballhaus and Glikson (1995) noted that olivine in the Giles intrusions shows a continuous range of Fo contents, in contrast to other layered intrusions such as the Bushveld Complex which lack olivines of composition Fo 60–80, normally interpreted to be the result of the peritectic reaction of olivine to pyroxene, temporarily destabilizing olivine. The authors proposed that the lack of an “olivine gap” in the Giles intrusions is due to polybaric fractionation.

## 8. Discussion

### 8.1. Nature of parent magmas to the Giles intrusions

Knowledge of the composition of the parent magma to cumulate rocks is of considerable interest to petrologists and economic geologists because this potentially allows to constrain the nature of the mantle source, the degree of crustal contamination of the magma, the crystallization history of an intrusion, and the prospectivity for magmatic mineral deposits. One of the most common approaches to estimate the parent magma composition is based on the study of chilled contact rocks of intrusions. However, such rocks are commonly contaminated and thus not necessarily representative of the primary magma. Another approach could be to examine microgabbroic rocks that are abundant within several Giles intrusions, but many of these rocks contain a cumulus component.

A technique that has been successfully applied in the Bushveld Complex and more recently in the Giles intrusions comprises the study of fine-grained sills or dykes associated with the intrusion (Sharpe, 1981; Barnes et al., 2010). For the ultramafic segments of the G1 intrusions, a suitable parent magma candidate would be the fine-grained low-Ti tholeiitic ‘plagioclase-rich dykes’ initially documented in the Bell Rock Range area by Howard et al. (2007). These dykes are compositionally equivalent to the NB1 dyke type of Godel et al. (2011). A further suitable parent magma type could be the unevolved members of the massive G2 gabbros. They contain ~10–13 wt.% MgO, 12 wt.% FeO<sub>T</sub>, 350 ppm Ni, up to 700 ppm Cr, and 10–15 ppb Pt and Pd each. Crystallization of the Wingellina Hills intrusion from either NB1- or primitive G2-type magma is consistent with the relatively low Ti content of these magmas (Fig. 53 in Maier et al., 2014). Modelling using the PELE software (Boudreau, 1999) indicates that at low to intermediate pressure NB1 has a crystallization order of chromite > olivine + chromite > olivine + chromite + clinopyroxene > chromite + clinopyroxene + plagioclase + orthopyroxene. This is broadly consistent with petrographic observations on the Pirntirri Mulari and Wingellina Hills intrusions, namely the occasional occurrence of chromite grains within olivine. The modelled Fo content at 1–5 kb is 87 mol%, consistent with analyses. Furthermore, calculations by Godel et al. (2011) indicate that NB1 reaches sulfur saturation after 30% crystallization, at about the time plagioclase appears on the liquidus, consistent with the stratigraphic position of the PGE reefs at the top of the ultramafic zone in the Wingellina Hills intrusion. None of the other c. 1070 Ma dyke suites analysed by Howard et al. (2006b) or Godel et al. (2011) provides a suitable fit for the ultramafic intrusions.

Considering the parental magmas to the gabbroic intrusions, possible candidates are the Nebo–Babel chilled margin (7–9 wt.% MgO, Mg# of 51–61) or the compositionally similar NB3 dyke type.

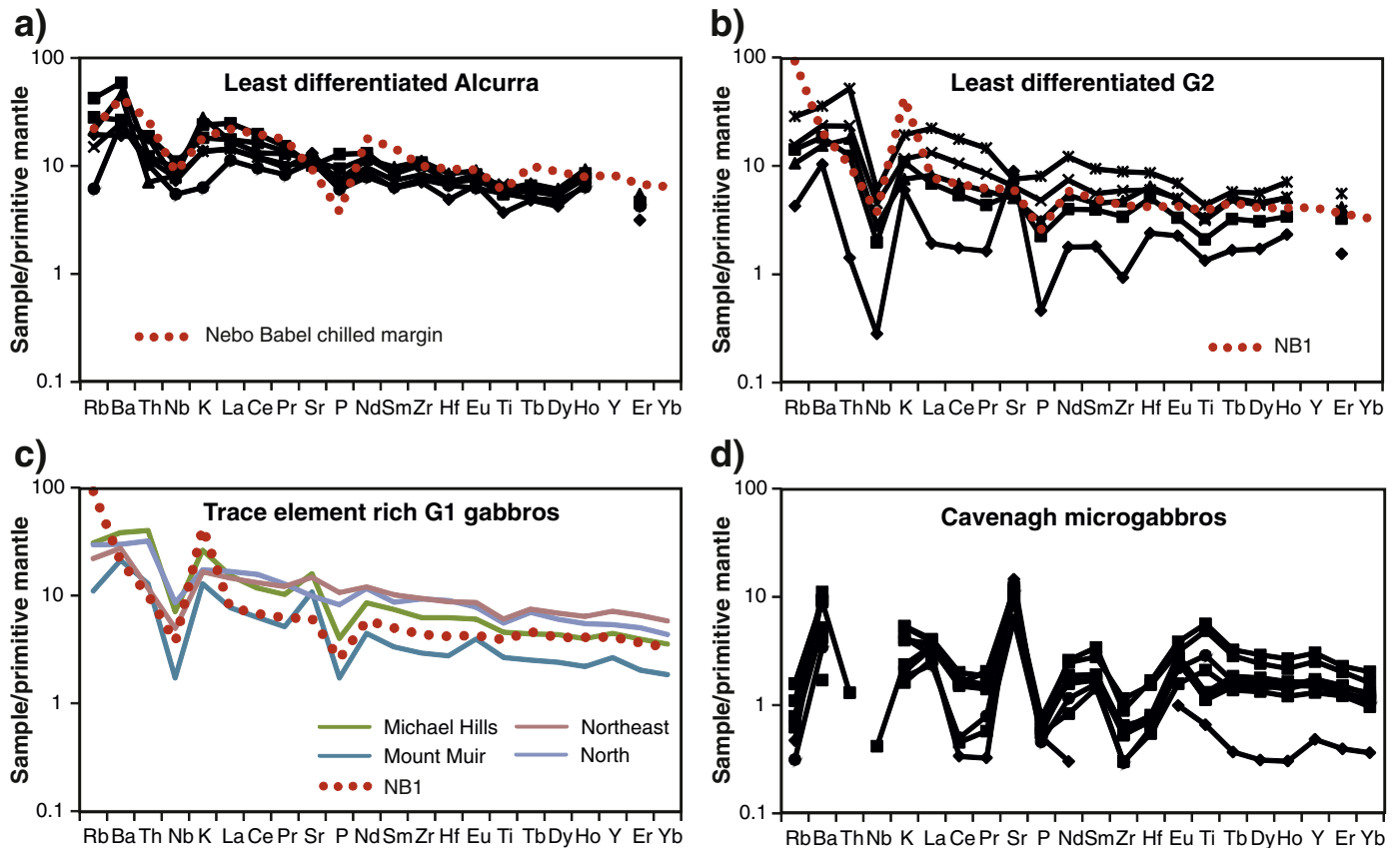


**Fig. 18.** Primitive mantle-normalized multi-element variation diagrams for rocks of the Giles Event that may be liquids, including: a) unevolved samples of the Alcurra dolerite suite; b) unevolved samples of the G2 gabbros; c) G1 gabbros enriched in incompatible trace elements; and d) Cavenagh microgabbros. Normalization factors are from Sun and McDonough (1989).

Adapted from Maier et al. (2014).

For the Halleys and Saturn intrusions, the Alcurra Dolerite suite (or the compositionally equivalent NB4 dyke type of Godel et al., 2011) would be a potential parent magma, based on similarities in incompatible trace element and noble metal ratios (e.g., high Cu/Pd) and common enrichment in mica and sulfide (Howard et al., 2009). The most primitive members of the Alcurra Dolerite suite have 8–9 wt.% MgO and Cr/V ratios of 2–4 (Table 1, supplementary data).

### 8.2. Mantle sources of the magmas

Godel et al. (2011) proposed that NB 1 magmas were derived from the sub-continental lithospheric mantle (SCLM). Their model was based on the relatively low Ti contents and MREE to HREE ratios in the magmas, implying the presence of amphibole in the source. However, several arguments can be made against this model: (i) Magmas believed to be derived from the SCLM, e.g. Bushveld B1 magmas, have much lower S contents (400 ppm, Barnes et al., 2010) than NB1, which has S contents typical of many other global basalts (~1000 ppm; Godel et al., 2011). (ii) SCLM derived magmas may have high Pt/Pd above unity (Maier and Barnes, 2004; Barnes et al., 2010) whereas NB1 has Pt/Pd below unity, in the range of most other basalts. (iii) Between c. 1220 and c. 1120 Ma, the west Musgrave Province experienced ultra-high temperature (UHT) metamorphism in the middle crust (Kelsey et al., 2009). Smithies et al. (2010, 2011) argued that this requires removal of the regional SCLM, consistent with a dramatic lowering in the pressure of crustal melting at the beginning of the Musgrave Orogeny. If there was SCLM at the beginning of the Giles Event, it must have formed after the Musgrave Orogeny, which means it would have been still young, hot, and weak, and have too radiogenic Nd isotopic compositions to be parental to the NB1 dykes

( $\epsilon\text{Nd} = -2$ ). Based on these data, we do not subscribe to the model of Godel et al. (2011). The evidence for an asthenospheric mantle source to NB1 is more persuasive, e.g., the resemblance of Yb–Ti–Zr–Nb concentrations of NB1 to those in MORB. The enrichment in LILE and LREE within NB1 could be modelled by low degree (<<5%) crustal contamination of asthenospheric high-Mg basalt.

The origin of the magma forming the Alcurra Dolerite suite also remains unresolved. Godel et al. (2011) proposed that the NB4 dykes, which they considered analogues of the Alcurra Dolerite suite, were plume melts. The main argument rests on the relatively high Ti contents and MREE/HREE ratios of NB4, ostensibly requiring the presence of residual garnet in a deep mantle source. However, the high La/Yb ratios of the Alcurra-type rocks (5–9.7) are not accompanied by depletions in Yb (average 3.34 ppm) with respect to MORB and are thus better explained through minor contamination (<<1%) with HFSE-rich crust. Crustal contamination could potentially also explain the relatively high Cu/Pd and Au/PGE ratios of the Alcurra-type magmas, whereas the origin of the elevated Pt/Pd remains presently poorly understood.

### 8.3. Crustal contamination of the magmas

The Giles intrusions have  $\epsilon\text{Nd}$  from +2 to –5 (Fig. 19 and Table 4, supplementary data). These data could be explained by variable crustal contamination, or melting of compositionally diverse mantle sources, or both. At least some degree of in situ crustal contamination is suggested by the field evidence, e.g. the mingling of the G2 gabbros with granite and abundant xenoliths in several G1 intrusions such as Hinckley Range (Fig. 6) and Kalka (Gray and Goode, 1989).

In the ultramafic intrusions, crustal contamination is suggested by the existence of 2 distinct crystallization paths. The basal portions

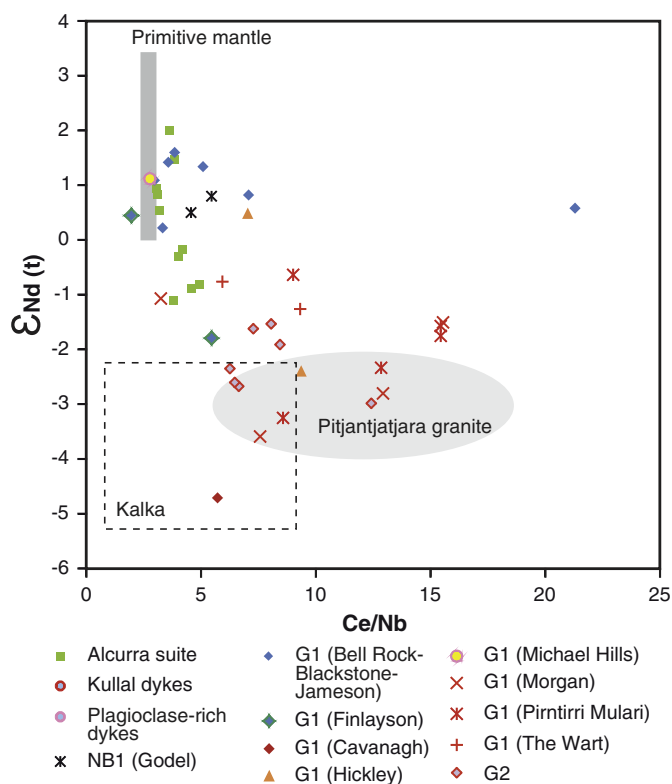


**Fig. 19.** Plot of  $\epsilon_{\text{Nd}}$  vs Ce/Nb for the Giles intrusions. Note that troctolitic G1 intrusions and the Alcurra Dolerite suite plot near the mantle range, whereas the other intrusions contain an enriched component. The compositional field of Pitjantjatjara granite contains the 10th–90th percentile of Ce/Nb data. Data for Kalka intrusion are from Wade (2006). Figure from Maier et al. (2014).

of the Wingellina Hills and Kalka (South Australia) intrusions, and most of the central portions of Pirntirri Mulari, have a crystallization sequence of olivine > orthopyroxene + olivine + chromite > orthopyroxene + clinopyroxene, in contrast to the central portion of the Wingellina Hills intrusion (Ballhaus and Glikson, 1995) which has a similar crystallization order as that modelled (using PELE) for NB1, i.e. chromite – olivine + chromite – olivine + chromite + clinopyroxene – chromite + clinopyroxene + plagioclase + orthopyroxene. Two distinct liquid lines of descent have also been found at the Muskox intrusion, Canada, where the basal rocks show a crystallization sequence of olivine > clinopyroxene + olivine, whereas the upper units show olivine > olivine + orthopyroxene, interpreted to result from contamination with partial melts of the roof (Irvine, 1970).

Amongst the gabbroic G1 intrusions, Cavanagh has the lowest  $\epsilon_{\text{Nd}}$  ( $\epsilon_{\text{Nd}}$  as low as  $-5$ ), overlapping with those of basalts of the Mummawarrawarra and Glyde Formations of the Bentley Supergroup (and Warakurna Supersuite). As there are no Musgrave crustal rocks currently known to have  $\epsilon_{\text{Nd}}$  values below  $-6$ , the required degree of contamination of the Cavanagh magma may seem unrealistically high. However, granites of the regionally occurring Pitjantjatjara Supersuite are extremely rich in HFSE, which may greatly reduce the required amounts of contamination (Kirkland et al., 2013). Relatively strong contamination of the Cavanagh intrusion is consistent with the high Ce/Sm and Ce/Nb ratios (Fig. 22). In contrast, Nd and Sr isotopic data for the troctolitic intrusions (namely Mantamaru) approximate the chondritic uniform reservoir (CHUR) ( $\epsilon_{\text{Nd}}$  mostly from 0 to  $+2$ ,  $\text{Isr} \sim 0.704$ ), and have markedly higher  $\epsilon_{\text{Nd}}$  or lower  $\text{Sr}$  than any Musgrave crust present at the time and relatively low Ce/Sm and Ce/Nb ratios (Fig. 22). These data indicate very minor (<5%) crustal contamination in most troctolitic intrusions.

The Alcurra Dolerite suite has slightly lower  $\epsilon_{\text{Nd}}$  ( $+1$  to  $-1$ ) than the Mantamaru intrusion. Smithies et al. (2013) showed that less than 10% bulk contamination of the most primitive samples of the Alcurra Dolerite suite with average Pitjantjatjara Supersuite granite can explain the entire isotopic variation and much of the highly incompatible trace element variation within the Alcurra Dolerite suite. If one assumes as contaminant a low-degree (20%) partial melt of average Pitjantjatjara Supersuite granite, the required assimilation is <4%. Such low degrees of contamination would produce only slight shifts to lower  $\epsilon_{\text{Nd}}$  isotope values, and it would thus appear unlikely that the mantle source was strongly depleted. Thus, the unevolved magmas of the Alcurra Dolerite suite were likely derived by relatively shallow melting (<80 km) of weakly depleted mantle, followed by early and very minor (<4%) contamination with highly enriched crustal material, and then closure of the continuously fractionating system to further contamination. The latter process can be applied to all Giles intrusions, consistent with the broad similarity in  $\epsilon_{\text{Nd}}$  within individual bodies, at variable Ce/Nb and La/Sm.

#### 8.4. Magma emplacement

The emplacement conditions of the Giles intrusions were discussed by Maier et al. (2014), from which the following summary has been compiled. Field relationships and compositional data indicate that the depth of emplacement varied considerably between intrusions. In the case of Mantamaru, country-rock inclusions and intrusive contacts indicate that the body was emplaced at the stratigraphic level of the Mummawarrawarra Basalt (Kunmarnara Group). Based on the low metamorphic grade (greenschist facies) of the basalts, it is argued that the Mantamaru intrusion crystallized in an upper crustal, extensional environment. Constraints on its crystallization age are the minimum depositional age of the Kunmarnara Group (defined by intrusion of granite at c. 1078 Ma; Sun et al., 1996; Howard et al., 2011b), and a direct U–Pb zircon date of  $1076 \pm 4$  Ma (Kirkland et al., 2011; GSWA 194762).

Particularly in the Hinckley Range, in the eastern part of the study area, massive G2 gabbro cuts the layered G1 intrusions and tends to show evidence of comingling with leucogranite. The latter may form pluton-scale bodies in the basement, for example the Tollu pluton. In the vicinity of major shear zones this bimodal gabbroic–granitic magmatism was accompanied by shearing and west–northwest folding, at between  $1078 \pm 3$  and  $1074 \pm 3$  Ma (Howard et al., 2011b). These dates overlap with the crystallization ages of the layered (G1) intrusions, but field relationships indicate that the G2 intrusions always post-date G1.

In the Blackstone Sub-basin, to the south of Blackstone Community, rhyolites of the Smoke Hill Volcanics directly overlie the G1 Blackstone Range without an obvious fault. Crystallization ages for the rhyolites [ $1071 \pm 8$  Ma (GSWA 191728; Coleman, 2009);  $1073 \pm 7$  Ma (GSWA 191706; Coleman, 2009), and  $1073 \pm 8$  Ma (GSWA 189561; C Kirkland, 2014, written comm.)] are within analytical error of the emplacement date of the G1 and G2 intrusions, and the composition of the rhyolites resembles that of leucogranites associated with the G2 intrusions. In addition, several field exposures indicate that the Blackstone intrusion was emplaced into the lower basaltic portions of the Kunmarnara Group (Bentley Supergroup). This requires extensive and rapid crustal uplift, erosion, and exhumation of the layered G1 intrusions, immediately followed by felsic volcanism.

Previous authors have proposed that some of the ultramafic Giles intrusions have been emplaced at relatively high pressure (Goode and Moore, 1975; Ballhaus and Berry, 1991), based on high Al concentrations of pyroxene, spinel exsolution in pyroxene and plagioclase, rutile exsolution in pyroxene, antiperthitic exsolution in plagioclase, and orthopyroxene–clinopyroxene–spinel–albite coronas between olivine and plagioclase. For example, Goode and Moore (1975) suggested that the Ewarara intrusion was emplaced at a pressure of 10–12 kbar. If

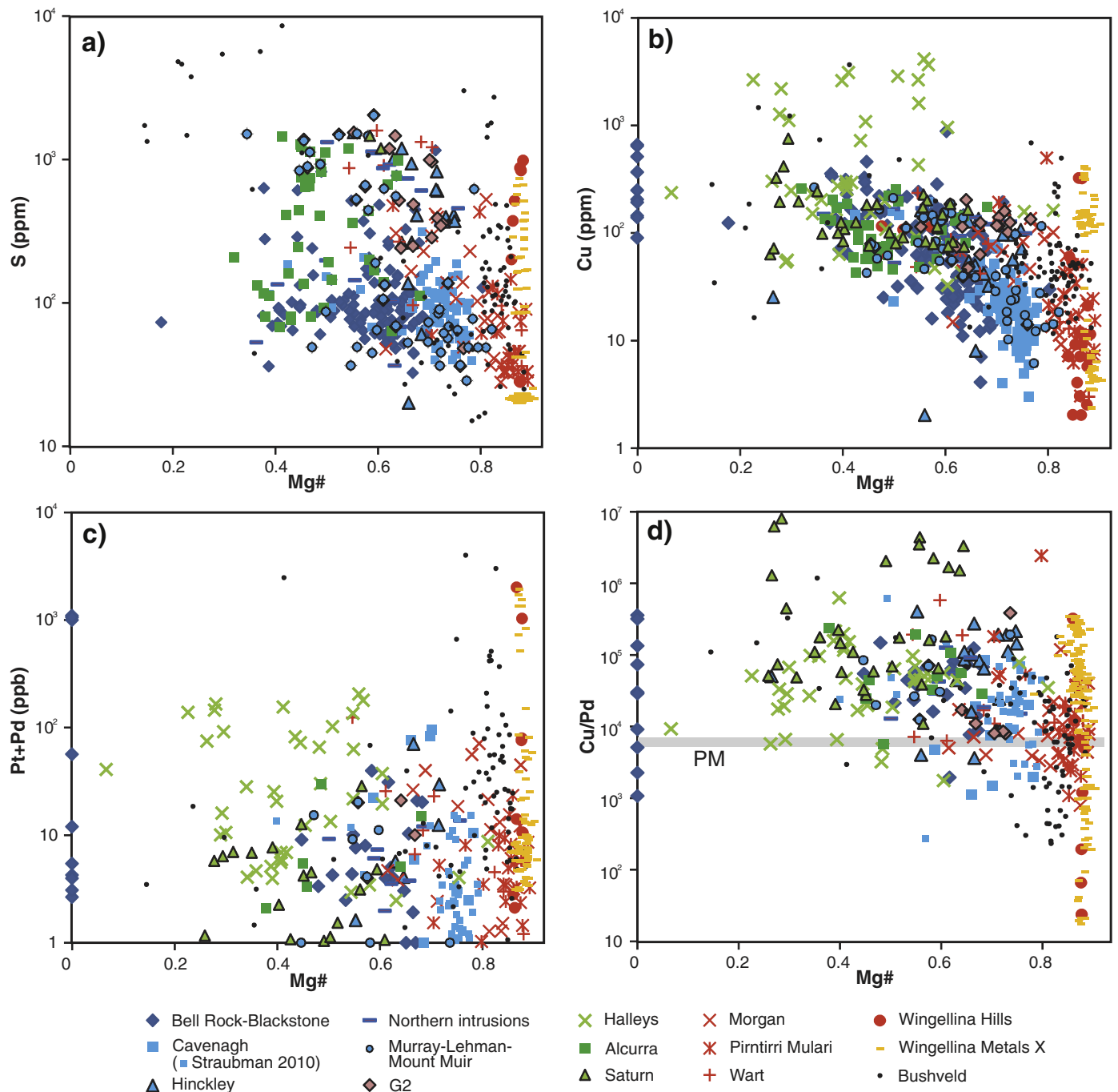


**Fig. 20.** Binary variation diagrams vs Mg# of: a) S; b) Cu; c) Pt + Pd; d) Cu/Pd. Primitive mantle value in d) is from Barnes and Maier (1999). Adapted from Maier et al. (2014).

the thickness of the crust at the end of the Musgrave Orogeny, just 40 my before the Giles event, was 35 km (Smithies et al., 2011), the Ewarara intrusion would have intruded near the base of the crust. Ballhaus and Glikson (1989) proposed an emplacement depth of 6.5 kbar (~20 km) for the Wingellina Hills and Pirntirri Mulari intrusions. However, because the coeval gabbroic intrusions are up to 10 km thick, the emplacement depth of the ultramafic bodies may have been as shallow as 10 km.

Emplacement into relatively deep crustal levels could explain why the ultramafic intrusions are less abundant than the gabbroic and troctolitic bodies, and why the former are proportionally more abundant in South Australia than in Western Australia – the South

Australian crust is exposed at a deeper level (Goode, 2002). Equally consistent with this model is the observation that the ultramafic intrusions tend to be exposed in the cores of regional folds (i.e., the anticline north of Blackstone Community which hosts the Pirntirri Mulari and Morgan Range intrusions), or along faults.

Field relationships also allow to place some constraints on emplacement dynamics. For example, the close spatial association of many microgabbros with fragments and schlieren of pyroxenite suggests that the emplacement of the microgabbros was accompanied by disaggregation of semi-consolidated pyroxene-rich cumulate slurries. This points to a semi-consolidated magma chamber that was frequently replenished by unevolved magma.



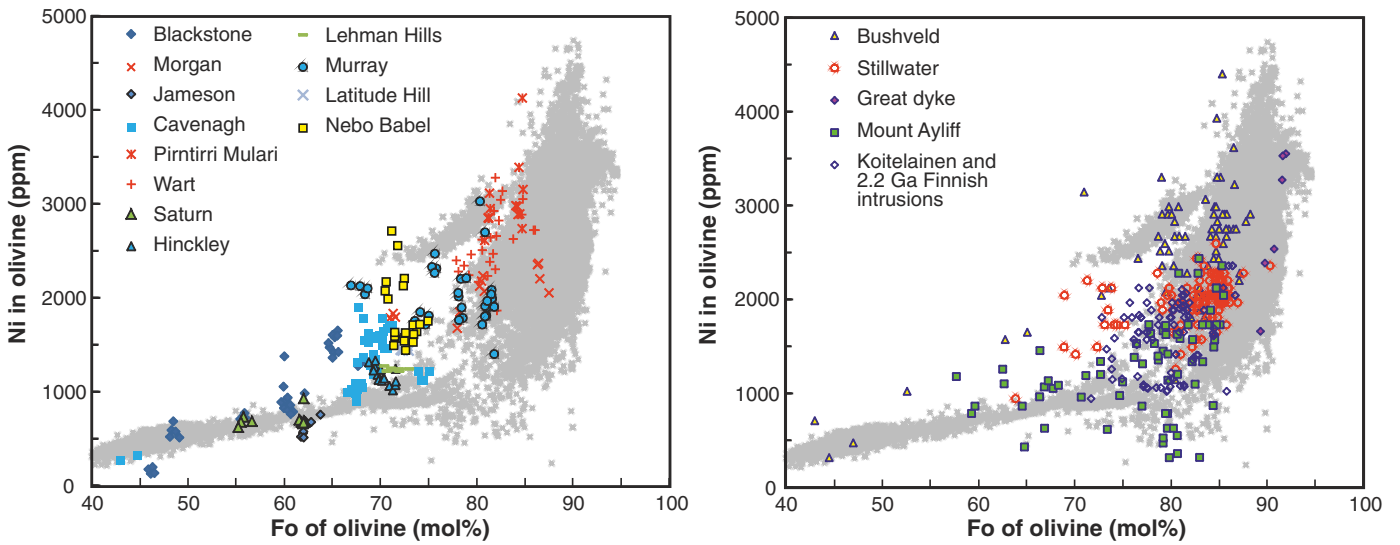


**Fig. 21.** Plot of Ni vs Fo in olivine: a) data from the west Musgrave Province; b) global data of layered intrusions (data compiled from Teigler and Eales, 1996; Maier and Eales, 1997; Lightfoot and Naldrett, 1983; Raedeke, 1982; E Hanski, unpublished data). Grey shading is background data on lavas, from Sobolev et al. (2011). Figure from Maier et al. (2014).

8.5. Fragmentation of intrusions

The idea that some or all of the Giles layered intrusions could be tectonically dismembered remnants of a much larger body can be traced back to Sprigg and Wilson (1959) and Nesbitt and Talbot (1966). Other authors who favoured this model include Glikson (1995), Smithies et al.

(2009), Howard et al. (2011b) and Aitken et al. (2013). Geophysical, lithological, and compositional data reported in the present study indicate that the Jameson–Finlayson, Blackstone, and Bell Rock intrusions are fragments of an originally contiguous body, named the Mantamaru intrusion by Maier et al. (2014). This has a minimum preserved size of 3400 km<sup>2</sup>, in the same range as the Great Dyke, Stillwater, Sept Iles,

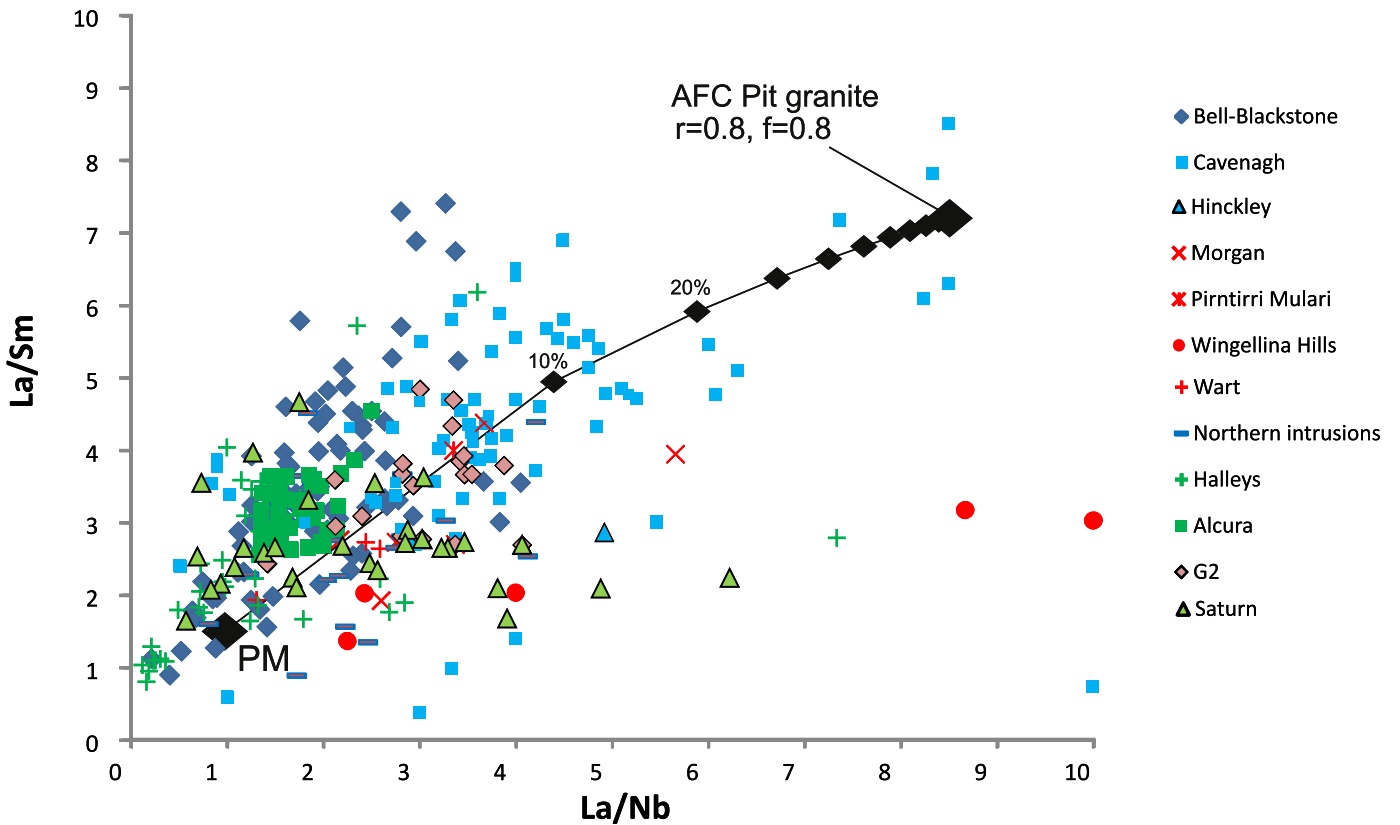


**Fig. 22.** Binary variation diagrams of La/Sm vs La/Nb: Most of the troctolitic intrusions (Mantamaru), the Alcurra Dolerite suite, and the Halleys and Saturn intrusions have primitive mantle-like trace element ratios, whereas many of the other intrusions (notably Cavenagh, Hinckley Range, Murray Range, and the ultramafic intrusions) contain a crustal component, possibly of Pitjantjarra granite (Pit granite). Solid line represents mixing line between picrite (with trace element contents assumed to be 4× primitive mantle, i.e. equivalent to ~25% partial mantle melting) and a contaminated magma produced by AFC ( $r = 0.8, f = 0.8$ ) of picrite with a 17% partial melt of Pitjantjarra granite (calculated by assuming modal proportions determined during experimental melting of biotite gneiss at 875°, 3 kbar, Patino Douce and Beard, 1995, and D values summarized in Rollinson, 2013).

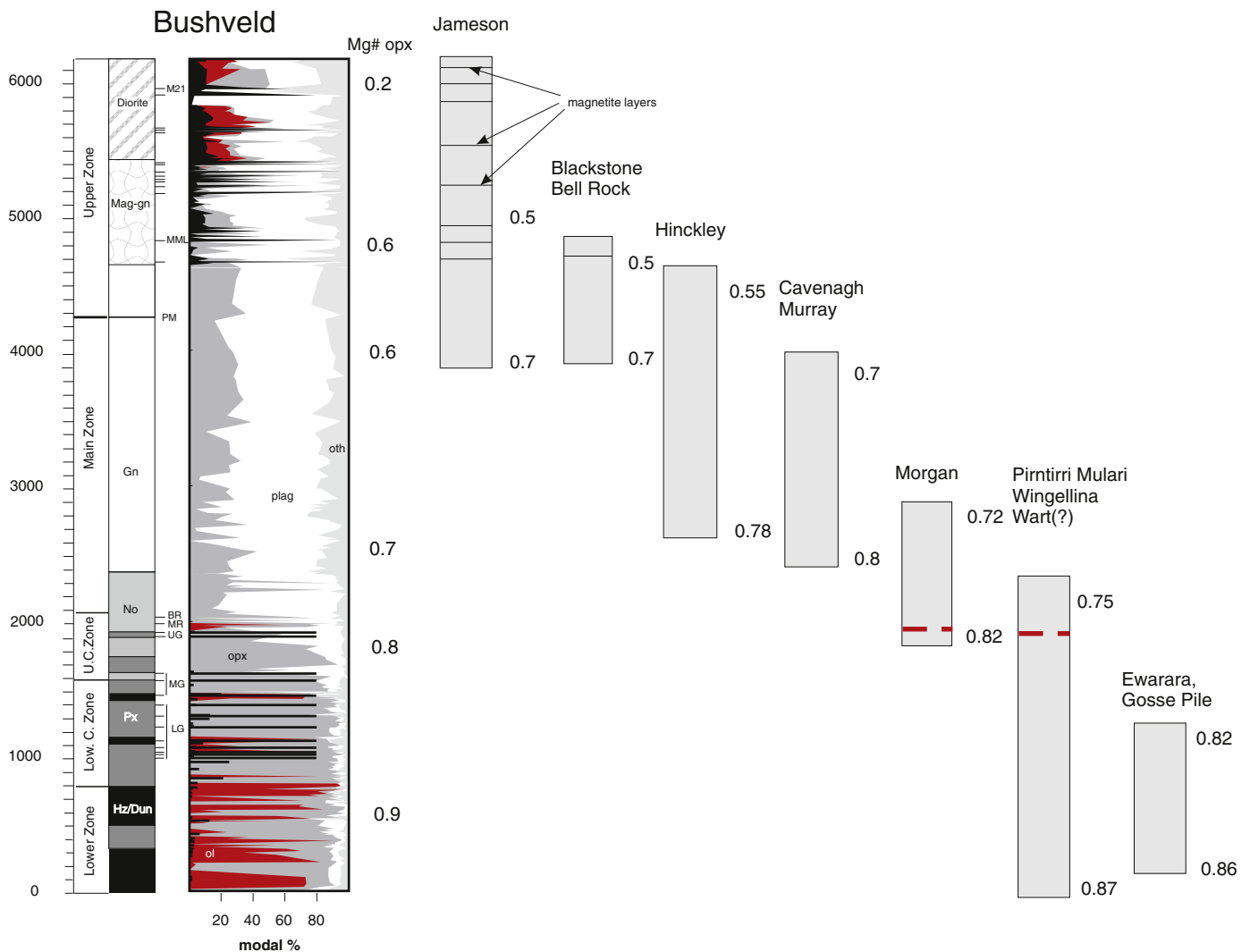


**Fig. 23.** Stratigraphic comparison of Giles intrusions with Bushveld Complex. (Bushveld log and data from Maier et al., 2013b). Low. C. Zone = Lower Critical Zone. U.C. Zone = Upper Critical Zone. Red stippled line indicates approximate position of (postulated) main PGE reef horizon. Figure from Maier et al. (2014).

and Dufek intrusions which measure between 3000 and 5000 km<sup>2</sup>. It has been further proposed that the Cavenagh intrusion may form the southern limb of the synclinal Blackstone intrusion (Nesbitt and Talbot, 1966; Aitken et al., 2013), potentially adding at least another 540 km<sup>2</sup> to the size of the Mantamaru intrusion. However, the Blackstone intrusion is much more differentiated than the Cavenagh intrusion, and it contains a massive magnetite layer that appears to be absent from the Cavenagh intrusion. Furthermore, the Cavenagh intrusion shows elevated PGE concentrations in its upper portion whereas the Blackstone intrusion is uniformly PGE depleted. Finally, the Blackstone intrusion has distinctly higher  $\epsilon$ Nd values than the Cavenagh intrusion. These data place some doubts on a possible connection between the Cavenagh and Blackstone intrusions, although other layered intrusions such as Bushveld and Kalka can have a wide range of trace element and isotopic compositions.

Based largely on compositional data, Seat et al. (2009) proposed that the Nebo and Babel intrusive blocks are overturned fragments of an originally single intrusion. This model is consistent with field evidence from, e.g., the western end of the Hinckley intrusion and the NW edge of the Blackstone Range, that deformation accompanied magmatism, locally developing open to tight folds.

It is tempting to speculate that all the ultramafic intrusions located in the Tjuni Purlka Zone (Wingellina Hills, Pirntirri Mulari, The Wart,

Morgan Range, Kalka, Gosse Pile, and Ewarara) originally formed a single body. This would imply lateral movement of up to 50 km within the Tjuni Purlka Zone. The intrusions share some similarities (e.g., olivine and pyroxene compositions, stratigraphic position of the Wingellina PGE reef and the Cu–PGE-rich horizon at Pirntirri Mulari) but they also show differences (e.g., thicker olivine and chromite rich segments and higher PGE concentrations at Wingellina Hills than in the other bodies, variation in plagioclase composition between Wingellina Hills and The Wart vs. Pirntirri Mulari). Further work is required to resolve this question.

#### 8.6. Comparison to other large layered intrusions

In order to better understand the petrogenesis and prospectivity of the Giles intrusions, it is useful to draw comparisons with other well-characterized and mineralized layered intrusions, e.g. the Bushveld Complex (Fig. 23). The Pirntirri Mulari, Wingellina Hills, and The Wart intrusions are the approximate stratigraphic and compositional equivalents of the Lower and Critical Zones of the Bushveld Complex. They have broadly similar olivine compositions and they show basal compositional reversals, thick ultramafic portions, and a number of ultramafic-mafic cyclic units. Reef-style PGE enrichments have been identified in the Wingellina Hills intrusion, and there are some indications that a

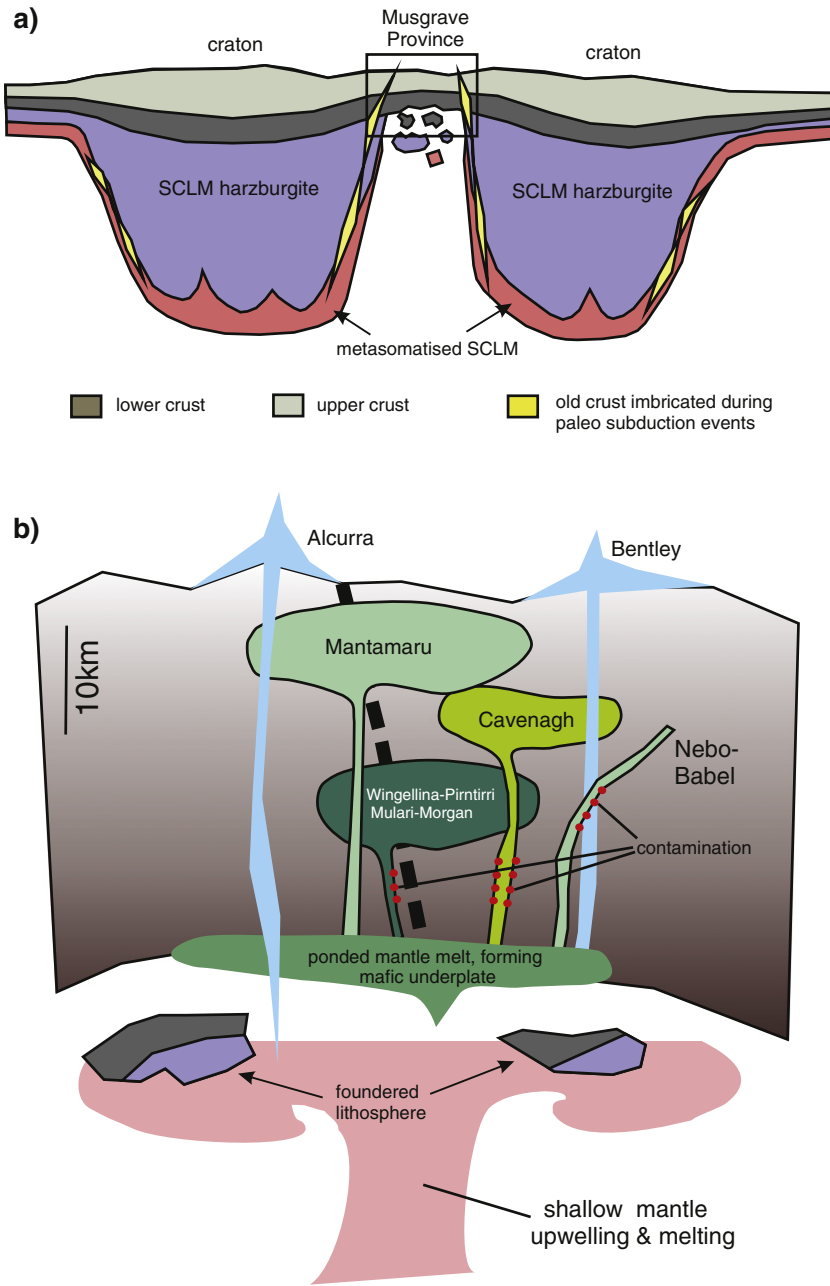


**Fig. 24.** Schematic model of emplacement of the Giles intrusions: a) foundering of crust and new SCLM; b) ponding and ascent of mantle melts. Note that the horizontal dimension is greatly compressed for added clarity. See text for discussion. SCLM = sub-continental lithospheric mantle. Figure from Maier et al. (2014).

similar horizon may exist in the Pirntirri Mulari intrusion. The equivalent prospective horizon of The Wart, Kalka, Ewarara, Gosse Pile, Ngulana, and Alvey Hills remains poorly studied, partly due to restricted access.

A major difference between the Giles ultramafic intrusions and the Bushveld Complex is that the former appear to lack chromitite seams. If this is due to the early crystallization of Cr-rich clinopyroxene, as suggested by Ballhaus and Glikson (1995), this would imply a low prospectivity for chromite deposits in the Giles intrusions.

The gabbroic Morgan Range intrusion contains a lens of ultramafic rocks at its northern edge and thus could represent the stratigraphic equivalent to the Upper Critical Zone–Main Zone transition of the Bushveld Complex, unless the ultramafic lens was tectonically adjoined to the Morgan Range. The lens does have some potential to host a PGE reef analogous to Wingellina Hills. In contrast, the Cavenagh, Michael

Hills, Latitude Hill, Hinckley Range, Murray Range, Lehman Hills, and Mt Muir intrusions have lower PGE prospectivity as they appear to be stratigraphic equivalents of the Bushveld Main Zone, sharing intermediate compositions and relatively subdued layering.

The Mantamaru intrusion is stratigraphically approximately equivalent to the upper Main Zone and Upper Zone of the Bushveld Complex. Both intrusions contain several magnetite layers (~25 in the Bushveld, at least 11 at Jameson) that can reach a thickness of more than 10 m (i.e., layer 1 at Jameson, magnetite layer 21 in Bushveld). In addition, in both intrusions the vanadium concentration progressively decreases from the basal to the upper magnetite layers (Fig. 24 in Maier et al., 2014), and also within individual layers. However, the vanadium contents of the Bushveld Main Magnetite Layer are twice as high as those at Jameson (13000 vs 7500 ppm). Other differences between the two intrusions include significantly higher PGE contents in the Jameson

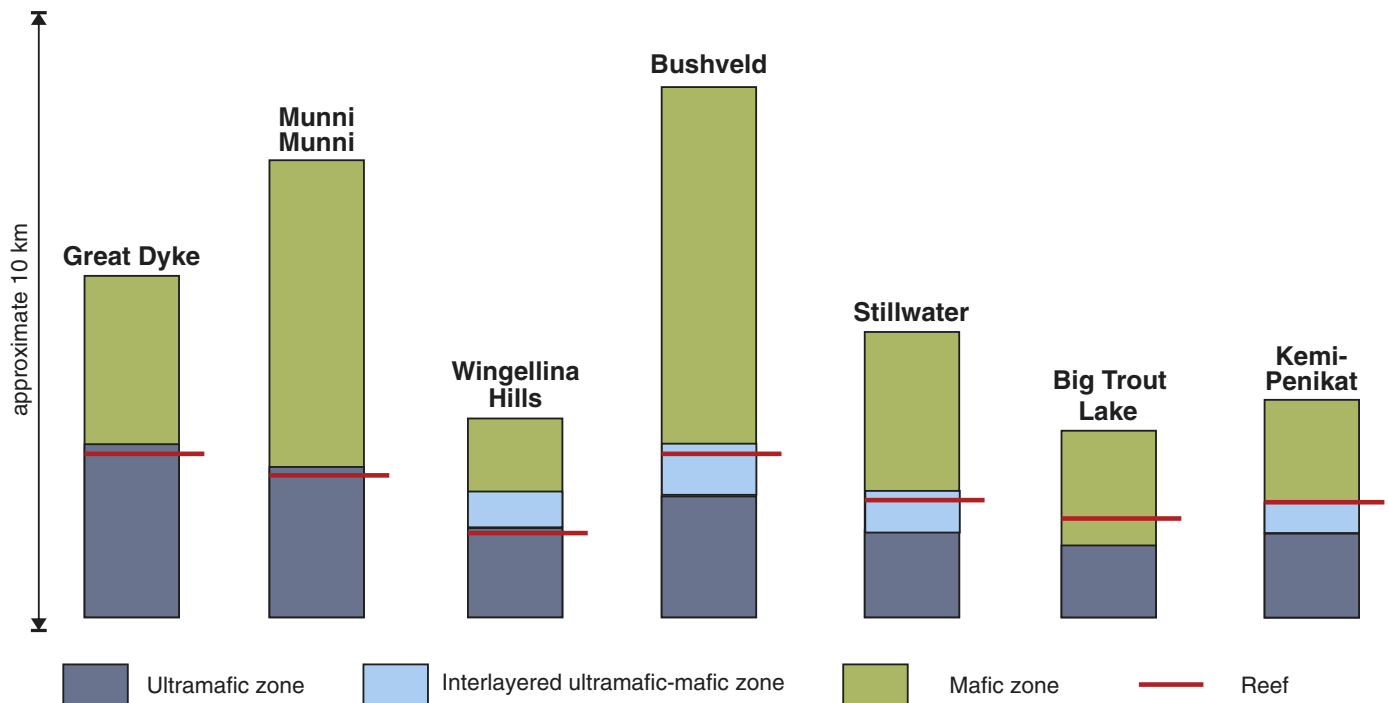


Fig. 25. Comparison of the positions of the PGE reef in a number of well-characterized layered intrusions. Figure from Maier et al. (2014).

basal magnetite seam and the apparent absence of an apatite-rich layer at Jameson.

### 8.7. Tectonic setting

The Musgrave Province is located between the lithospheric keels of the West Australian, South Australian, and North Australian Cratons. Channelling of mantle plumes along the cratonic keels could have resulted in strong adiabatic mantle partial melting and mafic magmatism (Begg et al., 2009). However, Smithies et al. (2011) argued that the >200 Ma time span of continuing mantle magmatism and UHT metamorphism is inconsistent with a mantle plume. The Musgrave Province instead represented a stationary zone of mantle upwelling, resulting in a persisting hot zone. Magmatism may have been driven by processes such as plate motions, lithospheric delamination, volatile transfer from the SCLM or the crust to the convecting mantle, or mantle flow along the irregular base of the lithosphere (Silver et al., 2006). Similar scenarios were envisaged by Silver et al. (2006) and Foulger (2010) for the Ventersdorp, Great Dyke, Bushveld, and Soutpansberg continental magmatic events in southern Africa.

The stage was set during and after the 1345–1293 Ma Mount West Orogeny which resulted in crustal thickening, partial melting, and densification of lower crust. The REE geochemistry of Musgrave granites suggests that at the beginning of the 1220–1150 Ma Musgrave Orogeny the depth of crustal melting changed from relatively deep to shallow, caused by delamination of residual lower crust and the underlying lithospheric mantle. The ensuing UHT metamorphism from 1220 to 1120 Ma testifies to a sustained regime of highly thinned crust and mantle lithosphere. Any magmatism was predominantly felsic because the lower crust had become a zone of melting, assimilation, storage, and homogenization (MASH), inhibiting ascent of relatively dense mafic magmas. This crustal thermal structure strongly influenced conditions at the beginning of the Giles Event (Smithies et al., 2015, in press). The latter was triggered by far-field forces acting on the margins of the West Australian Craton (Evins et al., 2010b; Smithies et al., 2015, in press). Initial subsidence and deposition of the Kunmarnara Group

was followed by draining of melts ponded at the base of the crust (G1, G2, Alcurra Dolerite suite). The relatively early G1 and G2 magmas were variably contaminated during ascent into the crust (Fig. 24). Subsequent magmas of the Alcurra Dolerite suite underwent relatively little contamination suggesting that the crust had become more refractory. At the same time, the Alcurra magmas are more differentiated because the crust thickened during the Giles event, allowing more intra-crustal ponding and fractional crystallization. The relatively low PGE concentrations, high Cu/Pd, Pt/Pd, and Au/PGE ratios of the Alcurra magmas could be explained by melting of hybrid crust-rich mantle, in response to foundering of crust and new SCLM (Fig. 24a).

### 8.8. Origin of mineralization

#### 8.8.1. PGE reefs within the Wingellina Hills layered intrusion

The bulk of the world's PGE resources occur in the form of stratiform layers or so-called reefs hosted by layered mafic–ultramafic intrusions. Economic deposits are presently confined to just three intrusions, namely the Bushveld Complex of South Africa, the Stillwater Complex in Montana, USA, and the Great Dyke of Zimbabwe, but sub-economic deposits that may be mined in the future occur in many other intrusions. The reefs consist of relatively narrow (<1–2 m), but laterally extensive layers of ultramafic or mafic rocks that typically contain <1–3% sulfides. The host intrusions are relatively sulfur poor, and most reefs show mantle-like sulfur isotopic signatures (Liebenberg, 1970; Li et al., 2008) suggesting that saturation of the magma in sulfide melt was reached due to fractionation rather than contamination. At least in the case of the Bushveld Complex, mixing between compositionally different magmas was probably not instrumental in reef formation because the magmas were highly sulfur undersaturated (Barnes et al., 2010). The concentration of the sulfides to form the reefs was possibly aided by hydrodynamic cumulate sorting in response to syn-magmatic subsidence of the intrusions (Maier et al., 2013b).

The main PGE reef of the Wingellina Hills intrusion shows certain similarities to the Great Dyke and Munni Munni PGE reefs, including the stratiform nature, the stratigraphic position towards the top of the ultramafic zone of the intrusion (Fig. 25), and the offset stratigraphic

positions of the various chalcophile elements. The bulk PGE content in the Wingellina Hills reef is in the same range as that in the Main Sulfide Zone of the Great Dyke. In both intrusions, there is no marked variation in trace element ratios across the reef (unpublished data of Maier). The origin of the Wingellina Hills main PGE reef can be explained by a model of sulfide saturation from fractionating NB1-type magma. The intrusion features several additional layers of PGE enrichment above the main PGE reef, but these have not been studied by us. They could reflect magma replenishments to the chamber, as the resident magma was likely relatively PGE depleted after the formation of the main reef.

The low PGE grade of the Wingellina Hills PGE reef relative to the Bushveld and Great Dyke reefs could reflect less-efficient metal concentration due to faster cooling rates in the relatively small Wingellina Hills intrusion, whereas the low sulfide contents may reflect metamorphic sulfur loss, consistent with sub-cotectic sulfide proportions in most Wingellina Hills rocks.

#### 8.8.2. Cu–Ni–PGE–Au mineralization at Halleys

Reef-style PGE–Cu–Au mineralization is typical of the upper portions of many layered intrusions (Maier, 2005). The enrichment of magnetite together with sulfide at the Halleys prospect could thus suggest that the Halleys intrusive body represents the evolved portion of an adjacent large layered intrusion, possibly the Blackstone Range of the Mantamaru intrusion, the Cavanagh Range, or the Saturn intrusion. A petrogenetic link to Blackstone and Cavanagh is presently considered unlikely as Halleys has much higher gold and sulfur concentrations as well as mica contents than Blackstone and Cavanagh. Furthermore, field relationships indicate that Halleys crosscuts the southern segment of the Blackstone Range. A petrogenetic relationship between Halleys and the Saturn intrusion is more plausible as both share the compositional features of the Alcurra Dolerite suite. However, a direct connection between Halleys and Saturn is inconsistent with the distinct magnetic signature of the intrusions.

An alternative model could be that the Halleys mineralization represents contact-style mineralization at the base or sidewall of a layered intrusion analogous to, e.g., the Platreef of the Bushveld Complex or the Suhanko deposit of the Portimo Complex, Finland. These deposits are considered to have formed through sulfide liquid saturation in response to fractional crystallization accompanied by floor contamination. The proximity of the floor and the resulting high cooling rate of the magma produced wide, disseminated mineralization rather than narrow reefs. Sulfides at Halleys have  $\delta^{34}\text{S}$  of  $-0.9$ , providing little added constraints on the nature of the sulfur source. More work is clearly required to further constrain the petrogenesis of the intrusion and its mineralization.

#### 8.8.3. Vanadium and PGE mineralization in magnetite seams of the Jameson Range, Mantamaru intrusion

Advanced fractional crystallization of basaltic magmas leads to cotectic crystallization of magnetite with silicates, resulting in magnetite-bearing gabbroic and dioritic rocks. The formation of massive oxide layers requires that magnetite is effectively separated from the silicate minerals as the cotectic proportions of magnetite and silicates are between 5 and 30% (Toplis and Carroll, 1996). The mechanism of oxide fractionation has been debated for decades. One of the main problems has been to explain the knife-sharp contacts of many magnetite layers, requiring extremely efficient separation of oxide crystals from silicate magma. The many structural similarities between layered cumulates and certain types of sedimentary rocks has led Irvine et al. (1998) to propose a mechanism of density currents sweeping down along the walls of magma chambers. Maier et al. (2013b) rejected this model for the Bushveld Complex because density currents would not preserve the abundant, highly elongated, sub-horizontally oriented anorthosite autoliths within many oxide seams. The authors instead suggested that oxide-silicate slurries were mobilized and sorted during subsidence of the Bushveld chamber. This process would be less

turbulent and may preserve some of the compositional layering of the cumulates. The slurries could be injected into the semi-consolidated crystal pile, and locally form transgressive pipes.

Other models for the formation of the oxide seams proposed in the past include shifts in phase stability fields of oxides caused by changes in pressure (Cameron, 1980; Lipin, 1993), temporary supersaturation in magnetite triggered by an increase in the oxygen fugacity of the magma in response to contamination (Ulmer, 1969), or a combination of magma mixing, pressure change, and oxidation in response to magma replenishment. However, one of the most popular models for the formation of massive magnetite layers remains iron oxide liquid immiscibility, originally advanced by Philpotts (1967). Experiments have produced immiscible iron oxide liquids in silicate liquids (Freestone, 1978; Roedder, 1978; Naslund, 1983), but whether the silicate melts used in the experiments are good analogues to natural magmas remains debated. Toplis and Carroll (1995, 1996) and Tollari et al. (2006, 2008) showed that using silicate melt compositions close to natural basalts and diorites, magnetite or ilmenite crystallize before the magmas become saturated with iron oxide liquid.

The potential for apatite deposits in the Giles intrusions remains unknown. Most of the samples analysed here are apatite free, although Traka Resources Ltd (2013) found somewhat elevated phosphorus concentrations (up to 250 ppm P) in seam 5 of the Jameson intrusion. Anglo American intersected elevated phosphorus concentrations (up to 8000 ppm P) in magnetite-rich rocks to the south of the Bell Rock intrusion, suggesting there could be apatite potential in unexposed magnetite seams. Minor amounts of apatite were also described from Kalka (Goode, 2002). Based on analogy with the Bushveld Complex where nelsonite forms the uppermost of the magnetite seams, the target horizon for apatite rich layers is at the very top of the intrusions.

#### 8.8.4. Nebo–Babel Ni–Cu deposit

Analogous to most other significant Ni–Cu deposits globally, Nebo–Babel is hosted by a tubular (chonolithic) body interpreted as a magma feeder conduit (Seat et al., 2007, 2009). The chilled margin contains sulfides, which led Seat et al. (2007) to propose that some of the magmas entrained sulfide liquid. The authors argued that the concentration of the entrained sulfides was in part controlled by changes in magma flow velocity, in turn related to changes in the shape of the conduit. However, in contrast to many other deposits elsewhere that are interpreted to have formed by addition of external sulfur to the magma, sulfide liquid saturation in the Nebo–Babel conduit was interpreted to have been triggered by magma mixing (of Alcurra-type magma with NB1-type magma) and contamination with orthogneiss, i.e. without addition of external sulfur (Seat et al., 2007; Godel et al., 2011). The orthomagmatic model is feasible in terms of sulfur mass balance: extracting 100 ppm S from 1 km<sup>3</sup> of magma can produce a massive sulfide lens 1 km long, 10 m high, and 20 m wide. However, orthomagmatic derivation of the Nebo Babel sulfides would require an extremely effective concentration mechanism as the cotectic proportion of sulfide precipitating from sulfur-saturated troctolitic–gabbroic magma is very small (perhaps as little as 0.1 wt.%).

Seat et al. (2007) based their model on the observation that the sulfides at Nebo Babel have mantle-like sulfur isotopic compositions, and that the rocks of the Pitjantjatjara Supersuite, which forms the immediate country rock to the deposit, tend to be sulfur-poor. However, mapping by GSWA has revealed that the Pitjantjatjara granites are only a very minor lithological component within this part of the Mamutjarra Zone. More abundant are rocks of the Wirku Metamorphics, Winburn Granite, and Bentley Supergroup. Amongst these, the Winburn Granite and volcanic and volcanoclastic rocks of the Bentley Supergroup typically contain visible pyrite and can locally be sulfide-rich, with up to 3000 ppm S in some samples of ignimbrite and rhyolite (see also Fig. 79 in Howard et al., 2011a, showing sulfide enrichment in drill hole WA02, Strzelecki Metals). The chamber system required for the Bentley volcanics must have been enormous – and even at the

current level of exposure, Nebo Babel is located only ~1 km north of unexposed (i.e., interpreted) areas of Bentley volcanics, and ~7 km east of the Winburn granite which is part of the felsic chamber system. It is possible that at a slightly deeper level, the NB magmas may have intruded into the Bentley volcanic system.

Deposition of the lower portion of the Bentley Supersuite (the Mount Palgrave Group and much of the Kaarna Group), pre-dates intrusion of the Nebo–Babel gabbro (Smithies et al., 2013). The presently available sulfur isotopic data for the units of the Bentley Supergroup indicate a range of compositions (Fig. 47 in Maier et al., 2014), with those from the lower part having  $\delta^{34}\text{S}$  between +1.8 and +7, potentially representing a suitable external sulfur source for the Nebo–Babel deposit. We thus argue that addition of external sulfur to the Nebo–Babel magma remains a possibility. The contamination model would be consistent with the relatively high Cu/Pd and Cu/Ni ratios (possibly reflecting addition of crustal Cu) and high Au/Pd ratios (possibly due to addition of crustal Au) (see data of Seat et al., 2007).

The question arises as to why only one major Ni–Cu deposit has so far been found in the Musgrave Province. Mineral deposits tend to form clusters, suggesting that more Ni–Cu deposits should occur in the Musgrave Province. Exploration during the last decade has identified several low-grade deposits (Halley's, Manchego, Succoth) suggesting the true potential of the west Musgrave Province for Ni–Cu sulfide deposits remains unrealized.

## 9. Conclusions

The Musgrave Province was the focus of long-lived mantle upwelling producing large volumes of magnesian basaltic to tholeiitic magma and their felsic derivatives. Magmatism led to crustal melting, lithospheric delamination, and a high crustal heat flux over >200 m.y. The Province contains one of the greatest concentrations of mafic–ultramafic layered intrusions globally, amongst them Mantamaru which is one of the world's largest layered intrusions. These data illustrate that large layered intrusions are not confined to cratons. What is required is a stable tectonic environment where magmas can ascend in locally extensional, possibly transpressional zones allowing the formation of thick sill-like bodies.

Due to the large size of the Giles intrusions, cooling rates were relatively slow. This led to crustal loading, subsidence of magma chambers, and sagging of cumulates prior to complete solidification. The mobilized cumulates unmixed and formed lenses and layers of peridotite and magnetite that are locally enriched in PGE. Syn- to post-magmatic tectonism led to fragmentation of many of the intrusions. The degree of crustal contamination was mostly relatively minor (<5%), although locally, basaltic magmas mingled with coeval granitic magmas.

The mineralization potential of the Giles intrusions and their host rocks is considerable. Large magmatic events, particularly those dominated by mafic–ultramafic magmas may cause increased heat flux into the crust, triggering crustal melting, devolatilization, and large-scale fluid flow. Deposit types favoured by such regimes include magmatic PGE–Cr–V–Fe–P deposits in large layered intrusions, Ni–Cu sulfide deposits in magma feeder conduits or at the base of layered intrusions, and hydrothermal deposits of variable style, notably in the roof and sidewalls of the largest intrusions.

Supplementary data to this article can be found online at <http://dx.doi.org/10.1016/j.oregeorev.2015.06.010>.

## Acknowledgements

Much of the work documented here arose through a regional-scale geological mapping project jointly coordinated through the Ngaanyatjarra Council and the Geological Survey of Western Australia (GSWA), and guided by the local Indigenous people in the region between the communities of Wingellina and Warburton. HMH and RHS publish with the permission of the executive director of the Geological

Survey of Western Australia. Richard Ernst and Steve Barnes are thanked for their constructive reviews.

## References

- Aitken, A.R., Dentith, M.C., Evans, S.F., Gallardo, L.A., Joly, A., Thiel, S., Smithies, R.H., Tyler, I.M., 2013. Imaging crustal structure in the west Musgrave Province from magnetotelluric and potential field data. Geological Survey of Western Australia, Report 114 (81 pp.).
- Ballhaus, C., Berry, R.F., 1991. Crystallization pressure and cooling history of the Giles Layered Igneous Complex, central Australia. *J. Petrol.* 32, 1–28.
- Ballhaus, C., Glikson, A.Y., 1989. Magma mixing and intraplate quenching in the Wingellina Hills intrusion, Giles Complex, central Australia. *J. Petrol.* 30, 1443–1469.
- Ballhaus, C., Glikson, A.Y., 1995. The petrology of layered mafic–ultramafic intrusions in the Giles Complex, western Musgrave block, central Australia. *AGSO J.* 16, 69–89.
- Barnes, S.J., 1993. Partitioning of the PGE and gold between silicate and sulphide magmas in the Munnii Munnii Complex, Western Australia. *Geochim. Cosmochim. Acta* 57, 1277–1290.
- Barnes, S.-J., Maier, W.D., 1999. The fractionation of Ni, Cu and the noble metals in silicate and sulphide liquids. In: Keays, R.R., Leshner, C.M., Lightfoot, P.C., Farrow, C.E.G. (Eds.), *Dynamic Processes in Magmatic Ore Deposits and Their Application to Mineral Exploration*. Geological Association of Canada; Short Course Notes 13, pp. 69–106.
- Barnes, S.-J., Maier, W.D., Curl, E., 2010. Composition of the marginal rocks and sills of the Rustenburg Layered Suite, Bushveld Complex, South Africa: implications for the formation of the PGE deposits. *Econ. Geol.* 105, 1491–1511.
- Becker, H., Horan, M.F., Walker, R.J., Gao, S., Lorand, J.-P., Rudnick, R.L., 2006. Highly siderophile element composition of the Earth's primitive mantle: constraints from new data on peridotite massifs and xenoliths. *Geochim. Cosmochim. Acta* 70, 4528–4550.
- Begg, G.C., Griffin, W.L., Natapov, L.M., O'Reilly, S.Y., Grand, S.P., O'Neill, C.J., Hronsky, J.M.A., Poudjom Djomani, Y., Swain, C.J., Deen, T., Bowden, P., 2009. The lithospheric architecture of Africa: seismic tomography, mantle petrology, and tectonic evolution. *Geosphere* 5, 23–50.
- Betts, P.G., Giles, D., 2006. The 1800–1100 Ma tectonic evolution of Australia. *Precambrian Research* 144, 92–125.
- Bodorkos, S., Wingate, M.T.D., 2008. 174589: quartz syenite dyke, Amy Giles Hill; *Geochronology Record* 715. Geological Survey of Western Australia (4 pp.).
- Bodorkos, S., Wingate, M.T.D., Kirkland, C.L., 2008a. 174538: metamonzogranite, Mount Daisy Bates; *Geochronology Record* 712. Geological Survey of Western Australia (4 pp.).
- Bodorkos, S., Wingate, M.T.D., Kirkland, C.L., 2008b. 174558: metamorphosed quartz diorite, Mount Fanny; *Geochronology Record* 713. Geological Survey of Western Australia (4 pp.).
- Bodorkos, S., Wingate, M.T.D., Kirkland, C.L., 2008c. 174736: granofelsic metasyenogranite, Mount Fanny; *Geochronology Record* 717. Geological Survey of Western Australia (4 pp.).
- Bodorkos, S., Wingate, M.T.D., Kirkland, C.L., 2008d. 174737: foliated metamonzogranite, Mount Fanny; *Geochronology Record* 718. Geological Survey of Western Australia (5 pp.).
- Bodorkos, S., Wingate, M.T.D., Kirkland, C.L., 2008e. 174747: metagabbro, Mount Fanny; *Geochronology Record* 719. Geological Survey of Western Australia (4 pp.).
- Boudreau, A.E., 1999. PELE – a version of the MELTS software programme for the PC platform. *Comput. Geosci.* 25, 201–203.
- Cameron, E.N., 1980. Evolution of the Lower Critical Zone, central sector, eastern Bushveld Complex. *Econ. Geol.* 75, 845–871.
- Campbell, I.H., Naldrett, A.J., 1979. The influence of silicate: sulfide ratios on the geochemistry of magmatic sulfides. *Econ. Geol.* 74, 1503–1505.
- Cawood, P.A., Korsch, R.J., 2008. Assembling Australia: Proterozoic building of a continent. *Precambrian Res.* 166, 1–38.
- Clarke, G.L., Sun, S.-S., White, R.W., 1995a. Grenville age belts and associated older terranes in Australia and Antarctica. *AGSO J. Aust. Geol. Geophys.* 16, 25–39.
- Clarke, G.L., Buick, I.S., Glikson, A.Y., Stewart, A.J., 1995b. Structural and pressure–temperature evolution of host rocks of the Giles Complex, western Musgrave Block, central Australia: evidence for multiple high-pressure events. *AGSO J. Aust. Geol. Geophys.* 16, 127–146.
- Coleman, P., 2009. Intracontinental orogenesis in the heart of Australia: structure, provenance and tectonic significance of the Bentley Supergroup, western Musgrave Block, Western Australia. *Geological Survey of Western Australia, Record* 2009/23 (48 pp.).
- Daniels, J.L., 1974. The geology of the Blackstone region, Western Australia. *Geol. Surv. West. Aust. Bull.* 123 (257 pp.).
- Edgoose, C.J., Scrimgeour, I.R., Close, D.F., 2004. *Geology of the Musgrave Block, Northern Territory*. Northern Territory Geological Survey, Report 15 (48 pp.).
- Eggs, S.M., Woodhead, J.D., Kinsley, L.P.J., Mortimer, G.E., Sylvester, P., McCulloch, M.T., Hergt, J.M., Handler, M.R., 1997. A simple method for the precise determination of >40 trace elements in geological samples by ICPMS using enriched isotope internal standardisation. *Chem. Geol.* 134, 311–326.
- Evins, P.M., Smithies, R.H., Howard, H.M. and Maier, W.D. 2009. *Holt, WA Sheet 4546: Geological Survey of Western Australia, 1:100000 Geological Series.*
- Evins, P.M., Smithies, R.H., Howard, H.M., Kirkland, C.L., Wingate, M.T.D., Bodorkos, S., 2010a. Redefining the Giles Event within the setting of the 1120–1020 Ma Ngaanyatjarra Rift, west Musgrave Province, Central Australia. *Geological Survey of Western Australia, Record* 2010/6 (36 pp.).

- Evins, P.M., Smithies, R.H., Howard, H.M., Kirkland, C.L., Wingate, M.T.D., Bodorkos, S., 2010b. Devil in the detail: the 1150–1000 Ma magmatic and structural evolution of the Ngaanyatjarra Rift, west Musgrave Province, Central Australia. *Precambrian Res.* 183, 572–588.
- Foulger, G.R., 2010. *Plates vs plumes*. Wiley-Blackwell, Chichester (328 pp.).
- Freestone, I.C., 1978. Liquid immiscibility in alkali-rich magmas. *Chem. Geol.* 23, 116–123.
- Gale, A., Dalton, C.A., Langmuir, C.H., Su, Y., Schilling, J.-G., 2013. The mean composition of ocean ridge basalts. *Geochem. Geophys. Geosyst.* 14 (3). <http://dx.doi.org/10.1029/2012GC004334>.
- The Giles mafic-ultramafic complex and environs, western Musgrave Block, central Australia. In: Glikson, A.Y. (Ed.), Thematic Issue. AGSO Journal of Geology and Geophysics vol. 16 (no. 1–2, 193 pp.).
- Giles, D., Betts, P.G., Lister, G.S., 2004. 1.8 – 1.5-Ga links between the North and South Australian Cratons and the Early–Middle Proterozoic configuration of Australia: *Tectonophysics*. v. 380, pp. 27–41.
- Glikson, A.Y., Stewart, A.T., Ballhaus, G.L., Clarke, G.L., Feeken, E.H.T., Level, J.H., Sheraton, J.W., Sun, S.-S., 1996. Geology of the western Musgrave Block, central Australia, with reference to the mafic-ultramafic Giles Complex. Australian Geological Survey Organisation, Bulletin 239 (206 p.).
- Godel, B., Seat, Z., Maier, W.D., Barnes, S.-J., 2011. The Nebo–Babel Ni–Cu–PGE sulfide deposit (West Musgrave Block, Australia): part 2 – constraints on parental magma and processes, with implications for mineral exploration. *Econ. Geol.* 106, 557–584.
- Goode, A.D.T., 1970. The petrology and structure of the Kalka and Ewarara layered basic intrusions, Giles Complex, central Australia: The University of Adelaide, Adelaide, PhD thesis (unpublished).
- Goode, A.D.T., 1976a. Small scale primary cumulus igneous layering in the Kalka layered intrusion, Giles Complex, central Australia. *J. Petrol.* 17, 379–397.
- Goode, A.D.T., 1976b. Sedimentary structures and magma current velocities in the Kalka layered intrusion, central Australia. *J. Petrol.* 17, 546–558.
- Goode, A.D.T., 1977a. Vertical igneous layering in the Ewarara layered intrusion, central Australia. *Geol. Mag.* 114, 215–218.
- Goode, A.D.T., 1977b. Flotation and remelting of plagioclase in the Kalka Intrusion, central Australia: petrological implications for anorthosite genesis. *Earth Planet. Sci. Lett.* 34, 375–380.
- Goode, A.D.T., 1977c. Intercumulus igneous layering in the Kalka layered intrusion, central Australia. *Geol. Mag.* 114, 215–218.
- Goode, A.D.T., 1978. High temperature, high strain rate deformation in the lower crustal Kalka Intrusion, central Australia. *Contrib. Mineral. Petrol.* 66, 137–148.
- Goode, A.D.T., 2002. The Western Musgrave Block – Australia. *Data Metallogenica, District Overview* (42 pp.).
- Goode, A.D.T., Krieger, G.W., 1967. The geology of Ewarara Intrusion, Giles Complex, central Australia. *J. Geol. Soc. Aust.* 14, 185–194.
- Goode, A.D.T., Moore, A.C., 1975. High pressure crystallisation of the Ewarara, Kalka and Gosse Pile intrusions, Giles Complex, central Australia. *Contrib. Mineral. Petrol.* 51, 77–97.
- Gray, C.M., 1971. Strontium isotope studies on granulites: The Australian National University, Canberra, PhD thesis (unpublished), 242p.
- Gray, C.M., Goode, A.D.T., 1989. The Kalka layered intrusion, central Australia: a strontium isotopic history of contamination and magma dynamics. *Contrib. Mineral. Petrol.* 103, 35–43.
- Howard, H.M., Smithies, R.H., Pirajno, F. and Skwarnecki, M.S. 2006a. Bates, WA Sheet 4646: Geological Survey of Western Australia, 1:100000 Geological Series.
- Howard, H.M., Smithies, R.H., Pirajno, F., 2006b. Geochemical and Nd isotopic signatures of mafic dykes in the western Musgrave Complex. Geological Survey of Western Australia Annual Review 2005–06, pp. 64–71.
- Howard, H.M., Smithies, R.H., Pirajno, F. and Skwarnecki, M.S. 2007. Bell Rock, WA Sheet 4645: Geological Survey of Western Australia, 1:100000 Geological Series.
- Howard, H.M., Smithies, R.H., Kirkland, C.L., Evins, P.M., Wingate, M.T.D., 2009. Age and geochemistry of the Alcurra Suite in the west Musgrave Province and implications for orthomagmatic Ni–Cu–PGE mineralization during the Giles Event. Geological Survey of Western Australia, Record 2009/16 (16 pp.).
- Howard, H.M., Smithies, R.H., Werner, M., Kirkland, C.L., Wingate, M.T.D., 2011a. Geochemical characteristics of the Alcurra Dolerite (Giles Event) and its extrusive equivalents in the Bentley Supergroup. Geological Survey of Western Australia, Record 2011/2pp. 27–30.
- Howard, H.M., Werner, M., Smithies, R.H., Kirkland, C.L., Kelsey, D.L., Hand, M., Collins, A., Pirajno, F., Wingate, M.T.D., Maier, W.D., Raimondo, T., 2011b. The geology of the west Musgrave Province and the Bentley Supergroup – a field guide. Geological Survey of Western Australia, Record 2011/4 (119 pp.).
- Howard, H.M., Smithies, R.H., Kirkland, C.L., Kelsey, D.E., Aitken, A., Wingate, M.T.D., Quentin de Gromard, R., Spaggiari, C.V., Maier, W.D., 2015. The burning heart – the Proterozoic geology and geological evolution of the west Musgrave Region, central Australia. *Gondwana Res.* 27, 64–94.
- Irvine, T.N., 1970. Crystallization sequences in magmas of the Muskox intrusion and some other layered intrusions. Geological Society of South Africa, Special Publication 1, pp. 441–476.
- Irvine, T.N., Andersen, J.C.O., Brooks, C.K., 1998. Included blocks (and blocks within blocks) in the Skaergaard Intrusion: geochemical relations and the origins of rhythmic modally graded layers. *Geol. Soc. Am. Bull.* 110, 1398–1447.
- Karykowski, B.T., 2014. Petrogenesis and Economic Potential of Orthomagmatic Ni–Cu–PGE Mineralization in the Jameson Range (West Musgraves), Western Australia, Diploma thesis, TU Bergakademie Freiberg (185 pp.).
- Kelsey, D.E., Hand, M., Evins, P., Clark, C., Smithies, H., 2009. High temperature, high geothermal gradient metamorphism in the Musgrave Province, central Australia: potential constraints on tectonic setting. In: Timms, N.E., Foden, J., Evans, K., Clark, C. (Eds.), Biennial conference of the Specialist Group for Geochemistry, Mineralogy and Petrology, Kangaroo Island November 2009. Geological Society of Australia Abstracts No. 96, p. 28.
- Kelsey, D.E., Hand, M., Smithies, H., Evins, P., Clark, C., Kirkland, C.L., 2010. What is the tectonic setting of long-lived Grenvillian-aged ultrahigh temperature, high geothermal gradient metamorphism in the Musgrave Province, central Australia? *Geol. Soc. Am. Abstr. Programs* 42 (5), 516.
- King, R.J., 2008. Using calculated pseudosections in the system NCKFMASHTO and SHRIMP II U–Pb zircon dating to constrain the metamorphic evolution of paragneisses in the Latitude Hills, West Musgrave Province, Western Australia. Geological Survey of Western Australia, Record 2009/15 (67 pp.).
- Kirkland, C.L., Wingate, M.T.D., Bodorkos, S., 2008a. 183496: orthogneiss, Mount West; Geochronology Record 747. Geological Survey of Western Australia (5 pp.).
- Kirkland, C.L., Wingate, M.T.D., Bodorkos, S., 2008b. 183459: charnockite, Latitude Hill, Geochronology Record 722. Geological Survey of Western Australia (5 pp.).
- Kirkland, C.L., Wingate, M.T.D., Bodorkos, S., 2008c. 183509: leucogranite dyke, Mount West; Geochronology Record 724. Geological Survey of Western Australia (4 pp.).
- Kirkland, C.L., Wingate, M.T.D., Bodorkos, S., 2008d. 193850: leucogranite dyke, Mount Fanny; Geochronology Record 748. Geological Survey of Western Australia (4 pp.).
- Kirkland, C.L., Wingate, M.T.D., Bodorkos, S., 2008e. 174761: porphyritic granite dyke, Bell Rock; Geochronology Record 721. Geological Survey of Western Australia (4 pp.).
- Kirkland, C.L., Wingate, M.T.D., Bodorkos, S., 2008f. 185509: leucogranite, Mount Aloysius; Geochronology Record 725. Geological Survey of Western Australia (4 pp.).
- Kirkland, C.L., Wingate, M.T.D., Smithies, R.H., 2011. 194762: leucogabbro, Mount Finlayson; Geochronology Record 966. Geological Survey of Western Australia (4 pp.).
- Kirkland, C.L., Smithies, R.H., Woodhouse, A.J., Howard, H.M., Wingate, M.T.D., Belousova, E.A., Cliff, J.B., Murphy, R.C., Spaggiari, C.V., 2013. Constraints and deception in the isotopic record: the crustal evolution of the west Musgrave Province, central Australia. *Gondwana Res.* 23, 759–781.
- Latypov, R., Hanski, E., Lavrenchuk, A., Huhma, H., Havela, T., 2011. A 'Three-Increase Model' for the Origin of the Marginal Reversal of the Koitelainen Layered Intrusion, Finland. *J. Petrol.* 52, 733–764.
- Leshner, C.M., Burnham, O.M., 2001. Multicomponent elemental and isotopic mixing in Ni–Cu–(PGE) ores at Kambalda, Western Australia. *Can. Mineral.* 39, 421–446.
- Li, Z.X., 2000. Palaeomagnetic evidence for unification of the North and West Australian craton by ca. 1.7 Ga: new results from the Kimberley Basin of northwestern Australia. *Geophys. J. Int.* 142, 173–180.
- Li, C., Ripley, E.M., 2010. The relative effects of composition and temperature on olivine-liquid partitioning: statistical deconvolution and implications for petrologic modeling. *Chem. Geol.* 275, 95–104.
- Li, C., Ripley, E.M., Oberthür, T., Miller Jr., J.D., Joslin, G.D., 2008. Textural, mineralogical and stable isotope studies of hydrothermal alteration in the main sulfide zone of the Great Dyke, Zimbabwe and the precious metals zone of the Sonju Lake Intrusion, Minnesota, USA. *Mineral. Deposita* 43, 97–110.
- Liebenberg, L., 1970. The sulfides in the layered sequence of the Bushveld igneous Complex. *Geol. Soc. S. Afr. Spec. Publ.* 1, 108–208.
- Lightfoot, P.C., Naldrett, A.J., 1983. The geology of the Tabankulu section of the Insizwa Complex, Transkei, Southern Africa, with reference to the nickel sulphide potential. *Trans. Geol. Soc. S. Afr.* 86, 169–187.
- Lipin, B.R., 1993. Pressure increases, the formation of chromite seams, and the development of the Ultramafic series in the Stillwater Complex, Montana. *J. Petrol.* 34, 955–976.
- Maier, W.D., 2005. Platinum-group element (PGE) deposits and occurrences: mineralization styles, genetic concepts and exploration criteria. *J. Afr. Earth Sci.* 41, 165–191.
- Maier, W.D., Eales, H.V., 1997. Correlation within the UG2 – Merensky Reef interval of the Western Bushveld Complex, based on geochemical, mineralogical and petrological data. *Geol. Surv. S. Afr. Bull.* 120 (56 pp.).
- Maier, W.D., Barnes, S.-J., 2004. Pt/Pd and Pd/Ir ratios in mantle-derived magmas: a possible role for mantle metasomatism. *S. Afr. J. Geol.* 107, 333–340.
- Maier, W.D., Barnes, S.J., Gartz, V., Andrews, G., 2003. Pt–Pd reefs in magnetites of the Stella layered intrusion, South Africa: a world of new exploration opportunities for platinum group elements. *Geology* 31, 885–888.
- Maier, W.D., Rasmussen, B., Li, C., Barnes, S.-J., Huhma, H., 2013a. The Kunene anorthosite complex, Namibia, and its satellite bodies: geochemistry, geochronology and economic potential. *Econ. Geol.* 108, 953–986.
- Maier, W.D., Barnes, S.-J., Groves, D.L., 2013b. The Bushveld Complex, South Africa: formation of platinum–palladium, chrome and vanadium-rich layers via hydrodynamic sorting of a mobilized cumulate slurry in a large, relatively slowly cooling, subsiding magma chamber. *Mineral. Deposita* 48, 1–56.
- Maier, W.D., Howard, H.M., Smithies, R.H., Yang, S., Barnes, S.-J., O'Brien, H., Huhma, H., Gardoll, S., 2014. Mafic-ultramafic intrusions of the Giles event, Western Australia: Petrogenesis and prospectivity for magmatic ore deposits. *GSWA Report 134* (82pp).
- Metals X Ltd, 2013. Globally significant nickel project, viewed 8 April 2014. (<[http://www.metalsx.com.au/system/assets/26/original/Nickel\\_Division.pdf](http://www.metalsx.com.au/system/assets/26/original/Nickel_Division.pdf)>).
- Morris, P.A., Pirajno, F., 2005. Geology, geochemistry, and mineralization potential of Mesoproterozoic sill complexes of the Bangemall Supergroup, Western Australia. Geological Survey of Western Australia of Western Australia, Report 99 (72 pp.).
- Morse, S.A., 1981. Kiglapait geochemistry IV: the major elements. *Geochim. Cosmochim. Acta* 45, 461–479.
- Naldrett, A.J., Lehmann, J., 1988. Spinel nonstoichiometry as the explanation for Ni-, Cu-, and PGE-enriched sulphides in chromitites. In: Prichard, H.M., et al. (Eds.), *Geo-Platinum 87*. Elsevier, Barking, pp. 93–109.
- Naslund, H.R., 1983. The effect of oxygen fugacity on liquid immiscibility in iron-bearing silicate melts. *Am. J. Sci.* 283, 1034–1059.
- Nesbitt, R.W., Talbot, J.L., 1966. The layered basic and ultrabasic intrusives of the Giles Complex, central Australia. *Contrib. Mineral. Petrol.* 13, 1–11.

- Nesbitt, R.W., Goode, A.D.T., Moore, A.C., Hopwood, T.P., 1970. The Giles Complex, central Australia: a stratified sequence of mafic and ultramafic intrusions. *Special Publications of the Geological Society of South Africa* vol. 1, pp. 547–564.
- Norrish, K., Hutton, J.T., 1969. An accurate X-ray spectrographic method for the analysis of a wide range of geological samples: *Geochemica et Cosmochimica Acta* 33, pp. 431–453.
- Norrish, K., Chappell, B.W., 1977. X-ray fluorescence spectrometry. In: Zussman, J. (Ed.), *Physical Methods in Determinative Mineralogy*, 2nd Edition Academic Press, London, pp. 201–272.
- Pascoe, A 2012. The geochemistry and petrogenesis of the mafic and ultramafic giles intrusions at Latitude Hill, west Musgrave Province, Western Australia: The University of Tasmania, Hobart, BSc Honours thesis (unpublished).
- Patino Douce, A.E., Beard, J.S., 1995. Dehydration-melting of Biotite Gneiss and Quartz Amphibolite from 3 to 15 kbar. *J. Petrol.* 36, 707–738.
- Philpotts, A.R., 1967. Origin of certain iron–titanium oxide and apatite rocks. *Econ. Geol.* 62, 303–315.
- Phosphate Australia Ltd, 2014. Manchego Prospect: Musgrave Project, Western Australia, viewed 6 May 2014. (<http://www.asx.com.au/asxpdf/20140103/pdf/42lz643zrngqwx.pdf>).
- Raedeke, LD 1982. Petrogenesis of the Stillwater Complex: The University of Washington, Seattle, PhD thesis (unpublished).
- Redstone Resources Ltd, 2008a. Quarterly report for the period ending June 30th 2008, viewed 6 May 2014. [http://www.redstone.com.au/investorcentre/press\\_releases/2008073101.pdf](http://www.redstone.com.au/investorcentre/press_releases/2008073101.pdf).
- Redstone Resources Ltd, 2008b. Report of the Annual General Meeting, viewed 8 April 2014. <http://www.asx.com.au/asxpdf/20081127/pdf/31dvzvjbkp7f5b.pdf>.
- Reynolds, I.M., 1985. The nature and origin of titaniferous magnetite-rich layers in the Upper Zone of the Bushveld Complex: a review and synthesis. *Econ. Geol.* 80, 1089–1108.
- Roedder, E., 1978. Silicate liquid immiscibility in magmas and in the system K<sub>2</sub>O–FeO–Al<sub>2</sub>O<sub>3</sub>–SiO<sub>2</sub>: an example of serendipity: *Geochemica et Cosmochimica Acta* 42, 1597–1617.
- Rollinson, H.R., 2013. Using Geochemical Data: Evaluation, Presentation, Interpretation. Routledge, Oxon, UK.
- Scrimgeour, I.R., Close, D.F., 1999. Regional high pressure metamorphism during intracratonic deformation: the Petermann orogeny, central Australia. *J. Metamorph. Geol.* 17, 557–572.
- Seat, Z 2008. Geology, petrology, mineral and whole-rock chemistry, stable and radiogenic isotope systematics and Ni–Cu–PGE mineralisation of the Nebo–Babel intrusion, west Musgrave, Western Australia: The University of Western Australia, Perth, PhD thesis (unpublished).
- Seat, Z., Beresford, S.W., Grguric, B.A., Waugh, R.S., Hronsky, J.M.A., Gee, M.M.A., Groves, D.I., Mathison, C.I., 2007. Architecture and emplacement of the Nebo–Babel gabbro–norite-hosted magmatic Ni–Cu–PGE sulfide deposit, West Musgrave, Western Australia. *Mineral. Deposita* 42, 551–582.
- Seat, Z., Beresford, S.W., Grguric, B.A., Gee, M.A., Grassineau, N.V., 2009. Reevaluation of the role of external sulfur addition in the genesis of Ni–Cu–PGE deposits: evidence from the Nebo–Babel Ni–Cu–PGE deposit: West Musgrave, Western Australia. *Econ. Geol.* 104, 521–538.
- Sharpe, M.R., 1981. The chronology of magma influxes to the eastern compartment of the Bushveld Complex, as exemplified by its marginal border group. *J. Geol. Soc. Lond.* 138, 307–326.
- Sheraton, J.W., Sun, S.-s., 1995. Geochemistry and origin of felsic igneous rocks of the western Musgrave Block. *AGSO J.* 16, 107–125.
- Silver, P.G., Behn, M.D., Kelley, K., Schmitz, M., Savage, B., 2006. Understanding cratonic flood basalts. *Earth Planet. Sci. Lett.* 245, 190–201.
- Smithies, R.H., Howard, H.M., Evins, P.M., Kirkland, C.L., Bodorkos, S., Wingate, M.T.D., 2009. The west Musgrave Complex – some new geological insights from recent mapping, geochronology, and geochemical studies. *Geological Survey of Western Australia, Record 2008/19* (20 pp.).
- Smithies, R.H., Howard, H.M., Evins, P.M., Kirkland, C.L., Kelsey, D.E., Hand, M., Wingate, M.T.D., Collins, A.S., Belousova, E., Allchurch, S., 2010. Geochemistry, geochronology and petrogenesis of Mesoproterozoic felsic rocks in the western Musgrave Province of central Australia, and implication for the Mesoproterozoic tectonic evolution of the region. *Geological Survey of Western Australia, Report 106* (73 pp.).
- Smithies, R.H., Howard, H.M., Evins, P.M., Kirkland, C.L., Kelsey, D.E., Hand, M., Wingate, M.T.D., Collins, A.S., Belousova, E., 2011. Mesoproterozoic high temperature granite magmatism, crust–mantle interaction and the intracontinental evolution of the Musgrave Province. *J. Petrol.* <http://dx.doi.org/10.1093/petrology/egr010>.
- Smithies, R.H., Howard, H.M., Kirkland, C.L., Werner, M., Medlin, C.C., Wingate, M.T.D., Cliff, J.B., 2013. Geochemical evolution of rhyolites of the Talbot Sub-basin and associated felsic units of the Warakurna Supersuite. *Geological Survey of Western Australia, Report 118* (74 pp.).
- Smithies, R.H., Kirkland, C.L., Korhonen, F.J., Aitken, A.R.A., Howard, H.M., Maier, W.D., Wingate, M.T.D., Quentin de Gromard, R., Gessner, K., 2015. The Mesoproterozoic thermal evolution of the Musgrave Province in central Australia – Plume vs. the geological record. *Gondwana Res.* 27, 64–94.
- Smithies, R.H., Howard, H.M., Kirkland, C.L., Korhonen, F.J., Medlin, C.C., Maier, W.D., Quentin de Gromard, R., Wingate, M.T.D., 2015. Piggyback supervolcanoes – long-lived, voluminous, juvenile rhyolite volcanism in Mesoproterozoic Central Australia. *J. Petrol.* <http://dx.doi.org/10.1093/petrology/egv015> (in press).
- Sobolev, S.V., Sobolev, A.V., Kuzmin, D.V., Krivolutskaia, N.A., Petrunin, A.G., Arndt, N.T., Radko, V.A., Vasiliev, Y.R., 2011. Linking mantle plumes, large igneous provinces and environmental catastrophes. *Nature* 477, 312–316.
- Sprigg, R.C., Wilson, R.B., 1959. The Musgrave mountain belt in South Australia. *Geol. Rundsch.* c47, 531–542.
- Staubmann, M 2010. The petrogenesis and economic potential of the Southern Cavenagh Range Intrusion (West Musgraves), Western Australia: The University of Tasmania, Hobart, BSc Honours thesis (unpublished).
- Stewart, A.J., 1995. Resolution of conflicting structures and deformation history of the Mount Aloysius granulite massif, western Musgrave Block, central Australia. *AGSO J. Aust. Geol. Geophys.* 16, 91–105.
- Sun, S.-s., McDonough, W.F., 1989. Chemical and isotopic systematics of oceanic basalts: implications for mantle composition and processes. In: Saunders, A.D., Norry, M.J. (Eds.), *Magmatism in the Ocean Basins*. Geological Society Special Publication 42, pp. 313–345.
- Sun, S.-s., Sheraton, J.W., Glikson, A.Y., Stewart, A.J., 1996. A major magmatic event during 1050–1080 Ma in central Australia, and an emplacement age for the Giles Complex. *AGSO J. Aust. Geol. Geophys.* 24, 13–15.
- Tegner, C., Wilson, J.R., Brooks, C.K., 1993. Intraplutonic quench zones in the Kap Edvard Holm layered gabbro complex, east Greenland. *J. Petrol.* 34, 681–710.
- Teigler, B., Eales, H.V., 1996. The Lower and Critical Zones of the western limb of the Bushveld Complex, as indicated by the Nooitgedacht boreholes. *Geol. Surv. S. Afr. Bull.* 111 (126 pp.).
- Tollari, N., Toplis, M.J., Barnes, S.-J., 2006. Predicting phosphate saturation in silicate magmas: an experimental study of the effects of melt composition and temperature. *Geochim. Cosmochim. Acta* 70, 1518–1536.
- Tollari, N., Baker, D., Barnes, S.-J., 2008. Experimental effects of pressure and fluorine on apatite saturation in mafic magmas, with reference to layered intrusions and massif anorthosites. *Contrib. Mineral. Petrol.* 156, 161–175.
- Toplis, M.J., Carroll, M.R., 1995. An experimental study of the influence of oxygen fugacity on Fe–Ti oxide stability, phase-relations, and mineral–melt equilibria in ferro-basaltic systems. *J. Petrol.* 36, 1137–1170.
- Toplis, M.J., Carroll, M.R., 1996. Differentiation of ferro-basaltic magmas under conditions open and closed to oxygen: implications for the Skaergaard intrusion and other natural systems. *J. Petrol.* 37, 837–858.
- Traka Resources Ltd, 2011. Quarterly Activities Report for the Three Months Ended 30 June 2011.
- Traka Resources Ltd, 2013. Musgrave Project, viewed 29 August 2013. <http://www.trakaresources.com.au>.
- Ulmer, G.C., 1969. Experimental investigation of chromite spinels. *Econ. Geol. Monogr.* 4, 114–131.
- Wade, BP 2006. Unravelling the tectonic framework of the Musgrave Province, central Australia: The University of Adelaide, Adelaide, PhD thesis (unpublished).
- Wade, B.P., Kelsey, D.E., Hand, M., Barovich, K.M., 2008. The Musgrave Province: stitching north, west and south Australia: *Precambrian Research* 166, 370–386.
- Waight, T.E., Maas, R., Nicholls, I.A., 2000. Fingerprinting feldspar phenocrysts using crystal isotopic composition stratigraphy: implications for crystal transfer and magma mingling in S-type granites. *Contrib. Mineral. Petrol.* 139, 227–239.
- White, R.W., Clarke, G.L., Nelson, D.R., 1999. SHRIMP U–Pb zircon dating of Grenville-age events in the western part of the Musgrave Block, central Australia. *J. Metamorph. Geol.* 17, 465–481.
- Wilson, A.H., Naldrett, A.J., Tredoux, M., 1989. Distribution and controls of platinum group element and base metal mineralization in the Darwendale subchamber of the Great Dyke, Zimbabwe. *Geology* 17, 649–652.
- Wingate, M.T.D., Evans, D.A.D., 2003. Palaeomagnetic constraints on the Proterozoic tectonic evolution of Australia. In: Yoshida, M., Windley, B.F., Dasgupta, S. (Eds.), *Proterozoic East Gondwana: Supercontinent Assembly and Breakup*. Geological Society, London, Special Publications 206, pp. 77–91.
- Wingate, M.T.D., Pirajno, F., Morris, P.A., 2004. Warakurna large igneous province: a new Mesoproterozoic large igneous province in west-central Australia. *Geology* 32, 105–108.
- Yang, S., Maier, W.D., Hanski, E., Lappalainen, M., Santaguida, F., Määttä, S., 2013a. Origin of ultra-nickeliferous olivine in the Kevitsa Ni–Cu–PGE mineralized intrusion, Lapland, Finland. *Contrib. Mineral. Petrol.* 166, 81–95.
- Yang, S., Maier, W.D., Lahaye, Y., O'Brien, H., 2013b. Strontium isotope disequilibrium of plagioclase in the Upper Critical Zone of the Bushveld Complex: evidence for mixing of crystal slurries. *Contrib. Mineral. Petrol.* <http://dx.doi.org/10.1007/s0041001309034>.
- Zhao, J.-X., McCulloch, M.T., Korsch, R.J., 1994. Characterisation of a plume-related ~800 Ma magmatic event and its implications for basin formation in central-southern Australia. *Earth Planet. Sci. Lett.* 121, 349–367.